

---

Theses and Dissertations

---

Fall 2010

# An investigation of the phototoxicity of decabromodiphenyl ether and triclosan

Yang-Won Suh  
*University of Iowa*

Copyright 2010 Yang-Won Suh

This dissertation is available at Iowa Research Online: <http://ir.uiowa.edu/etd/892>

---

## Recommended Citation

Suh, Yang-Won. "An investigation of the phototoxicity of decabromodiphenyl ether and triclosan." PhD (Doctor of Philosophy) thesis, University of Iowa, 2010.  
<http://ir.uiowa.edu/etd/892>.

---

Follow this and additional works at: <http://ir.uiowa.edu/etd>



Part of the [Occupational Health and Industrial Hygiene Commons](#)

AN INVESTIGATION OF THE PHOTOTOXICITY OF  
DECABROMODIPHENYL ETHER AND TRICLOSAN

by  
Yang-Won Suh

An Abstract

Of a thesis submitted in partial fulfillment  
of the requirements for the Doctor of  
Philosophy degree in Occupational and Environmental Health  
in the Graduate College of  
The University of Iowa

December 2010

Thesis Supervisor: Associate Professor Gabriele Ludewig

## ABSTRACT

Decabromodiphenylether (deca-BDE) and triclosan (2,4,4'-trichloro-2'-hydroxydiphenylether) are used in consumer products as flame retardant and bactericide, respectively. Dermal contact is a major human exposure pathway. Deca-BDE and triclosan are known to be photolytically degraded to compounds like lower-BDEs and dioxins. My hypothesis is that photolysis of deca-BDE and triclosan generates free radicals and degradation products which cause toxic effects including cytotoxicity, growth inhibition, oxidative stress and genotoxicity in skin. To test this hypothesis radical formation and photolytic products of deca-BDE and toxic effects of deca-BDE and triclosan alone/with UV-exposure were determined using immortal human keratinocytes (HaCaT) and primary human skin fibroblasts (HSF).

My electron paramagnetic resonance and GC-MS studies indicate that deca-BDE is photoreactive and UV irradiation of deca-BDE in organic solvents generates free radicals and lower-BDEs. The free radical formation is wavelength-dependent and positively related to the irradiation time and deca-BDE concentration.

In structure-activity relationship studies with deca-BDE, octa-BDE, PBB 209, PCB 209 and diphenyl ether, the presence of halogen atoms (Br > Cl), and/or an ether bond enhance free radical formation. Debromination and hydrogen abstraction from the solvents are the mechanism of radical formation with deca-BDE, which raises concerns about possible toxic effects in UV-exposed skin.

In cell culture experiments high levels of triclosan plus UV irradiation and repetitive deca-BDE and UV exposures caused synergistic cytotoxicity in HaCaT. However, neither triclosan nor deca-BDE can be regarded as a phototoxicant following the OECD test and evaluation guidelines. In HSF, no synergistic cytotoxicity was observed, although HSF were more sensitive to deca-BDE and triclosan alone than HaCaT. Contrary to expectations, the photodegradation products of triclosan were less

toxic than triclosan itself to HaCaT. However, UV irradiation of triclosan-exposed cells produced a dose dependent increase in intracellular oxidative stress (dichlorofluorescein formation). Comet experiments did not show consistent results of genotoxicity in HaCaT. Overall, deca-BDE and triclosan had no or weak phototoxic potential in cells with the experimental conditions employed.

To my knowledge, my research is the first prove of free radical formation during UV irradiation of deca-BDE and the first investigation of phototoxicity of deca-BDE and triclosan in human skin cells.

Abstract Approved: \_\_\_\_\_  
Thesis Supervisor  
\_\_\_\_\_  
Title and Department  
\_\_\_\_\_  
Date



AN INVESTIGATION OF THE PHOTOTOXICITY OF  
DECABROMODIPHENYL ETHER AND TRICLOSAN

by  
Yang-Won Suh

A thesis submitted in partial fulfillment  
of the requirements for the Doctor of  
Philosophy degree in Occupational and Environmental Health  
in the Graduate College of  
The University of Iowa

December 2010

Thesis Supervisor: Associate Professor Gabriele Ludewig

Graduate College  
The University of Iowa  
Iowa City, Iowa

CERTIFICATE OF APPROVAL

---

PH.D. THESIS

---

This is to certify that the Ph.D. thesis of

Yang-Won Suh

has been approved by the Examining Committee  
for the thesis requirement for the Doctor of Philosophy  
degree in Occupational and Environmental Health at the December 2010  
graduation.

Thesis Committee: \_\_\_\_\_  
Gabriele Ludewig, Thesis Supervisor

\_\_\_\_\_  
Larry W. Robertson

\_\_\_\_\_  
Garry R. Buettner

\_\_\_\_\_  
Michael W. Duffel

\_\_\_\_\_  
Jerald L. Schnoor

## ACKNOWLEDGMENTS

I would like to thank my adviser, Dr. Ludewig, for guiding me to find an exciting research field and advising me with a profound knowledge of science, generosity and endurance as a mentor for my research and life. I also want to thank Dr. Robertson for his insightful advice and suggestions for my PhD research with continuous supports and consideration. Dr. Buettner provided me with considerable help to understand free radical formation and interpret results from EPR experiments and study photochemistry. Dr. Duffel gave me critical suggestions for objective and reasonable interpretation of research data and presentation. Dr. Schnoor gave me excellent feedback for my research plan and progress.

I have to tell significant help from Dr. Garcia-Boy who taught me cell culture and other biology laboratory techniques. Dr. Venkataraman helped me to simulate and interpret EPR data. Dr. Treimer analyzed photodegradation samples and provided GC-MS data. Brett Wagner and Karl Niggemeyer instructed me to use EPR machine and set up experimental conditions. I also would like to thank everybody in our laboratory and the Department of Occupational and Environmental Health.

Finally, I would like to express my special thanks to my wife, Miae Yun and my parents and parents-in-law for their sacrificial and endless support whenever I was frustrated and needed encouragement.

## ABSTRACT

Decabromodiphenylether (deca-BDE) and triclosan (2,4,4'-trichloro-2'-hydroxydiphenylether) are used in consumer products as flame retardant and bactericide, respectively. Dermal contact is a major human exposure pathway. Deca-BDE and triclosan are known to be photolytically degraded to compounds like lower-BDEs and dioxins. My hypothesis is that photolysis of deca-BDE and triclosan generates free radicals and degradation products which cause toxic effects including cytotoxicity, growth inhibition, oxidative stress and genotoxicity in skin. To test this hypothesis radical formation and photolytic products of deca-BDE and toxic effects of deca-BDE and triclosan alone/with UV-exposure were determined using immortal human keratinocytes (HaCaT) and primary human skin fibroblasts (HSF).

My electron paramagnetic resonance and GC-MS studies indicate that deca-BDE is photoreactive and UV irradiation of deca-BDE in organic solvents generates free radicals and lower-BDEs. The free radical formation is wavelength-dependent and positively related to the irradiation time and deca-BDE concentration.

In structure-activity relationship studies with deca-BDE, octa-BDE, PBB 209, PCB 209 and diphenyl ether, the presence of halogen atoms (Br > Cl), and/or an ether bond enhance free radical formation. Debromination and hydrogen abstraction from the solvents are the mechanism of radical formation with deca-BDE, which raises concerns about possible toxic effects in UV-exposed skin.

In cell culture experiments high levels of triclosan plus UV irradiation and repetitive deca-BDE and UV exposures caused synergistic cytotoxicity in HaCaT. However, neither triclosan nor deca-BDE can be regarded as a phototoxicant following the OECD test and evaluation guidelines. In HSF, no synergistic cytotoxicity was observed, although HSF were more sensitive to deca-BDE and triclosan alone than HaCaT. Contrary to expectations, the photodegradation products of triclosan were less

toxic than triclosan itself to HaCaT. However, UV irradiation of triclosan-exposed cells produced a dose dependent increase in intracellular oxidative stress (dichlorofluorescein formation). Comet experiments did not show consistent results of genotoxicity in HaCaT. Overall, deca-BDE and triclosan had no or weak phototoxic potential in cells with the experimental conditions employed.

To my knowledge, my research is the first prove of free radical formation during UV irradiation of deca-BDE and the first investigation of phototoxicity of deca-BDE and triclosan in human skin cells.

## TABLE OF CONTENTS

LIST OF TABLES .....	viii
LIST OF FIGURES .....	ix
CHAPTER 1. BACKGROUND INFORMATION ON POLYBROMINATED DIPHENYL ETHERS AND TRICLOSAN .....	1
Polybrominated Diphenyl Ethers.....	1
Production and Uses.....	1
Levels in the Environment and in Humans .....	3
Biotic Environment and Food .....	4
Abiotic Environment.....	4
Human .....	6
Exposure Routes.....	7
Toxic Effects .....	8
Neurotoxicity.....	8
Hormonal Interruption.....	9
Interactions with the AhR Receptor .....	10
Carcinogenicity .....	10
Other Effects .....	10
Regulations .....	10
Biological and Physicochemical Transformation.....	11
Biological Transformation .....	11
Physicochemical Transformation.....	11
Triclosan .....	12
Production, Uses and Regulations.....	12
Levels and Exposure Routes .....	14
Toxic Effects .....	15
Acute Toxicity.....	15
Irritation and Sensitization .....	15
Repeat Dose Toxicity .....	16
Genotoxicity .....	16
Carcinogenicity .....	16
Reproductive and Developmental Toxicity.....	17
Bacterial Resistance .....	17
Ecotoxicity .....	17
Physicochemical transformation .....	17
Photolytic Transformation.....	17
Outline of Thesis .....	18
CHAPTER 2. PHOTOACTIVITY AND RADICAL FORMATION POTENTIAL OF DECA-BDE IN THE PRESENCE OF LIGHT .....	24
Introduction.....	24
Literature Review .....	24
Research Hypothesis .....	25
Materials and Methods .....	25
Experimental Design .....	25
Materials.....	25

Methods .....	26
UV-VIS Spectroscopy .....	26
Irradiation .....	26
GC-MS .....	27
EPR.....	28
Results and Discussion .....	29
Absorption Spectra .....	29
Photodegradation of Deca-BDE with Lower-BDE Formation .....	29
Radical Formation from Irradiation of Deca-BDE.....	30
Wavelength Dependency of the Radical Formation.....	31
Radical Formation Changes by Deca-BDE Concentration and Irradiation Time.....	31
Conclusions.....	31
CHAPTER 3. MECHANISMS OF THE RADICAL FORMATION OF DECA- BDE IN THE PRESENCE OF LIGHT .....	44
Introduction.....	44
Literature Review .....	44
Research Hypothesis .....	45
Materials and Methods .....	45
Experimental Design .....	45
Materials.....	46
Methods .....	46
UV-VIS Spectroscopy.....	46
Irradiation .....	46
EPR.....	47
Results and Discussion .....	48
Absorption Spectra of Structurally Related Compounds .....	48
EPR Spectra of Structurally Related Compounds.....	48
Relationship between Structure and Radical Yield.....	48
Effect of Deca-BDE on the Radical Species .....	49
Sources of Hydrogen Involved in the Radical Formation.....	52
Photochemistry of the Free Radical Formation of Deca-BDE in the Presence of UV Light.....	53
Conclusions.....	54
CHAPTER 4. BIOLOGICAL EFFECTS OF DECA-BDE/TRICLOSAN, LIGHT, AND THE COMBINATION OF BOTH IN SKIN CELLS.....	66
Introduction.....	66
Literature Review .....	67
PBDEs .....	67
Triclosan.....	68
Chlorpromazine.....	68
Research Hypothesis .....	70
Materials and Methods .....	70
Experimental Design .....	70
Materials.....	70
Chemicals.....	70
Cell Culture .....	70
Irradiation and UV-VIS Spectroscopy .....	71
Methods .....	71
Irradiation .....	71

Spectral Changes after UV Irradiation .....	72
Cell Culture Experiment.....	72
Cytotoxicity Test (protocol A) for Studying Dose- response Relationship for Test Compounds and UV Dose.....	73
OECD Test (protocol C) Paired with Cytotoxicity Test with UVB (protocol B) .....	74
Toxicity of Photodegradation Products.....	76
Oxidative Stress .....	76
Genotoxicity.....	77
Statistical Analyses .....	80
Results and Discussion .....	80
Absorption Spectra and Their Changes after UV Irradiation.....	80
Cytotoxicity with Confluent Cells and UVA & B: Concentration and UV-dose Response.....	81
Toxicity Test with Growing Cells (OECD test) and Confluent Cells.....	83
OECD Test .....	83
Cytotoxicity Test with Confluent Cells, UVB-centered .....	83
Toxicity of Photodegradation Products .....	85
Oxidative Stress.....	86
Genotoxicity .....	87
Conclusions.....	88
 CHAPTER 5. SUMMARY AND FUTURE PERSPECTIVES .....	 115
Summary.....	115
Future Perspectives .....	118
 REFERENCES .....	 121



## LIST OF TABLES

Table 1.1. Profiles of congeners (mass %) in commercial PBDE mixtures. ....	22
Table 1.2. Estimated human adult intakes of PBDEs (exposures in units of ng/day). ....	23
Table 2.1. Molecular structures of deca-BDE and organic solvents.....	33
Table 3.1. Molecular structures of the compounds structurally related to deca-BDE, MNP spin trap agent and deuterated THF. ....	57
Table 4.1. Intensity and energy of artificial light sources and natural sunlight.....	111
Table 4.2. Molar absorptivities ( $\epsilon$ ) of deca-BDE, chlorpromazine, and triclosan indicate that they need to be tested for phototoxicity. ....	113
Table 4.3. IC50 values and phototoxicity parameters of chlorpromazine, triclosan and deca-BDE. ....	114

## LIST OF FIGURES

Figure 1.1. Chemical structure of polybrominated diphenyl ethers (PBDEs). .....	20
Figure 1.2. Chemical structure of triclosan.....	21
Figure 2.1. Irradiation spectra of natural solar light and the xenon lamp are similar.....	34
Figure 2.2. Absorption spectra of test compounds and solvents; transmittance (%) of cut-off filters. ....	36
Figure 2.3. Photodegradation of deca-BDE.....	38
Figure 2.4. Irradiation of deca-BDE produces free radicals as seen by EPR spin trapping with DMPO.....	40
Figure 2.5. Effective wavelength for radical formation.....	42
Figure 2.6. Free radical formation increases with time of light exposure and concentration of deca-BDE. ....	43
Figure 3.1. Absorption spectra of test compounds; transmittance (%) of cut-off filters.....	58
Figure 3.2. EPR spectra of structurally related compounds.....	59
Figure 3.3. Radical formation by structurally related compounds, relation to UV molar absorption coefficient ( $\epsilon$ ). ....	60
Figure 3.4. Computer simulations of EPR spectra of DMPO spin adducts in (A) THF with BHT alone, (B) with deca-BDE.....	61
Figure 3.5. Proposed mechanism of radical formation during irradiation of the deca-BDE in THF.....	62
Figure 3.6. EPR spectra produced by MNP adducts in (A) THF, (B) toluene. ....	63
Figure 3.7. Computer simulation of EPR spectra with MNP spin trap.....	64
Figure 3.8. Solvent effects on the radical formation of deca-BDE.....	65
Figure 4.1. Chemical structure of chlorpromazine. ....	90
Figure 4.2. Irradiation spectra of UV lamps and absorption spectrum of a plate lid.....	91
Figure 4.3. Spectral change of chlorpromazine after UV exposure.....	92
Figure 4.4. Spectral change of triclosan after UV exposure.....	93
Figure 4.5. Spectral change of deca-BDE after UV exposure. ....	94
Figure 4.6. UV energy dependent spectral changes of triclosan.....	95

Figure 4.7. Positive control for measurements of oxidative stress and viability. ....	96
Figure 4.8. Dose-response study of cytotoxicity of chlorpromazine and UV light on HaCaT. ....	97
Figure 4.9. Dose-response study of cytotoxicity of triclosan and UV light on HaCaT. ....	98
Figure 4.10. Dose-response study of cytotoxicity of deca-BDE and UV light on HaCaT. ....	99
Figure 4.11. Dose-response study of cytotoxicity of deca-BDE and UV light on HSF. ....	100
Figure 4.12. Toxicity of combined exposures of exponentially growing (OECD test) and confluent HaCaT cells to UVB-centered light and chlorpromazine. ....	101
Figure 4.13. Toxicity of combined exposures of exponentially growing (OECD test) and confluent HaCaT cells to UVB-centered light and triclosan. ....	102
Figure 4.14. Toxicity of combined exposures of exponentially growing (OECD test) and confluent HaCaT cells to UVB-centered light and deca-BDE. ....	103
Figure 4.15. Cytotoxicity of combined exposures of HSF to UV light and triclosan or deca-BDE. ....	104
Figure 4.16. Effects of pre-irradiated triclosan on growing HaCaT cells. ....	105
Figure 4.17. Effects of pre-irradiated deca-BDE on growing HaCaT cells. ....	106
Figure 4.18. Oxidative stress of triclosan and/or UVB-centered light in confluent HaCaT. ....	107
Figure 4.19. Oxidative stress of deca-BDE and/or UVB-centered light in confluent HaCaT cells. ....	109
Figure 4.20. Combined genotoxicity of deca-BDE + UV on HaCaT. ....	110

CHAPTER 1  
BACKGROUND INFORMATION ON  
POLYBROMINATED DIPHENYL ETHERS AND TRICLOSAN

Polybrominated Diphenyl Ethers

Production and Uses

Polybrominated diphenyl ethers (PBDEs) are a group of brominated organic compounds consisting of two phenyl rings and an ether bond between the two rings (Figure 1.1). PBDEs are synthesized by a reaction between bromine and diphenyl ether with an inorganic catalyst (ATSDR, 2004). The degree of bromination is determined by the amount of bromine and the reaction time and bromine is added to the molecular backbone in a stepwise manner generating lower to higher BDEs (US EPA, 2010). There are 209 congeners with different number and location of bromine atoms attached to the phenyl rings.

In 1871, the first two brominated diphenyl ethers (BDEs), a mono and a di-BDE were synthesized and a tetra-BDE was synthesized in 1910 (Vonderheide *et al.*, 2008). Three commercial mixtures were produced and used as penta-, octa-, and decabrominated diphenyl ether (BDE) mixtures, named in this way to indicate the average number of bromines on the diphenyl ether core structure. The congener profiles of the commercial mixtures are displayed in Table 1.1. In 1960, penta-BDE was patented as the first PBDE mixture to be used as a flame retardant and five years later, products including PBDEs began to be sold on the market (Vonderheide *et al.*, 2008). Brominated flame retardants (BFRs) such as PBDEs and polybrominated biphenyls (PBBs) were categorized as a class of flame retardants in 1978 and since then, PBDEs have been the major BFR in the production and uses (Vonderheide *et al.*, 2008).

Annual worldwide production of PBDEs was 40,000 metric tons (MT) in 1999, 67,000 MT in 2002 and about 56,000 MT in 2003 (US EPA, 2010). In 2001, deca-BDE

accounted for 83% of global production of PBDEs while 11% was penta-BDE and, 6% by octa-BDE (US EPA, 2010). The American continents consumed about 95% of the worldwide production of penta-BDE, 40% of octa-BDE, and 44% of deca-BDE (US EPA, 2010). Based upon reports of the Toxics Release Inventory (TRI), 32.2 MT of deca-BDE was released to the environment in 2007. The highest amount of released deca-BDE, 53.9 MT, was recorded in 1999 and this level of release was not significantly changed before releases decreased in 2003. After 2003, the level declined in 2005, 2006, and 2007, except for an increased release of 44.8 MT in 2004 (US EPA, 2010).

The mixtures are applied as flame retardant additives to a variety of products.

Lists of uses for specific commercial PBDE mixture are as follows:

#### Penta-BDE

- Flexible polyurethane foam (FPUF) in mattresses, home and automobile furniture
- Materials for packaging and carpet
- Textile fabrics used in upholstery for furniture and automobile seat covers
- Epoxy resins (EPs) used as protective coatings on circuit boards
- Unsaturated polyesters; paper laminates; flexible polyvinyl chloride used as electrical wire coatings; rubber; paints and lacquers; rigid polyurethane foam; and adhesives and automotive parts.

#### Octa-BDE

- Acrylonitrile Butadiene Styrene (ABS)-based plastics and high impact polystyrene (HIPS), polybutylene terephthalate (PBT), polyamide polymers, polycarbonate, nylon, polyolefin, and phenol-formaldehyde resins used in the cases of office equipment and PC.

### Deca-BDE

- HIPS-based plastics used in television housings and back panels, cases of audio and video equipment, mobile phones, remote controls, PCs, and PC monitors.
- The polyethylene (PE)-based plastics used in the insulation of wire and cables of electrical equipment.
- The polypropylene (PP)-based plastics used in communication cables, capacitor films, building, cables, pipes, stadium seats, lamp sockets and holders, and kitchen hoods.
- The PBT-based plastics used in connectors in electrical and electronic equipment.
- Unsaturated polyesters (UPE) used in building and construction materials as reinforced plastic panels.
- Nylon and the back coating of upholstery textiles used in sofas, chairs, and office furniture, electrical and electronic equipment, circuit breakers, and coils.

(This list was excerpted from (US EPA, 2010))

### Levels in the Environment and in Humans

PBDEs are used as additives, i.e. not covalently bound to the polymers, and therefore easily released from the consumer products into the air, water, food and house dust (D'Silva *et al.*, 2004). PBDEs are also structurally similar to the polyhalogenated biphenyls (PBBs and PCBs) and, like them are highly lipophilic and bioaccumulate. Therefore, they are a global environmental issue because of their ubiquitous presence in human blood, breast milk and tissues, in our indoor and outdoor environment, and in ecosystems (Tanabe *et al.*, 2008; Vonderheide *et al.*, 2008; Ward *et al.*, 2008).

### Biotic Environment and Food

In 1979, deca-BDE was first detected in the environment and in 1981, tetra to hexa-BDE congeners were found in fish with a maximum level of 27,000 ng g<sup>-1</sup> (Vonderheide *et al.*, 2008). In 1987, PBDEs were found in samples of sea birds living in the Arctic, the Baltic, and the North Sea, suggesting that PBDEs are distributed widely and an international environmental issue (Jansson *et al.*, 1987; Vonderheide *et al.*, 2008). Monitoring levels of halogenated organic compounds in birds is a good way to study distribution and uses of the chemicals in different locations (Chen and Hale, 2010). Higher levels of PBDEs in North American and Chinese birds are possibly connected to larger demand and human activities of penta-BDE and deca-BDE in the regions (Chen and Hale, 2010). Exposure studies of birds in nature and laboratory studies revealed that BDE-209 could be degraded to lower BDEs. Therefore, although BDE-209 is often considered to be less toxic than lower BDEs, to protect the environment and humans, production and uses of deca-BDE need to be controlled (Chen and Hale, 2010).

Studies of levels of persistent halogenated organic compounds in over 600 kinds of seafood items in South China, found PBDEs levels between non-detectable and 5.93 ng/g (Guo *et al.*, 2010). Using survey results for the same region, intake of PBDEs from seafood for persons of all ages were calculated to be 4.7–18.5 ng/day (0.27–0.46 ng/kg bw/day). It was suggested that seafood intake of PBDEs might not be significantly related to human health risk (Guo *et al.*, 2010). However, other routes of exposure may be of higher importance.

### Abiotic Environment

In Korean sediment samples, 29 PBDE congeners were found and among them BDE-209 was dominant (Hong *et al.*, 2010). While the average of the sum of PBDEs levels (5.7 ng/g dry weight) was lower than that of PCBs values (7.2 ng/g) in surface sediment samples, the average of the sum of PBDE levels (9.3 ng/g dry weight) was

higher than that of the levels of PCBs (4.6 ng/g dry weight) in core sediment samples. Overall, the temporal trend of the levels of PBDEs and PCBs in sediment core, indicated that PBDEs increase while PCBs decrease. Disposal of various types of waste was related to of the contamination of the environment with PBDE (Hong *et al.*, 2010).

Recent studies reported very high levels of PBDEs in indoor dust of US houses (8.2  $\mu\text{g/g}$ ) and houses and cars in Great Britain (260 and 340  $\mu\text{g/g}$  dust, respectively) (Lorber, 2007; Stuart *et al.*, 2008), with deca-BDE as the dominant congener. One study compared the PBDE levels in dust samples from homes to the levels in offices; median levels of the total of 8 PBDEs (BDE-47, 99, 100, 154, 153, 197, 196 and 203) and BDE-209 in offices were higher than in homes. For the total PBDEs, the levels in homes and offices were between 4 and 1,214  $\text{ng g}^{-1}$  dw (median 27) and 59 and 10,088 (median 138), respectively. BDE 209 levels in homes and offices ranged between  $<5$ – $5.30 \times 10^3$   $\text{ng g}^{-1}$  dw (median 313) and 69– $1.20 \times 10^4$   $\text{ng g}^{-1}$  dw (median 443), respectively (D'Hollander *et al.*, 2010). In one area near electronic waste storage places in Thailand, PBDE levels in outdoor air ranged from 8 to 150  $\text{pg m}^{-3}$ , while the indoor levels ranged from 46 to 350  $\text{pg m}^{-3}$  (Muenhor *et al.*, 2010). An occupational exposure model estimated that the exposure level of BDE-99 for the e-waste storage workers is beyond a U.S. EPA Health Based Limit Value for the congener calculated using inhalation and dust ingestion rates. BDE-209 exposure was lower than the reference dose of the US EPA.

Recent studies of PBDE levels and profiles of their congeners suggested that PBDEs are degraded by natural sunlight (Gevao *et al.*, 2010; Li *et al.*, 2010a). Organic films were placed on indoor and outdoor windows in South China and analyzed to study PBDE levels (Li *et al.*, 2010a). The highest value of BDE-209 was 4000  $\text{ng m}^{-2}$ . Generally, PBDE levels on the outdoor films were higher than indoor films and BDE-209 was the most dominant congener, indicating that the sources of PBDEs found in the study are outside of the buildings while other study reported that indoor levels of PBDEs are



higher than their outdoor levels (Muenhor *et al.*, 2010). While the organic films were growing, the PBDE levels on the films on the window did not increase accordingly, indicating that photodegradation of PBDEs may occur on the window surface. During and after a severe dust storm in Kuwait City, PBDE levels were measured over a five day period (Gevao *et al.*, 2010). Total PBDE concentrations were between 51 and  $1.31 \times 10^3$   $\text{pg m}^{-3}$  during the dust storm and the levels were down to 20-148  $\text{pg m}^{-3}$  for the next three days. The congener profile in the gas phase was inversely related to solar irradiation suggesting the occurrence of photodegradation of PBDEs in the gas phase.

### Human

There have been historical findings by which PBDEs have gained global attention as follows: PBDEs, with the maximum level of 1 ng/g, were detected in human adipose tissues (1990); a striking increase of PDBE levels was seen in Swedish breast milk (1998); the highest total PBDE concentration (9,630 ng/g) was reported in adipose tissue of a person living in New York (2005) (Vonderheide *et al.*, 2008). High levels of PBDEs were found in archived breast adipose tissues of Californian women, suggesting that large use of PBDEs in California is related to the high levels of PBDEs (Petreas *et al.*). Many recent studies also reported that various congeners of PBDEs remain in humans.

In breast milk samples for women in New Hampshire, the total PBDE concentrations were between 6.5 to 166.7 ng/g lipid, with a median of 29.7 ng/g (Dunn *et al.*, 2010). BDE-47 and BDE-153 were dominant congeners. BDE-153, age, postpartum saturated fat consumption, and the home model were positively correlated suggesting that dietary habit and living environment could affect levels of PBDEs. A study of PBDE levels in breast milk of Chinese women reported that average PBDE levels ranged from 3.42 ng/g fat to 4.16 ng/g fat (Sun *et al.*, 2010). The samples included deca, nona, octa, hexa, tetra, tri and di-BDE congeners. Total levels of PBDEs were not related to food consumption.

Serum samples were taken from police officers in Guinea-Bissau between 1990 and 2007 (Linderholm *et al.*, 2010). The levels of PBDEs detected in them were low. However, the temporal trend of BDE-153 was increasing, unlike the trends of other halogenated organic compounds like 1,1,1-trichloro-2,2-bis(4-chlorophenyl)ethane (4,4'-DDT) and PCBs.

From blood samples of fish consumers in the Great Lakes regions the levels of total PBDEs, BDE-47 and 99 increased from 1994/1995 to 2001/2003 and total PBDEs and BDE-99, 100, and 153 increased between 1994/1995 and 2004/2005. From 2001–2003 to 2004–2005, total PBDEs and levels of BDE congeners did not vary significantly (Vizcaino *et al.*). A Spanish study reported that in blood and cord blood serum samples from pregnant women and their babies, dominant PBDE congeners were BDE-47, 99, 153, 154 and 209 (Vizcaino *et al.*).

While PBDE levels on human skin have not yet been thoroughly investigated, a recent analysis found PBDE concentrations normalized to skin surface area in the range of 3 - 1970 pg/cm<sup>2</sup> (Stapleton *et al.*, 2008).

### Exposure Routes

PBDEs are transferred to humans via external and internal pathways such as breast milk and maternal blood to next generation (Frederiksen *et al.*, 2009). Dermal contact with dust may contribute more to the body burden of PBDEs than food intake and inhalation, which stands in contrast to other halogenated organic compounds (Lorber, 2007), although PBDEs could also be accumulated in fatty tissues because of their lipophilicity and persistence (Frederiksen *et al.*, 2009). According to the estimation of adult intakes of PBDE congeners by the US EPA, dust ingestion is the most dominant pathway accounting for 73% of the total estimated intake, while dust dermal contact is the second dominant pathway accounting for 17% (Table 1.2) (US EPA, 2010). Among the congeners, BDE 209 (deca-BDE) is the most dominant congener accounting for 28 %

of the total estimated intake. BDE 99 is the second dominant congener accounting for 27 % of the total estimated intake. For deca-BDE, dust ingestion (74 %) and dermal contact (18 %) are also the most dominant exposure pathways. Dust exposure of PBDEs is more critical for toddlers than adults (Frederiksen *et al.*, 2009).

Human exposure in North America has been generally reported to be higher than in European and Asian countries. It is not only due to the different food intakes, but also caused by higher uses of PBDEs following differing regulations for fire safety (Frederiksen *et al.*, 2009).

### Toxic Effects

Toxic effects of PBDEs including neurotoxicity, disruption of the homeostasis of hormones such as thyroid hormones and androgens, retarded menstrual period, carcinogenicity and the interactions of PBDEs with the aryl hydrocarbon receptor (AhR) as biomarkers have been observed (NTP (National Toxicology Program), 1986; Lorber, 2007; Fossi *et al.*, 2008; Vonderheide *et al.*, 2008; Ward *et al.*, 2008; Chao *et al.*, 2010; Christen *et al.*, 2010; Wahl *et al.*, 2010; Wang *et al.*, 2010; Yan *et al.*, 2010; Zhang *et al.*, 2010a; Zhang *et al.*, 2010b).

#### Neurotoxicity

BDE-209 interrupted the outgrowth of neurite and neural stem cells (NSCs). These did not differentiate normally into neurons, and the effects were dose-dependent, while BDE-209 stimulated NSCs to be differentiated into glial cells (Zhang *et al.*, 2010b). In rat primary hippocampal neurons, BDE-209 enhanced apoptosis, p38 MAPK expression, the calcium ion concentration, oxidative stress, and decreased the number of

viable cells. N-acetylcysteine (NAC) showed protective effects on cytotoxicity caused by BDE-209 (Zhang *et al.*, 2010a).

### Hormonal Interruption

Individuals living in the area near electronic waste recycling facilities, as well as workers at the facilities were investigated for relationships between levels of thyroid hormones (THs), thyrotropins (TSH) and BFR exposures (Wang *et al.*, 2010). For workers and residents in the area, the levels of Triiodothyronine (T<sub>3</sub>), free triiodothyronine (fT<sub>3</sub>) and thyroxine (fT<sub>4</sub>) were lower than the control group, though the thyroxine (T<sub>4</sub>) levels for both groups were not significantly different from the control group. The TSH levels (0.00-5.00  $\mu$ IU/mL with a mean 1.26  $\mu$ IU/mL) for the workers were lower than the control group (0.03-5.54  $\mu$ IU/mL with a mean 1.57  $\mu$ IU/mL). In addition, BDE-205 and 126 had a positive relation to the levels of T<sub>4</sub>.

Influences of PBDEs on the reproductive system were investigated by analyzing the relationships between PBDE levels in breast milk samples and menstrual cycle changes (Chao *et al.*, 2010). The average total PBDE level was 3.42 ng/g lipid. The levels of PBDEs were significantly correlated to the length of menstruation, irregular menstrual cycle, the age when regular menstruation began. With caution due to small sample size, it was suggested that higher brominated BDEs may extend the menstrual cycle on average and delay the time when the first regular menstrual cycle begins. In the MDA-kb2 cells, BDE-100 and BDE-155 stimulated androgenic activity via testosterone-dependent activation of gene expression, which responds to the androgen receptor (Christen *et al.*, 2010).

### Interactions with the AhR Receptor

In skin biopsies and fibroblasts of a Mediterranean cetacean, induction of CYP1A1 and CYP2B was detected by Western blot analysis (Fossi *et al.*, 2008). In zebrafish embryos, PBDEs interrupted the signaling process of AhR and caused malformations (Wahl *et al.*, 2010).

### Carcinogenicity

In 1986, a U.S. National Toxicology Program (NTP) study reported that PBDEs increased neoplastic nodes in the rat liver (NTP (National Toxicology Program), 1986). Based upon this finding, the U.S. EPA classified deca-BDE as a possible human carcinogen in 1995 (Vonderheide *et al.*, 2008).

### Other Effects

BDE-47 caused dose-dependent apoptosis of Jurkat cells, increased ROS formation and down-regulated MMP which are involved in mitochondrial functions (Yan *et al.*, 2010).

### Regulations

In 1989, production and use of deca-BDE voluntarily stopped in Germany (Vonderheide *et al.*, 2008). The penta and octa commercial PBDE mixtures were banned in Europe and voluntarily phased out of the U.S. market in 2004 (Vonderheide *et al.*, 2008). In 2006, the Canadian EPA listed deca-BDE as toxic substance and in 2007, deca-BDE uses in cables, furniture and textiles were prohibited in Sweden (BSEF, 2010). In 2008, the states of Maine and Washington began restriction of deca-BDE uses in

furniture and mattresses, and later Oregon and Vermont set up the regulations of deca-BDE (Vonderheide *et al.*, 2008; BSEF, 2010). In 2009, the U.S. EPA decided to stop production, sales, and import of deca-BDE in the U.S. for most uses by 2012 and for all uses by 2013 (US EPA, 2010).

In China and Korea, deca-BDE has been excluded from the lists of regulated chemicals for electric and electronic equipment uses and in Japan, the amount of production, uses, import and wastes of deca-BDE must be reported to the government (BSEF, 2010).

### Biological and Physicochemical Transformation

#### Biological Transformation

In fish plasma, OH-tetra-BDEs and OH-penta-BDEs were identified as products of fish metabolism and 4'-OH-BDE-49 and 4'-OH-BDE-101 were identified as metabolites of BDE-47 and BDE-99, respectively (Munschy *et al.*). OH-metabolites of PBDEs were also found in juvenile sole (Munschy *et al.*).

OH-octa-BDEs such as 6-OH-BDE196 and 6-OH-BDE199 and one OH-nona-BDE (OH-BDE206) were identified in human serum samples of residents in an e-waste facility in South China and all of the metabolites had *ortho*-hydroxy groups (Yu *et al.*, 2010). It was suggested that higher BDEs could be metabolized to OH-BDEs and the metabolites may persist in human blood (Yu *et al.*, 2010).

#### Physicochemical Transformation

PCBs and PBBs are known to undergo photolytic dehalogenation to lower halogenated biphenyls, and may form dibenzofurans, and other by-products from secondary and tertiary reactions (Robertson *et al.*, 1983; Bunce *et al.*, 1989; Miao *et al.*, 1999; Manzano *et al.*, 2004; von der Recke and Vetter, 2007). Similarly PBDEs in pure

solvents (acetonitrile, ethanol, methanol, hexane, THF, and toluene), aqueous solutions, mixtures like methanol/water, sediment and other media were shown to photolytically degrade to products that are more toxic and more bioavailable (Hua *et al.*, 2003; Rayne *et al.*, 2003; Bezares-Cruz *et al.*, 2004; Eriksson *et al.*, 2004b; Soderstrom *et al.*, 2004; Ahn *et al.*, 2006; Hagberg *et al.*, 2006a; Rayne *et al.*, 2006a). In these matrices, PBDEs absorbed UVC (250 - 280 nm), UVB (280 - 320 nm) and part of UVA (320 – 350 nm) from artificial UV light sources or natural solar light and degraded to lower BDEs and other compounds, including polybrominated dibenzofurans (PBDFs), brominated 2-hydroxybiphenyls and bromobenzene (Watanabe and Tatsukawa, 1987; Soderstrom *et al.*, 2004; Hagberg *et al.*, 2006a; Rayne *et al.*, 2006b). Using light intensities in the range of natural solar light, this required exposure times of only minutes to weeks. It has been hypothesized that free radical processes are involved in the photodegradation *via* light-induced homolytic breakage of aryl-Br and/or ether bonds of PBDEs, thereby generating aryl and bromine radicals (Watanabe and Tatsukawa, 1987; Rayne *et al.*, 2003; Rayne *et al.*, 2006a).

Recent studies reported that halogenated diphenyl ethers such as OH-PBDEs and triclosan [5-chloro-2-(2,4-dichlorophenoxy)phenol] are converted to dioxin compounds such as polybrominated dibenzo-p-dioxins (PBDDs) and polychlorinated dibenzo-p-dioxins (PCDDs) by solar or artificial UV light irradiation in aqueous environments (Sanchez-Prado *et al.*, 2006; Bastos *et al.*, 2009; Steen *et al.*, 2009).

### Triclosan

#### Production, Uses and Regulations

Triclosan, a.k.a. Irgasan, is a hydroxylated derivative of trichlorinated diphenyl ether (Figure 1.2) and synthesized by reaction between 2,4,4'-trichloro-2'-methoxydiphenyl ether and aluminum chloride under reflux in benzene (NICNAS, 2009). Triclosan is mainly used as an antibacterial agent and a bactericide whose mechanism of

action mechanism involves alteration of membrane function and interruption of bacterial enoyl-acyl carrier protein reductase (FDA, 2008). Triclosan has also been used as an antiplaque agent, material preservative, biocide and fungicide (FDA, 2008). The U.S. EPA and the U.S. Food and Drug Administration (FDA) are governmental bodies regulating triclosan (US EPA, 2008).

Triclosan is used in a variety of consumer products as follows:

#### Regulated by the FDA

- Personal hygiene items: facial tissues, hand soaps, toothpastes, deodorants, ; laundry items: detergent and fabric softeners; medical items: antiseptics and medical devices

#### Regulated by the EPA

- Biocide: bacteriostat, deodorizer, fungistat, and mildewstat
- Commercial, institutional and industrial premises and equipment: conveyor belts, dye bath vats, fire hoses, and ice makers; residential and public access premises: HVAC coils
- Material preservative: adhesives, fabrics, tents, mattresses, clothing, vinyl, shower curtains, plastics for toys and toothbrushes, polyethylene, polyurethane, polypropylene, floor wax emulsions, rubber, textiles, paints, insulation, sealants, refuse container liners, concrete mixtures, grouts, caulking compounds, brooms, mulch, awnings, toilet bowls, urinals, and garbage cans.

(List excerpted from (US EPA, 2008))

From 1976 to April 2008, over 2000 patents issued by the U. S. Patent and Trademark Office included contents related to triclosan (FDA, 2008). As of 2001 in the U.S., triclosan was used in all liquid antibacterial soaps and 16% of bar type antibacterial soaps (FDA, 2008).



Because triclosan is not related to direct food intake, a tolerance level or exemption has not been set up. Risk assessments for triclosan were conducted for the indirect food uses in/on adhesives, cutting boards, conveyor belts, counter top, ice maker, and paper (US EPA, 2008).

In 2008, the FDA recommended that further studies of dermal toxicity of triclosan such as animal studies of skin carcinogenesis and phototoxicity need be performed to have proper dermal toxicity data (FDA, 2008). Currently, the FDA is in the process of a scientific and regulatory review of triclosan for products regulated by FDA (FDA, 2010) and the EPA is also joining their studies to evaluate endocrine effects of triclosan (EPA, 2010).

#### Levels and Exposure Routes

The National Report on Human Exposure to Environmental Chemicals from the Center for Disease Control and Prevention (CDC) indicated that average levels of triclosan in human urine have increased by approximately 40 % from 13.0 µg/L (2003-2004) to 18.5 µg/L (2005-2006) (CDC, 2009).

Principle exposure routes of triclosan include dermal contact with consumer products, ingestion of personal hygiene items, such as mouth washes, toothpastes, and dentifrices, intakes of food and drinking water contaminated with triclosan, and inhalation (FDA, 2008). From 1981 to 1983, the National Institute for Occupational Safety and Health (NIOSH) conducted The National Occupational Exposure Survey (NOES) and reported that workers potentially exposed to triclosan numbered over 180,000 (FDA, 2008). According to the “U. S. Geological Survey Triclosan” (1999-2000), triclosan was listed as one of the 7 major organic pollutants in wastewater (FDA, 2008). The maximum level of triclosan in lakes and a river in Switzerland was 74 ng/L and in wastewater treatment facilities in the U.S., Denmark, Sweden, and Switzerland,

triclosan levels were between 0.1 and 16.6 µg/L in the influent with levels in the effluent of 0.1-2.7 µg/L and levels in the sludge between 0.028 and 15.6 µg/L (FDA, 2008).

According to a Chinese study of triclosan in bottled and tap water, 18 out of 21 bottled water samples contained triclosan with the range of concentrations of 0.6 to 9.7 ng/L (Li *et al.*, 2010b). In the same study, the highest levels of triclosan in tap water was 14.5 ng/L and it was estimated that daily intakes of triclosan for adults was 10 ng/day and for infants 5 ng/day (Li *et al.*, 2010b).

## Toxic Effects

### Acute Toxicity

According to a report, triclosan has a relatively low level of acute toxicity (LD50 >5000 mg/kg bw) by oral exposure, and in a rat study, there was no indication of toxicity with a 4 h exposure to 0.15 mg triclosan/L aerosol and the LC50 was higher than the maximum dose (NICNAS, 2009). In an inhalation toxicity test of triclosan in rats with a repeat dose, LC50 was estimated as <1300 mg/m<sup>3</sup> and for dermal exposure only, low acute toxicity was suggested with an LD50 higher than >9300 mg/kg bw while acute toxicity could be increased by IV injection (NICNAS, 2009).

### Irritation and Sensitization

In rabbits, irritation of skin and eye by triclosan was reported, and, in rats, triclosan irritated the respiratory tract (NICNAS, 2009). The skin sensitisation potential of triclosan was reported to be very weak based upon guinea-pig studies (NICNAS, 2009).

### Repeat Dose Toxicity

In a study of 21-day inhalation exposures of rats, systemic toxicity was indicated at 1300 mg/m<sup>3</sup> with clinical signs and death, and a No Observed Adverse Effect Concentration (NOAEC) was estimated as 0.05 mg/L (NICNAS, 2009). A No Observed Adverse Effect Level (NOAEL) of 40 mg/kg bw/day was determined for male rats, and a NOAEL of 56 mg/kg bw day was calculated for female rats in a carcinogenicity study with changes in clinical chemistry and histopathology of the liver for males, and loss of body weight gain for females (NICNAS, 2009). For local effects of irritation in a study of 14-day exposure of male and female rats, a NOAEL of 7.5 and 3.5 mg/kg bw/day respectively was obtained, and there was no systemic toxicity though in 14-day mouse studies. Histological changes in the mouse liver were found and NOAEL values in males and females were determined at 20 and 24 mg/kg bw/day, respectively (NICNAS, 2009).

### Genotoxicity

Though there is a small scale study indicating a weak positive genotoxic effect in bacteria with a very high dose, most studies of bacterial genotoxicity reported negative results, and no evidence of mutagenesis in fungi or mammalian cells was found (NICNAS, 2009). For chromosome aberration, positive and negative results were mixed, while all of Unscheduled DNA Synthesis (UDS) assays showed negative results (NICNAS, 2009). Therefore, *in vitro* studies indicate no significant genotoxicity (NICNAS, 2009). From *in vivo* studies, there was no strong indication of genotoxicity either, possibly because of limitation of the methods (NICNAS, 2009).

### Carcinogenicity

Animal studies of carcinogenicity using rat or hamster did not indicate carcinogenicity (NICNAS, 2009).

### Reproductive and Developmental Toxicity

There was no clear indication of fertility toxicity from a two-generation dietary study and repeat dose studies for longer than 90 days with investigation of the reproductive organs in the rat (NICNAS, 2009). Developmental effects were not found in a rat and rabbit study, no postnatal developmental toxicity was shown either and for both developmental and maternal toxic effect, the NOAEL was set at 50 mg/kg bw/day (NICNAS, 2009).

### Bacterial Resistance

Though several mechanisms for bacterial resistance to triclosan have been suggested in mostly laboratory studies, investigations of clinical samples indicate that uses of biocides including triclosan may not cause antibiotic bacterial resistance (NICNAS, 2009).

### Ecotoxicity

Triclosan was tested for its toxicity on biofilm algae and bacteria in laboratory channels and increased death rate of bacteria with a No Effect Concentration (NEC) of  $0.21 \mu\text{g L}^{-1}$ , a level of triclosan within the range of concentrations which were found in river and wastewater ( $0.027\text{--}2.7 \mu\text{g L}^{-1}$ ) (Ricart *et al.*, 2010). Triclosan was more toxic to bacteria than algae, and photosynthesis was interrupted with an NEC of  $0.42 \mu\text{g L}^{-1}$  and diatom cell viability was changed with concentrations of triclosan (Ricart *et al.*, 2010).

## Physicochemical transformation

### Photolytic Transformation

Triclosan is converted to potential toxicants like PCDDs and halogenated phenol compounds by solar or artificial UV light irradiation in aqueous environments (Sanchez-Prado *et al.*, 2006).

In the process of waste water treatment, transformations of triclosan such as chemical oxidation by free chlorine, ozonation and UV photolysis with a catalyst like

TiO<sub>2</sub> have been used, and unfavorable byproducts including halogenated phenols, trihalomethanes (THMs), chloroform, DCDD were generated (Bokare *et al.*, 2010)

### Outline of Thesis

UV irradiation of patients treated with potassium bromide resulted in severe skin ulceration and necrosis, suggesting that UV irradiation of a bromide produces a bromine radical which can damage the skin tissue (Diener *et al.*, 1998). Linemen and cable splicers, typical outdoor occupations, had significantly higher risk for melanoma after long term dermal exposure to PCBs (Loomis *et al.*, 1997). These observations suggest potentiated toxicity (synergism) by co-exposure to UV light and halogenated compounds, most likely due to radical formation, which could also play a role for triclosan and PBDEs.

**The overall hypothesis for the thesis is that photolysis of halogenated diphenyl ethers and their hydroxylated derivatives generates free radicals and degradation products which cause toxic effects including cytotoxicity, growth inhibition, oxidative stress and genotoxicity on skin.**

Chapter 2 describes the findings from studies of photo reactivity and radical formation potential of deca-BDE in the presence of light. The findings include the photo reactivity of deca-BDE, free radical generation during the photolytic degradation of deca-BDE in various organic solvents, wavelength-dependent radical formation of deca-BDE for UVB and UVA, relationships among radical formation and irradiation time and deca-BDE concentration.

The next chapter describes studies of mechanisms of the radical formation of deca-BDE in the presence of light as follows: structure-activity relationships between

radical yield and structurally related compounds, such as deca-BDE, octa-BDE, PBB 209, PCB 209 and DE; importance of debromination paired with hydrogen abstraction from the solvents in the radical formation.

Chapter 4 includes studies of biological effects of deca-BDE/triclosan, light, and the combination of both, in human skin cells. It is suggested that repeated UV irradiation and deca-BDE exposures cause synergistic cytotoxic effects in skin cells. Tests following OECD guidelines are also described to see the phototoxic potential of deca-BDE and triclosan. UV irradiation of triclosan causes a synergistic increase in oxidative stress at higher concentrations of triclosan in skin cells. UV irradiation of deca-BDE could cause more genotoxic effects than the expected additive effect on skin cells though the genotoxicity test needs to be confirmed.

These findings suggest that deca-BDE is photolytically active and generates free radicals by UV irradiation and deca-BDE and triclosan may have weak phototoxic potential in human skin cells. The toxicological mechanism is related to oxidative stress and possibly genotoxicity.

Figure 1.1. Chemical structure of polybrominated diphenyl ethers (PBDEs).

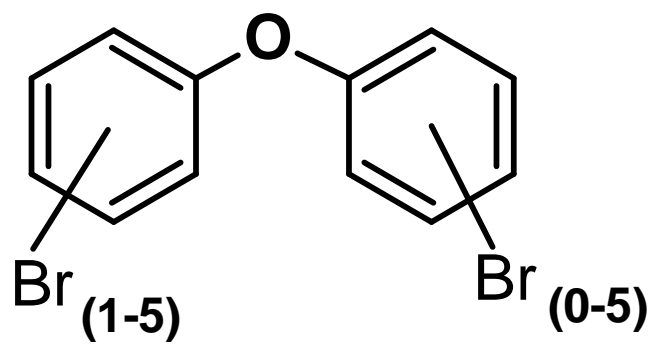
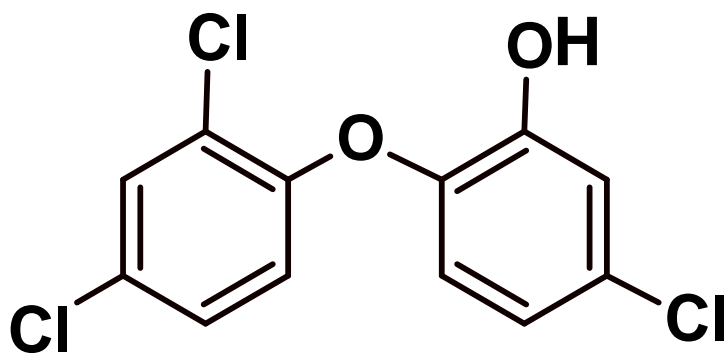


Figure 1.2. Chemical structure of triclosan.





**Table 1.1. Profiles of congeners (mass %) in commercial PBDE mixtures.**

<b>PBDE Congeners</b>	<b>Commercial PBDE mixtures</b>		
	<b>Penta</b>	<b>Octa</b>	<b>Deca</b>
<b>Tri-BDEs</b>	0-1		0.00001
<b>Tetra-BDEs</b>	24-38		
<b>Penta-BDEs</b>	50-62		0.002
<b>Hexa-BDEs</b>	4-12	10-12	0.001
<b>Hepta-BDEs</b>		43-58	0.003
<b>Octa-BDEs</b>		26-35	
<b>Nona-BDEs</b>		8-14	2.5
<b>Deca-BDE (BDE 209)</b>		0-3	97.5

Source: US EPA (2010). An exposure assessment of polybrominated diphenyl ethers. (NCEA, Ed.). National Technical Information Service, Springfield, VA, Washington, DC.

**Table 1.2. Estimated human adult intakes of PBDEs (exposures in units of ng/day).**

<b>Exposure routes</b>	<b>Tri-BDEs</b>	<b>Tetra-BDEs</b>	<b>Penta-BDEs</b>	<b>Hexa-BDEs</b>	<b>Hepta-BDEs</b>	<b>Octa-BDE</b>	<b>Nona-BDE</b>	<b>Deca-BDE</b>	<b>Total (%)</b>
<b>House dust ingestion</b>	0.00	82.2	147	25.5	2.86	0.08	0.01	105	363 (73)
<b>House dust dermal contact</b>	0.00	19.7	35.3	6.11	0.69	0.02	0.00	25.2	87.0 (17)
<b>Inhalation</b>	0.42	2.20	1.25	0.15	0.00	0.00	0.00	1.45	5.47 (1)
<b>Water/Food ingestion</b>	0.25	19.0	12.4	1.18	0.65	0.25	0.51	10.8	45.0 (9)
<b>Total</b>	0.67	123	196	32.9	4.20	0.35	0.52	142	500 (100)

Source: US EPA (2010). An exposure assessment of polybrominated diphenyl ethers. (NCEA, Ed.). National Technical Information Service, Springfield, VA, Washington, DC.

BDE congeners included for the data are as followings: BDE 17 and 28 (tri-BDEs); BDE 47 and 66 (tetra); BDE 85, 99 and 100 (penta); BDE 138, 153 and 154 (hexa); BDE 183 (hepta); BDE 197 (octa); BDE 206 (nona); BDE 209 (deca).

## CHAPTER 2

### PHOTOACTIVITY AND RADICAL FORMATION POTENTIAL OF DECA-BDE IN THE PRESENCE OF LIGHT

#### Introduction

Halogenated hydrocarbons such as PCBs and PBBs, which are structurally related to PBDEs, have been known to undergo photolytic dehalogenation to lower halogenated biphenyls, and may form dibenzofurans, and other by-products from secondary and tertiary reactions (Robertson *et al.*, 1983; Bunce *et al.*, 1989; Miao *et al.*, 1999; Manzano *et al.*, 2004; von der Recke and Vetter, 2007). PBDEs have also been known to be photolytically degraded producing degradation products (Hua *et al.*, 2003; Rayne *et al.*, 2003; Bezares-Cruz *et al.*, 2004; Eriksson *et al.*, 2004a; Söderström *et al.*, 2004; Ahn *et al.*, 2006; Hagberg *et al.*, 2006c; Rayne *et al.*, 2006a) and, during the degradation process, the formation of free radicals has been suggested (Watanabe and Tatsukawa, 1987; Rayne *et al.*, 2003; Rayne *et al.*, 2006a).

#### Literature Review

PBDEs in pure solvents (acetonitrile, ethanol, methanol, hexane, THF, and toluene), aqueous solutions, mixtures like methanol/water, sediment and other media were shown to photolytically degrade to products that are more toxic and more bioavailable (Hua *et al.*, 2003; Rayne *et al.*, 2003; Bezares-Cruz *et al.*, 2004; Eriksson *et al.*, 2004a; Söderström *et al.*, 2004; Ahn *et al.*, 2006; Hagberg *et al.*, 2006c; Rayne *et al.*, 2006a). In these matrices, PBDEs absorbed UVC (250 - 280 nm), UVB (280 - 320 nm) and part of UVA (320 – 350 nm) from artificial UV light sources or natural solar light and degraded to lower BDEs and other compounds, including polybrominated dibenzofurans (PBDFs), brominated 2-hydroxybiphenyls and bromobenzene (Watanabe and Tatsukawa, 1987; Söderström *et al.*, 2004; Hagberg *et al.*, 2006c; Rayne *et al.*, 2006b). Using light intensities in the range of natural solar light, this required exposure

times of only minutes to weeks. It has been hypothesized that free radical processes are involved in the photodegradation *via* light-induced homolytic breakage of aryl-Br and/or ether bonds of PBDEs, thereby generating aryl and bromine radicals (Watanabe and Tatsukawa, 1987; Rayne *et al.*, 2003; Rayne *et al.*, 2006a).

### Research Hypothesis

Our research hypothesis is that free radicals are generated by UV irradiation of deca-BDE during its photodegradation.

### Materials and Methods

#### Experimental Design

First of all, the absorption spectra of deca-BDE and solvents were measured to choose the proper range of wavelengths of light and cutoff filters for efficient irradiation. Photoreactivity of deca-BDE and functionality of the irradiation system was tested by identification of photodegradation products using GC-MS. In three different organic solvents, EPR studies were conducted to examine the potential of radical formation from irradiation of deca-BDE and any solvent effects on it. An EPR study was conducted with different cutoff filters to find the most active wavelength for the free radical formation. Dose-dependent studies were performed to find influential factors on the free radical formation.

#### Materials

The commercial deca-BDE mixture DE-83R (>98% BDE-209) was a gift from Great Lakes Chemical Co. (West Lafayette, U.S.A.). In this thesis, the term deca-BDE indicates DE-83R and BDE-209 indicates the deca-BDE congener. 5,5-Dimethylpyrrolone-N-oxide (DMPO) was from Dojindo (Gaithersburg, MD). Tetrahydrofuran (THF) with butylated hydroxytoluene (BHT) and dimethylformide (DMF) were from Acros (New Jersey, U.S.A.). THF without BHT, and toluene were

from Burdick & Jackson (Muskegon, MI, U.S.A.). THF was selected as a solvent because it has been used in previous photodegradation studies of PBDEs due to its very good solvent activity compared to other solvents and known to be a good hydrogen donor, which facilitates debromination of PBDEs (Eriksson *et al.*, 2004b). DMF and toluene were included as solvents for deca-BDE to study solvent effects on the radical formation. The structures of chemicals are depicted in Tables 2-1.

## Methods

### UV-VIS Spectroscopy

Absorption spectra were measured using a Perkin-Elmer Lambda 650 UV/Vis spectrophotometer at room temperature and a standard 1 cm quartz cuvette (Cat. No. 3-Q-10, Atascadero, CA).

### Irradiation

A 150 W Photomax xenon arc lamp (Oriel, Stratford, CT) was used to irradiate the samples. The power of the lamp was set at 30 W. The irradiation spectrum of the lamp was similar to that of natural solar light (Figure 2.1). All samples were irradiated at room temperature for 14 min in mixtures and with DMPO, unless otherwise indicated. A 309 nm (WG 305), 280 nm (WG 280), or 400 nm (BG 12) cutoff filter (cutting off the shorter wavelengths; specification 50% transmittance at 309, 280, or 400 nm and less than 1% transmittance at below 291, 260, and 387 nm respectively) from Schott (Duryea, PA) was inserted into the lamp to minimize the photodegradation of spin traps and solvents at shorter wavelengths. Widths of EPR spectra from preliminary experiments were too broad and it was speculated that small peaks could be overlapping with each other and undistinguishable from each other. Since oxygen broadens the EPR lines, thus lowering the resolution, the samples were bubbled with argon to partially remove oxygen and then transferred to a flat quartz cell. By reducing the amount of oxygen in samples,

EPR spectra became sharper and previously hidden peaks could be observed. The path length for UV irradiation of the flat quartz cell was 0.3 mm. The cell was placed into the TM cavity, and the sample was irradiated (xenon lamp at ~50 cm distance) while in the EPR cavity. For photodegradation studies, samples in a standard 1 cm quartz cuvette were exposed to light from the xenon lamp with a 309 nm cutoff filter. An IL1400 BL radiometer with a UV GAL.NIT detector from International Light Inc. (Peabody, MA) was used to measure the intensity of UVB and UVA light. The light intensity was 2.3 and 3.5 mW/cm<sup>2</sup> with the 309 and 280 nm filters, respectively, for both the EPR and cuvette photodegradation studies. The intensity of light through each filter was in the range of natural solar UV light (Godar, 2006; Svobodova *et al.*, 2006).

#### GC-MS

Hexachlorobenzene (Accustandard Inc.) was used as an internal standard (ISTD). To 100 µL samples, 50 µL ISTD was added, agitated thoroughly and run. To 150 µL method blank, 50 µL ISTD was added and corrected for concentration. A combined single point calibrator included DE-83R (Great Lakes Chemical Co.), BDE-203 and BDE-206 standards (Wellington Laboratories, Guelph, Ontario, Canada). To 150 µL combined single-point calibrator, 50 µL ISTD was added and corrected for concentration.

An Agilent 6890 gas chromatograph with 5975 mass spectrometer (Palo Alto, CA, USA) was used with a J&W DB5-MS (or Restek Rtx-5MS w/Integra Guard) column, 30 m, 0.25 mm bore, 0.25 µm film thickness, 1.1 mL/min constant He flow. The oven ramp was 100 (or 90)°C initial for 0.5 (or 0.7) min, 20°C/min to 300 (or 320)°C and held for 45 (or 33) min. The volume of an injection was 20 µL. The temperature of the split-splitless inlet was 290°C. The GC was operated in the ramped flow mode: initial flow 1.1 mL/min for 10 m, 1 mL/min to 2.1 mL/min for 40 min, 1 mL/min to 1.1 mL/min. The transfer line temperature was kept at 290°C. The ion source of the mass spectrometer was EI. The ion source temperature was held at 230°C and the quad

temperature was 150°C. Autotune was performed and used in methods. The solvent delay was set at 7 min. For semi-quant studies, the selected ion mode (SIM) was used with parameters: group 1 (7 - 10 min, ions 284, 79 dwell 100 ms), group 2 (10 - 20.5 min, ions 79, 321, 641, 801 dwell 50 ms), group 3 (20.5 - 29 min, ions 79, 360, 719, 879 dwell 50 ms), and group 4 (29 - 45.2 min, ions 79, 400, 799, 959 dwell 50 ms). For qualitative studies, the full scan mode was used and the scan range of m/z was 50 - 1050 daltons. The combined single point calibrator was used for identification and quantification. Relative response factors of DE-83R, BDE-206 and BDE-203 were used for calculation of concentration of deca-BDE, nona- and octa-BDE congeners, respectively.

### EPR

A Bruker EMX EPR spectrometer (Karlsruhe, Germany) equipped with a 4103TM cavity was used. Typical instrument settings were: microwave frequency, 9.8 GHz (X-band); microwave power, 20 mW; modulation amplitude, 1.0 G; time constant, 0.2 s; scan rate, 80 G/84 s; receiver gain,  $2 \times 10^2$  -  $3 \times 10^4$ . Test compounds were dissolved in the appropriate solvent. Spin traps were added to obtain a final concentration of 25 mM DMPO (from a 1 M aqueous stock). Estimates of absolute concentrations of spin adduct were accomplished by double integration of spectra and comparison to a standard of 3-carboxyproxyl (3-CxP) using the same instrument settings and physical setup (Venkataraman *et al.*, 2000). Simulation of EPR data was accomplished using WinSim software (NIEHS) and Bruker WinEPR (Karlsruhe, Germany). The Spin Trap Database (NIEHS) was referred to interpret and simulate EPR spectra (Li *et al.*, 1988). Simulated spectra correlated well with corresponding experimental spectra (correlation coefficient >0.99).

## Results and Discussion

### Absorption Spectra

Deca-BDE absorbs readily in the wavelength range passed by a 309 nm filter, but there is no absorbance above ~350 nm (Figure 2.2). THF, DMF, toluene, and DMPO ( $\epsilon_{228} = 7.8 \times 10^3 \text{ M}^{-1} \text{ cm}^{-1}$ ) (Buettner, 1990) do not absorb significantly in this range (Figure 2.2). The irradiation spectrum of the light from the xenon lamp covers the absorption spectrum of deca-BDE while the UV absorption of the solvents and spin trap is limited (Figure 2.1 and 2.2). Therefore, the range of the irradiation of the light source is proper for possible photoreaction of deca-BDE.

### Photodegradation of Deca-BDE

#### with Lower-BDE Formation

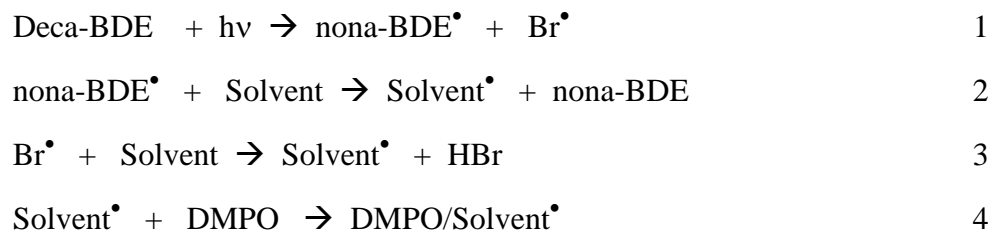
When 0.5 mM deca-BDE in toluene was exposed to UV light (1 cm quartz cuvette with a 309 nm cutoff filter) a loss of BDE-209 was observed with a concomitant formation of degradation products (Figure 2.3). This loss of BDE-209 and formation of photoproducts increased with time of exposure. Three nona-BDE congeners (BDE-206, 207, and 208) and an octa-BDE congener (BDE-203) were identified with GC-MS data of the calibration standards for nona-BDE (BDE-206) and octa-BDE (BDE-203). In details, five peaks were observed in the range of the retention time for group 2 and four of them were matched with the fragmented  $m/z$  data of BDE-203 indicating that those four peaks were signals of octa-BDE congeners and the retention time and MS data for one peak was same as the data for the BDE-203 standard and it was identified as BDE-203. Three peaks were observed in the range of the retention time for group 3 and the MS data for all of them were matched with the fragmented  $m/z$  data of BDE-206 indicating that those three peaks were signals of nona-BDE congeners and the retention time and MS data for one peak was the same as the date for the BDE-206 standard and it was identified as BDE-206. One peak was the same as the GC-MS data for the DE-83R



standard and it was identified as BDE-209. The lag-time required before the octa-BDE congeners appear suggests that these degradation products were derived from the newly formed nona-BDE congeners. This is in agreement with previous reports (Bezares-Cruz *et al.*, 2004; Eriksson *et al.*, 2004b; Soderstrom *et al.*, 2004; Ahn *et al.*, 2006). One unknown peak close to the octa-BDE congeners was observed (Figure 2.3-B), probably a hexabromodibenzofuran (hexa-BDF) congener considering its retention time and mass data.

#### Radical Formation from Irradiation of Deca-BDE

EPR spin trapping experiments with DMPO demonstrate that high levels of free radicals are produced during irradiation of deca-BDE (Figure 2.4). Irradiation of solvent alone produces much weaker background EPR signals (Figure 2.4 spectra B and C of each panel). The radical yields from deca-BDE in THF, DMF, and toluene were about 9-, 4-, and 7-fold higher than from solvent alone, respectively, indicating that deca-BDE is directly involved in increased radical formation. Previous studies have suggested that the hydrogen-donating ability of a solvent significantly affects the rate of photodegradation of PBDE (Rayne *et al.*, 2003). This is in agreement with our observation that THF, which is a good hydrogen-donor, facilitates the spin adduct formation more than the other solvents. The EPR spectra of the DMPO spin adducts formed during deca-BDE irradiation show different spectral features in each of the three organic solvents used (THF, Figure 2.4 A-a; DMF, B-a; toluene, C-a). This suggests that the different spin adducts arise because of the different solvents, not from the BDE. The concentrations of deca-BDE used were 2 mM in THF and DMF, and 1 mM in toluene while the concentration of solvent is  $\approx 10$  M and that of DMPO only 25 mM. Thus, oxidants produced by the interaction of BDE and light will kinetically have the highest probability of reacting with solvent; the resulting solvent-derived radicals will in turn be trapped by DMPO. A general mechanism in agreement with these observations is:



### Wavelength Dependency of the Radical Formation

When a 400 nm cut-off filter is used, only a very weak solvent radical spectrum is observed (Figure 2.5). Deca-BDE absorbs readily in the wavelength range passed by a 309 nm filter, but there is no absorbance above ~350 nm (Figure 2.2). THF, DMF, toluene, and DMPO ( $\epsilon_{228} = 7.8 \times 10^3 \text{ M}^{-1} \text{ cm}^{-1}$ ) (Buettner, 1990) do not absorb significantly in this range. Thus, the activating wavelength for radical formation from deca-BDE is in the UVA (400-320 nm) to UVB (320-280 nm) range.

### Radical Formation Changes by

#### Deca-BDE Concentration and Irradiation Time

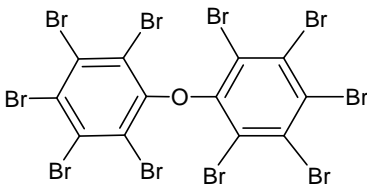
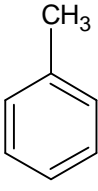
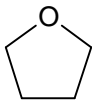
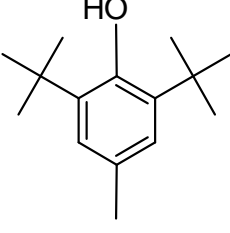
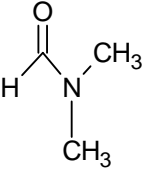
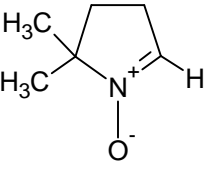
The total amount of spin adducts formed increased with irradiation time (309 nm cut-off) for all solvents (Figure 2.6 A) and with concentration of deca-BDE in THF and DMF (Figure 2.6 B). With either increase in time-of-exposure or concentration of deca-BDE an apparent steady-state level of spin adducts is approached or attained, consistent with both formation and expected loss of spin adduct. The solvent-only derived spin adduct barely changed with exposure time (data not shown). Thus, deca-BDE presence was essential for strong spin adduct generation.

### Conclusions

Our data from UV spectroscopy confirmed that deca-BDE in our solvent systems absorbs UVB and UVA light which are biologically relevant. GC-MS study showed that with increasing UV dose, deca-BDE is degraded to lower-BDEs such as three nona-BDE congeners (BDE-206, 207 and 208), one identified octa-BDE (BDE 203) and three

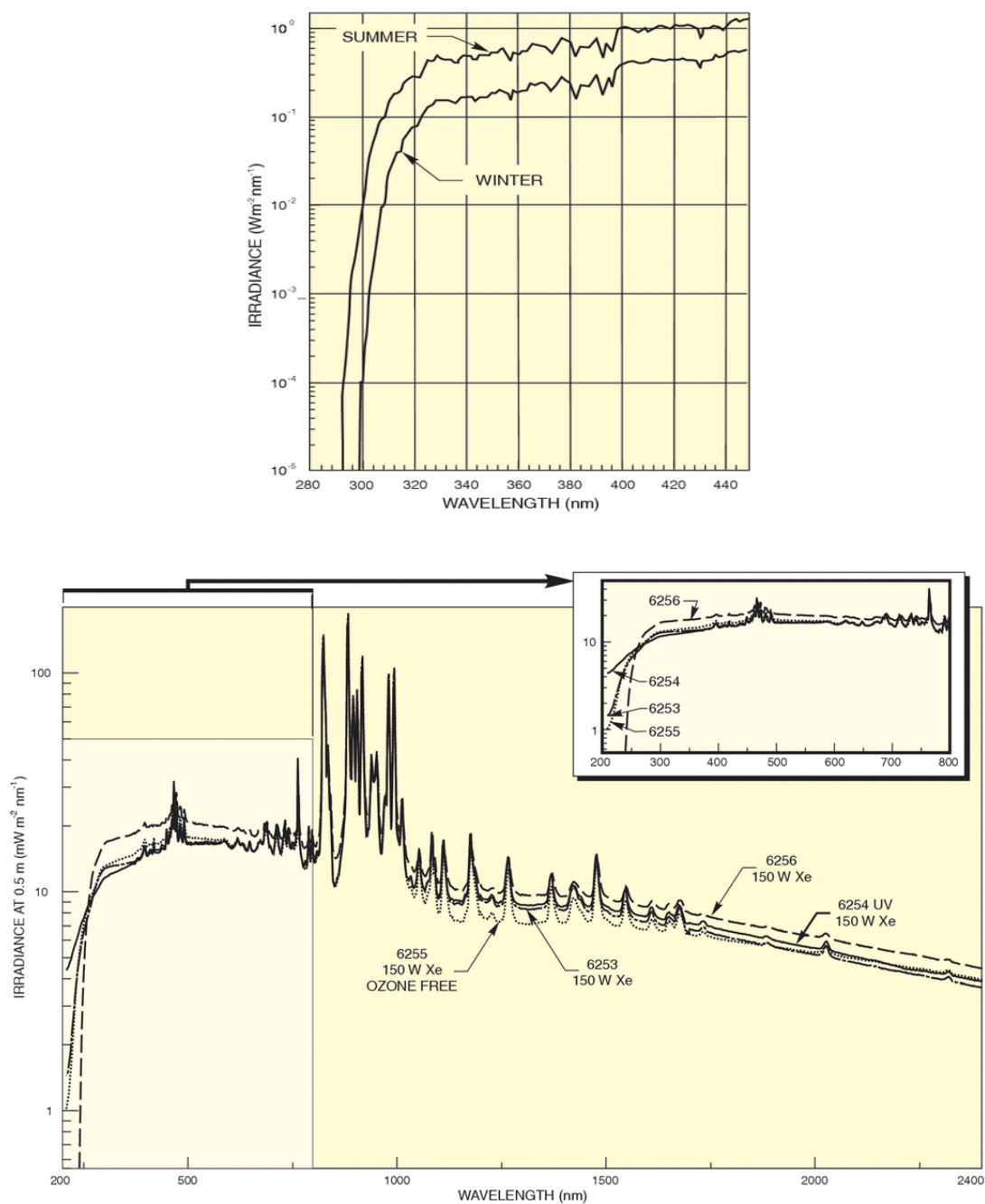
unidentified four octa-BDE congeners and one tentatively identified hexa-BDE. EPR study with DMPO spin trap revealed that the free radicals are produced by deca-BDE in the presence of light whose wavelengths are in the range of UVB and UVA. The irradiation time and deca-BDE concentration were positively related to the free radical formation, suggesting that they are main factors dominating the free radical formation.

**Table 2.1. Molecular structures of deca-BDE and organic solvents.**

Name	Molecular structure	Name	Molecular structure
Deca-BDE (De-83R) <sup>1</sup>		Toluene	
THF		BHT	
DMF		DMPO	

<sup>1</sup> The deca-BDE used in this study is the commercial mixture DE-83R, which contains >98% decabromodiphenyl ether.

**Figure 2.1.** Irradiation spectra of natural solar light and the xenon lamp are similar.



**Top:** Irradiation spectra of natural solar light.

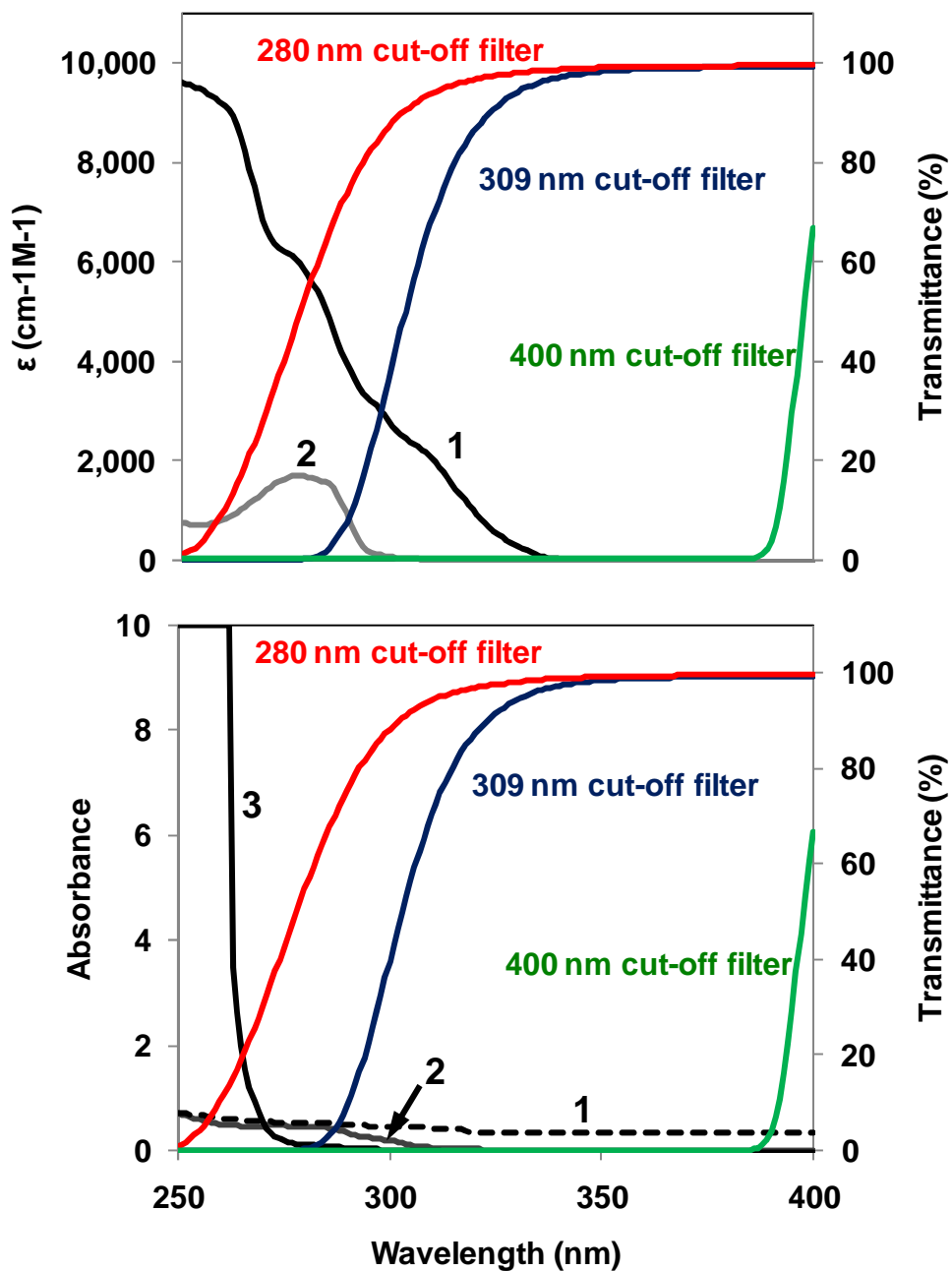
Figure 2.1 continued, above the footnote, p.34.

Source: “Photochemistry and Photobiology”  
(<http://www.newport.com/store/genContent.aspx/Photochemistry-and-Photobiology/412053/103>) and edited.

**Bottom**: Irradiation spectra of the xenon lamp (6256 150W Xe).

Source: A catalogue of Oriel (Oriel, Stratford, CT).

Figure 2.2. Absorption spectra of test compounds and solvents; transmittance (%) of cut-off filters.



**Top:** 1. deca-BDE (DE-83R); 2. BHT. All compounds were dissolved in THF without BHT.

**Bottom:** 1. Toluene; 2. THF, 3. DMF. All solvents were neat. DMPO has an absorption peak at  $\approx 230$  nm (Hall *et al.*, 1991).

Figure 2.2 continued, above the footnote, p.36.

Source: Data provided from Schott (Duryea, PA, USA; “Optical Glass Filters Datasheets, calculation prog.”

([http://www.us.schott.com/advanced\\_optics/english/download/optical\\_filters\\_download\\_vers.zip?](http://www.us.schott.com/advanced_optics/english/download/optical_filters_download_vers.zip?)) were used to draw the transmission curves for the cut-off filters.



Figure 2.3. Photodegradation of deca-BDE.

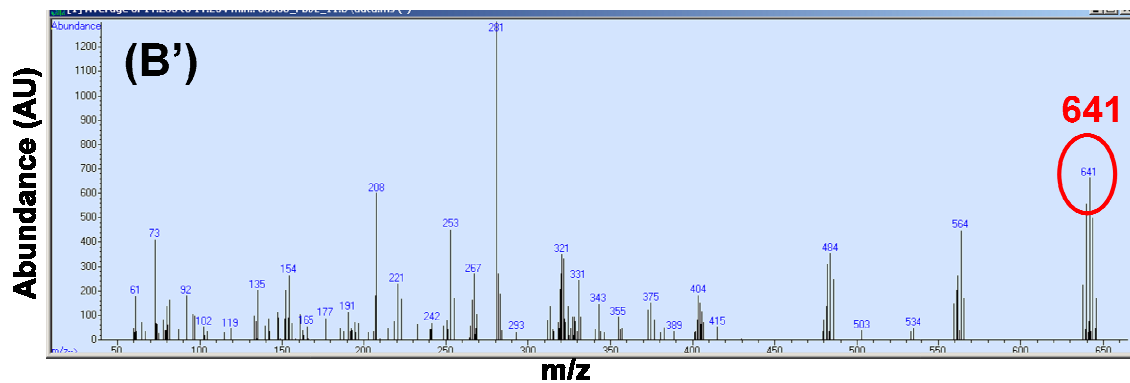
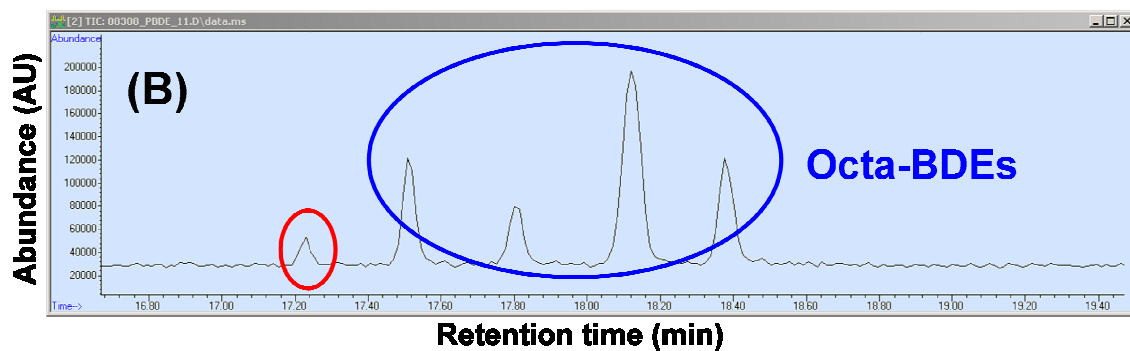
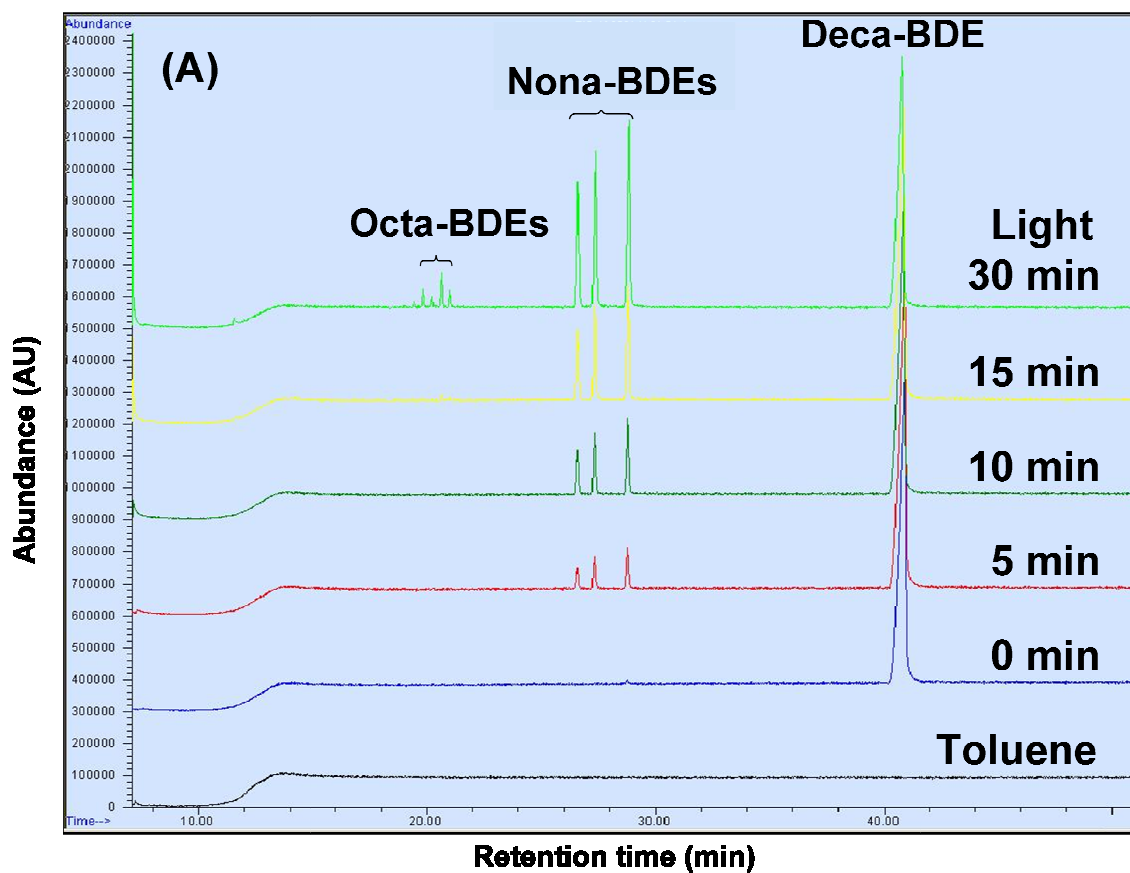


Figure 2.3 continued, above the Figure material, p.38.

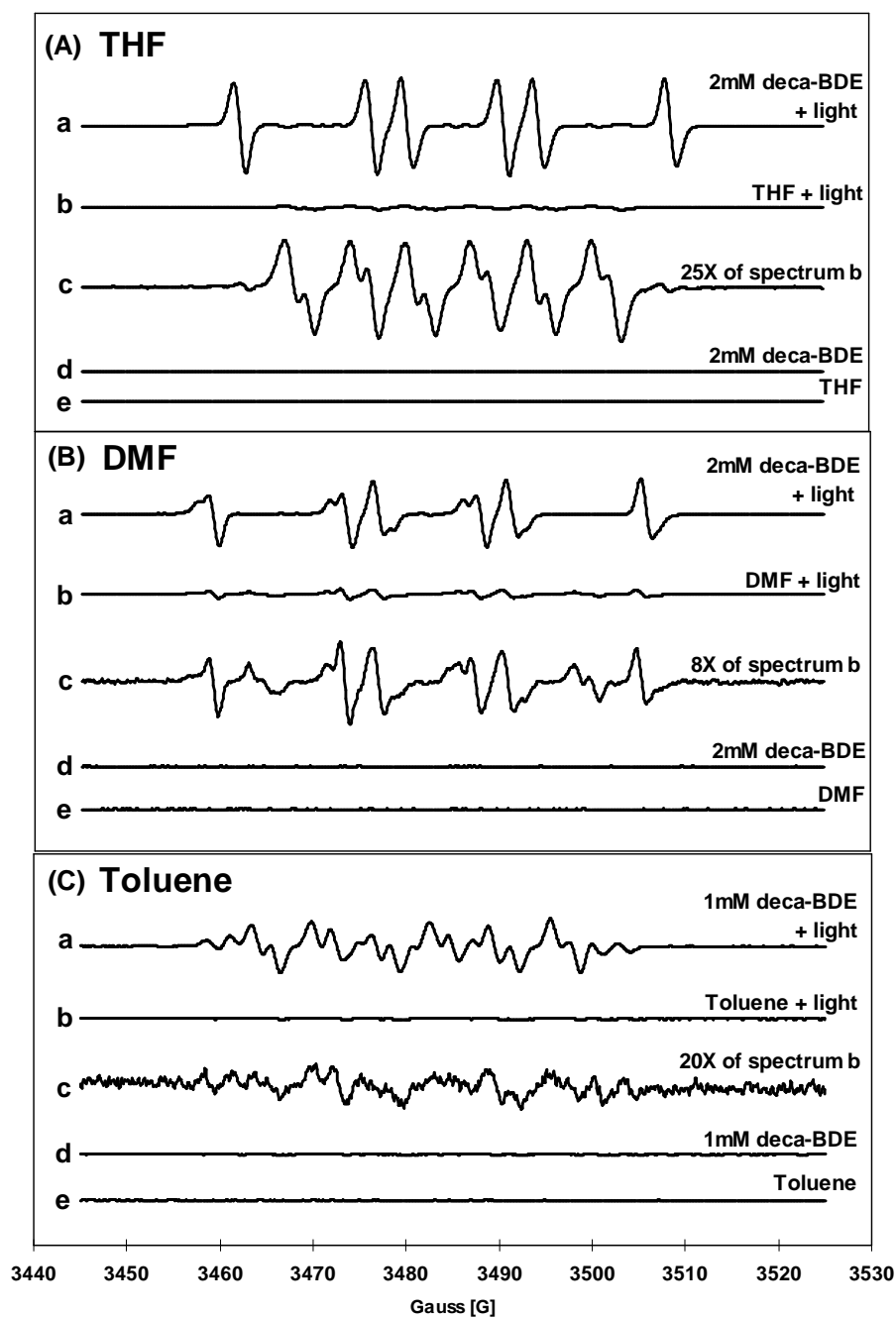
---

Deca-BDE (0.5 mM in toluene) was exposed to light with a 309 nm cut-off filter.

**(A)** GC chromatograms of deca-BDE and photodegradation products. **(B)** GC chromatogram and **(B')** mass spectrum of an unidentified peak (in red circles).

The peak is with the same group of four octa-BDE congeners (in a blue circle). Its distribution of mass cluster is very different from a typical mass cluster distribution of octa-BDEs. Theoretical mass data of a hexa-BDE or hexabromodibenzofuran (hexa-BDF) match with the mass data of the unidentified peak. Considering its mass and retention time, the peak is most likely a hexa-BDF congener.

Figure 2.4. Irradiation of deca-BDE produces free radicals as seen by EPR spin trapping with DMPO.



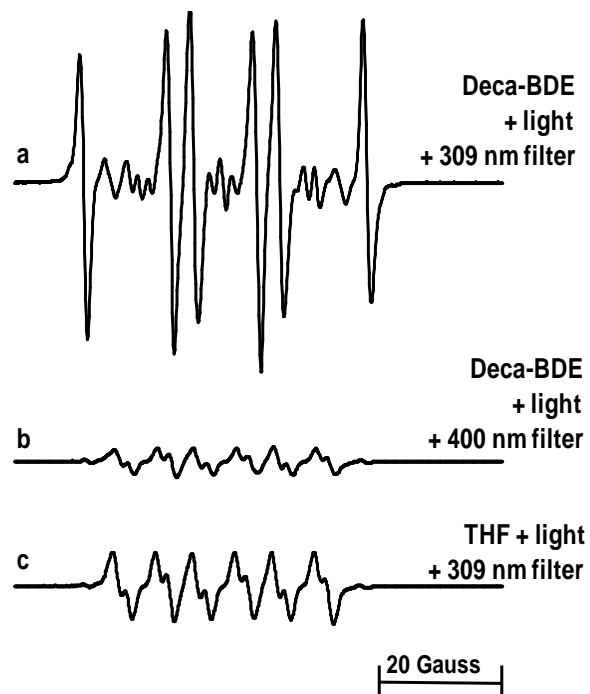
Deca-BDE was dissolved in (A) THF with BHT, (B) DMF, or (C) toluene. a: deca-BDE + light; b: solvent alone + light; c: spectrum b amplified by the factor shown; for

Figure 2.4 continued, above the footnote, p.40.

example, 25X implies the experimental intensities were multiplied by 25 for display.; d and e: controls without light.

The concentration of spin adducts in spectrum (A)-a is approximately  $10 \times 10^{-6}$  M, using 3-CxP as a standard (Venkataraman *et al.*, 2000).

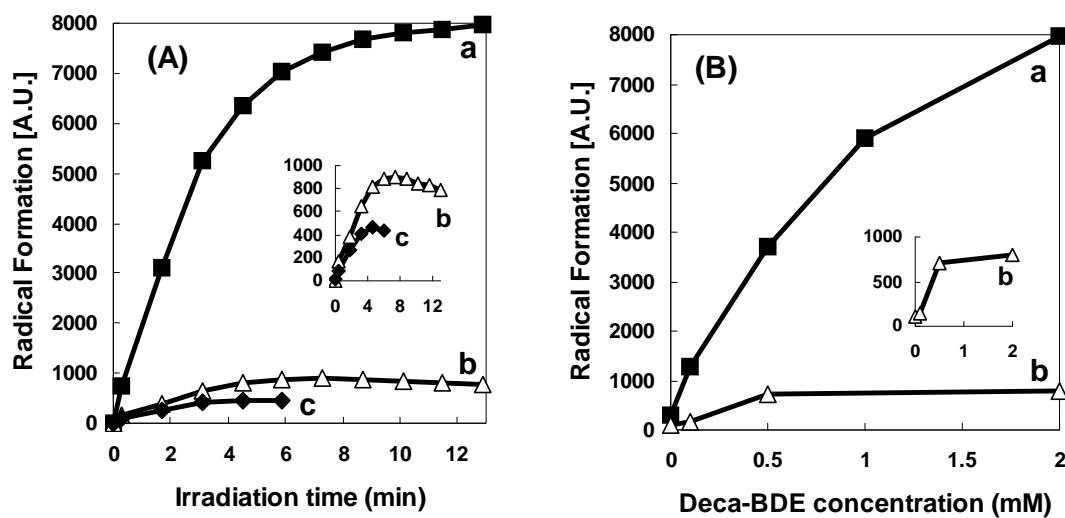
**Figure 2.5. Effective wavelength for radical formation.**



---

(a, b) Deca-BDE (1 mM) in THF with BHT or (c) THF with BHT alone was irradiated using a (a, c) 309 nm cut-off filter, (b) 400 nm cut-off filter.

**Figure 2.6. Free radical formation increases with time of light exposure and concentration of deca-BDE.**



Radical formation (A.U., derived from signal heights, peak-to-peak) correlated to (A) irradiation time with (a) deca-BDE (2 mM) in THF with BHT; (b) deca-BDE (2 mM) in DMF; (c) deca-BDE (1 mM) in toluene; (B) concentration of deca-BDE in (a) THF with BHT; (b) DMF with 14 minutes irradiation time.

CHAPTER 3  
MECHANISMS OF THE RADICAL FORMATION OF DECA-BDE  
IN THE PRESENCE OF LIGHT

Introduction

Various types of radicals and reactive species are generated by light irradiation in skin. They include reactive oxygen species (ROS) such as hydrogen peroxide ( $\text{H}_2\text{O}_2$ ), hydroxyl radical ( $\text{HO}\cdot$ ), singlet oxygen ( $^1\text{O}_2$ ) and superoxide anion radical ( $\text{O}_2\cdot^-$ ), reactive nitrogen species (RNS) like nitric oxide and nitric dioxide, and lipid radicals ( $\text{L}\cdot$ ) (Jurkiewicz and Buettner, 1996; Venkataraman *et al.*, 2004; Herrling *et al.*, 2006; Svobodova *et al.*, 2006). EPR is useful for the detection of UV-induced radicals in skin *in vitro* and *in vivo* (Jurkiewicz and Buettner, 1996). Spin trap agents such as  $\alpha$ -(4-Pyridyl-1-oxide)-*N-tert*-butylnitron (POBN) and 5,5-Dimethyl-pyrroline-1-oxide (DMPO) are used to detect lipid radicals in EPR studies (Venkataraman *et al.*, 2004). It has been proposed that the mechanism of the phototoxic effect is related to the formation of reactive species (de Gruijl and van der Leun, 2002). It is suggested that irradiation of deca-BDE generates free radicals. Therefore, deca-BDE in the presence of UV light can enhance significantly free radical formation and the formation mechanism needs to be investigated to explore potential biological effects of combined exposures of humans to UV and deca-BDE.

Literature Review

Reductive debromination is probably the main mechanism of photodegradation of PBDEs (Watanabe and Tatsukawa, 1987; Hua *et al.*, 2003; Rayne *et al.*, 2003; Sanchez-Prado *et al.*, 2005; Rayne *et al.*, 2006a). It has been suggested that the homolytic dissociation of aryl-Br bonds leads to the debromination of PBDEs generating aryl and bromine radicals and subsequently lower brominated DEs, PBDFs and other degradation products (Sanchez-Prado *et al.*, 2005; Rayne *et al.*, 2006a). The aryl radicals are then

proposed to abstract hydrogen atoms from their matrices thereby completing the reductive debromination process (Rayne *et al.*, 2003; Sanchez-Prado *et al.*, 2005; Rayne *et al.*, 2006a). The analysis of photodegradation products of irradiated BDE 15 (4,4'-dibromodiphenyl ether) suggested homolytic cleavage of C-Br as a dominant process since no O-aryl bond breakage products were formed, probably because the Br-aryl bond dissociation energy (~335 kJ/mol) is weaker than the O-aryl bond dissociation energy (335 - 390 kJ/mol) (Rayne *et al.*, 2003; Schutt and Bunce, 2004). Other researchers suggest that photodegradation of PBDEs involve also aryl-oxygen bond cleavage with the generation of phenoxy and aryl radicals (Watanabe and Tatsukawa, 1987; Rayne *et al.*, 2006a).

### Research Hypothesis

Our research hypothesis is that debromination and hydrogen abstraction are key steps for the mechanism of the free radical formation of deca-BDE in the presence of light.

### Materials and Methods

#### Experimental Design

For a structure-activity relationship study, firstly, the absorption spectra of deca-BDE and structurally related compounds were measured to choose a proper range of wavelengths of light and cutoff filters for efficient irradiation. Secondly, the relationships between the radical yields from irradiation of the compounds and their abilities of UV absorption were investigated to find influential factors for the free radical formation.

With different types of spin traps and isotopes, EPR studies were conducted to identify free radical species from irradiation of deca-BDE. Based upon experimental



results from the EPR studies, EPR spectra were simulated to confirm identification of spin adducts of the free radicals.

The mechanism of the free radical formation was suggested by considering the factors affecting the free radical formation and free radical species identified by the simulation.

### Materials

The commercial deca-BDE mixture DE-83R (>98% BDE-209) and the octa-BDE mixture DE-79 (containing BDE-209 (<0.70%), nona-BDEs (<10%), octa-BDEs (<33%), hepta-BDEs (<45%), hexa-BDEs (<12%), penta-BDEs (<0.50%)) were a gift from Great Lakes Chemical Co. (West Lafayette, U.S.A.). In this paper, the term deca-BDE and octa-BDE indicate DE-83R and DE-79, respectively. BDE-209 indicates the deca-BDE congener. Decabromobiphenyl (PBB 209) and decachlorobiphenyl (PCB 209) were purchased from Accustandard Inc. (New Haven, U.S.A.). 5,5-Dimethylpyrroline-N-oxide (DMPO) was from Dojindo (Gaithersburg, MD) and 2-methyl-2-nitrosopropane (MNP) was from Sigma (St. Louis, U.S.A.). DE, THF with butylated hydroxytoluene (BHT), deuterated THF (THF-d<sub>8</sub>) without BHT and DMF were from Acros (New Jersey, U.S.A.). THF without BHT and toluene were from Burdick & Jackson (Muskegon, MI, U.S.A.). The structures of chemicals are depicted in Table 3-1.

### Methods

#### UV-VIS Spectroscopy

Absorption spectra were measured using a Perkin-Elmer Lambda 650 UV/Vis spectrophotometer at room temperature and a standard 1 cm quartz cuvette.

#### Irradiation

A 150 W Photomax xenon arc lamp (Oriel, Stratford, CT) was used to irradiate the samples. The power of the lamp was set at 30 W. All samples were irradiated at room

temperature for 14 min and with DMPO, unless otherwise indicated. A 309 (WG 305) or 280 (WG 280) nm cutoff filter (cutting off the shorter wavelengths; specification 50% transmittance at 309, 280, or 400 nm, respectively) from Schott (Duryea, PA) was inserted into the lamp to minimize the photodegradation of spin traps and solvents at shorter wavelengths. Since oxygen broadens the EPR lines, thus lowering the resolution, the samples were bubbled with argon to partially remove oxygen and then transferred to a flat quartz cell. The path length for UV irradiation of the flat cell was 0.3 mm. The cell was placed into the TM cavity, and the sample was irradiated (xenon lamp at ~50 cm distance) while in the EPR cavity. An IL1400 BL radiometer with a UV GAL.NIT detector from International Light Inc. (Peabody, MA) was used to measure the light intensity. The light intensity was 2.3 and 3.5 mW/cm<sup>2</sup> with the 309 and 280 nm filters, respectively, for both the EPR and cuvette photodegradation studies.

### EPR

A Bruker EMX EPR spectrometer (Karlsruhe, Germany) equipped with a 4103TM cavity was used. Typical instrument settings were: microwave frequency, 9.8 GHz (X-band); microwave power, 20 mW; modulation amplitude, 1.0 G; time constant, 0.2 s; scan rate, 80 G/84 s; receiver gain,  $2 \times 10^2 - 3 \times 10^4$ . Test compounds were dissolved in the appropriate solvent. Spin traps were added to obtain a final concentration of 25 mM DMPO (from a 1 M aqueous stock) or 10 mM MNP (prepared in the dark). Estimates of absolute concentrations of spin adduct were accomplished by double integration of spectra and comparison to a standard of 3-carboxypropyl (3-CxP) using the same instrument settings and physical setup (Venkataraman *et al.*, 2000). Simulation of EPR data was accomplished using WinSim software (NIEHS) and Bruker WinEPR (Karlsruhe, Germany). The Spin Trap Database (NIEHS) was referred to interpret and simulate EPR spectra (Li *et al.*, 1988). Simulated spectra correlated well with corresponding experimental spectra (correlation coefficient >0.99).

## Results and Discussion

### Absorption Spectra of Structurally Related Compounds

The UV absorption spectra show that deca-BDE absorbs at longer wavelengths than the other compounds (Figure 3.1) (MacNeil *et al.*, 1976; Eriksson *et al.*, 2004a).

### EPR Spectra of Structurally Related Compounds

We investigated the radical yield of deca-BDE compared to similar organic compounds, i.e. octa-BDE, PBB 209, PCB 209, and DE. Irradiation of 1 mM solutions of each compound in THF, using a 309 nm cut-off filter, resulted in formation of the same DMPO spin adducts and similar spectral patterns, but the radical yields were very different (Figures 3.2). The EPR signal intensity from brominated biphenyl was clearly higher than of chlorinated biphenyl. A possible reason could be the red-shift in the spectrum of PBB compared to PCB as well as the lower bond dissociation energy of C-Br (330-345 kJ/mol) compared to C-Cl (350-400 kJ/mol) in aryl halides (Rayne *et al.*, 2003; Schutt and Bunce, 2004), as proposed (Alonso *et al.*, 2008). The ether bridge in PBDE further increases the red shift, accompanied by an increased yield of radicals compared to PBB 209.

### Relationship between Structure and Radical Yield

The spin adduct yield from deca-BDE was ~2-fold higher than from octa-BDE and PBB 209, ~3-fold higher than PCB 209, and ~6-fold higher than DE or solvent alone (Figure 3.3). Use of a 280 nm cut-off filter resulted in a general increase in radical formation by maintaining the same order of compounds, although the increase was higher with the other halogenated compounds compared to deca-BDE. The UV absorption spectra show that deca-BDE absorbs at longer wavelengths than the other compounds (Figure 3.1) (MacNeil *et al.*, 1976; Eriksson *et al.*, 2004b); the actual quantum yields of degradation are quite similar (Eriksson *et al.*, 2004b). Additionally, the integrated UV

spectra correlate positively with the radical yields (Figure 3.3-B-a/b). This demonstrates that the rate of degradation depends on the degree of UV absorption by the compound. Heat of formation ( $\Delta H_f$ ), bond dissociation energy, and energy of the highest occupied molecular orbital ( $E_{\text{HOMO}}$ ) and lowest unoccupied molecular orbital ( $E_{\text{LUMO}}$ ) have been used to predict degradation rates of PBDEs and PCBs during irradiation (Hu *et al.*, 2005; Niu *et al.*, 2006; Li *et al.*, 2008; Zeng *et al.*, 2008). Photodegradation rates of PBDEs increase with number of C-Br bonds (Eriksson *et al.*, 2004b). Thus, it is suggested that higher bromine content results in a smaller ( $E_{\text{LUMO}} - E_{\text{HOMO}}$ ) and higher  $\Delta H_f$ , which in turn will result in a greater yield of free radicals (Hu *et al.*, 2005). An inverse correlation was found between phototoxicity and dE of polycyclic aromatic hydrocarbons (PAHs) and suggested to be related to the ease of radical formation (Mekenyan *et al.*, 1994).

The EPR signal intensity from brominated biphenyl was clearly higher than of chlorinated biphenyl. A possible reason could be the red-shift in the spectrum of PBB compared to PCB as well as the lower bond dissociation energy of C-Br (330-345 kJ/mol) compared to C-Cl (350-400 kJ/mol) in aryl halides (Rayne *et al.*, 2003; Schutt and Bunce, 2004), as proposed (Alonso *et al.*, 2008). The ether bridge in PBDE further increases the red shift, accompanied by an increased yield of radicals compared to PBB 209. This shows that PBDEs will be significantly more photoactive upon exposure to solar UV light than parallel chlorinated compounds and/or halogenated biphenyls.

#### Effect of Deca-BDE on the Radical Species

To assist in the identification of the observed spin adducts with DMPO we simulated key spectra (Figure 3.4). The weak solvent spectra, Figure 3.4 A-a (and Figures 2.4-A-b,c and 2.5) have the appearance and splitting constants consistent with the spin trapping of superoxide (or hydroperoxyl radical  $\text{HOO}^\bullet$ ) in an organic solvent ( $a^{\text{N}} = 13.0 \text{ G}$ ;  $a_{\beta}^{\text{H}} = 7.07 \text{ G}$ ;  $a_{\gamma}^{\text{H}} = 2.05 \text{ G}$ ,  $\text{NoH} = 1.84$ ) forming adduct A (Figure 3.5). ( $\text{NoH}$  is the ratio of the nitrogen hyperfine splitting to the hydrogen hyperfine splittings ( $\text{NoH} =$

$a^N/a^H$ )) (Buettner, 1987; Li *et al.*, 1988). Adduct B would be formed in the absence of oxygen (Figure 3.5).

The asymmetric line width with an apparent 1:1 ratio of two species is also consistent with that observed for DMPO/•OOH (Buettner, 1990). Autoxidation of THF with oxygen and/or UV could form furan hydroperoxide (Figure 3.5) (Clark, 2001). UV would homolytically cleave the furan hydroperoxide to a furan alkoxy radical (Figure 3.5, radical I) and HO•. The alkoxy radical would rapidly rearrange to form a carbon-centered radical that will react rapidly with dissolved oxygen, producing an unstable peroxy radical (radical II). The peroxy radical will release superoxide (or hydroperoxy radical HOO•) *via* its transition state, which will be captured by DMPO (radical III and spin trap adduct A) (Bothe *et al.*, 1978a; Bothe *et al.*, 1978b; Das *et al.*, 1988; von Sonntag, 1988). As oxygen is consumed over time, the alkoxy radical (I) would be more likely to be captured by DMPO, forming spin adduct B ( $a^N = 13.04$  G;  $a_\beta^H = 7.51$  G, NoH = 1.74) (Buettner, 1987; Li *et al.*, 1988). Hydroxyl radical would initiate new oxidation chains forming a carbon-centered radical (radical IV) and the activated hydrogens next to the ethereal oxygen (carbon 2) will be the center of radical formation (Bothe *et al.*, 1978b; Clark, 2001). The carbon-centered radical will react with dissolved oxygen forming a peroxy radical and oxidation chains leading to release of superoxide (or hydroperoxy radical HOO•) (Bothe *et al.*, 1978a; Symons, 2000b). The carbon-centered radical could also be captured by DMPO directly. The splitting constants and especially NoH of the carbon-centered radical spin adduct ( $a^N = 14.1-14.2$  G;  $a_\beta^H = 17.3-18.0$  G; and NoH = 0.79-0.82) (Figure 3.4 A-e, B-e and Figure 3.5, spin trap adduct C) indicated the spin trapping of an oxygenated carbon-centered radical, consistent with the mechanism suggested (Buettner, 1987; Li *et al.*, 1988). The computer simulation of the THF-DMPO spectra is consistent with this proposed mechanism, indicating a prevalence of spin adducts A and B (Figure 3.4 A-c,d,e, Figure 3.5).

The spectra obtained from deca-BDE with DMPO in THF are quite different from those of DMPO in THF alone. The presence of deca-BDE (2 mM) results in a much more intense spin adduct EPR signal than observed from THF alone, 25-fold more (Figure 3.4 A/B-a). This spin adduct appears to be identical to adduct C derived from the carbon-centered radical IV in Figure 3.5 observed with THF alone (Figure 3.4 A/B-e). Because neat THF is  $\approx 10$  M, and DMPO is only 25 mM, oxidants produced from photoexcited deca-BDE ( $\text{Br}^\bullet$  and a BDE-carbon-centered radical (V)) will react preferentially with THF forming the THF radical and lower BDE, *e.g.* nona-BDE *via* hydrogen abstraction; DMPO will then trap solvent-derived radicals, producing adduct C (Figure 3.5). The EPR simulations indicate that the spectra obtained from irradiated solvent alone and from irradiating deca-BDE in THF share the same set of spin adducts, but in very different proportions. With THF alone,  $\text{DMPO}/\bullet\text{OR}$  and  $\text{DMPO}/\bullet\text{OOH}$  are dominant ( $A + B = >98\%$  of total adducts), while light exposure of deca-BDE produced predominantly the  $\text{DMPO}/\text{tetrahydrofuranlyl}$  spin adduct (C), increasing this adduct from 1.6% to  $>86\%$  of all adducts.

Because DMPO does not typically demonstrate observable hyperfine splittings from nuclei on the trapped radical, we used MNP, a nitroso spin trap to learn more about the carbon-centered radicals trapped by DMPO. The disadvantage of MNP is that oxygen-centered spin adducts are very short-lived and thus not observable in steady-state experiments; in addition, the photolytic cleavage (at the wavelengths used) of the C-N nitroso bond, produces a *tert*-butyl radical which will be trapped by MNP thus forming the di-*tert*-butylnitroxide (DTBN,  $\text{MNP}/\text{tert-butyl}^\bullet$ ) with a simple 1:1:1 triplet spectrum (Figure 3.5, E) (Makino *et al.*, 1981). As expected, all MNP samples contained varying levels of the triplet spectrum which increased with irradiation (Figure 3.6, 3.7 and 3.8). The presence of deca-BDE weakened the triplet spectrum from DTBN (Figure 3.6 A-a/b-1 and Figure 3.6 B-a/b-1), most likely due to significant light absorption by deca-BDE, thereby limiting the photochemistry for its formation. Alternatively, since the intensity of

DTBN is pH dependent (Makino *et al.*, 1981), the effect could be due to production of HBr from irradiation of deca-BDE, which dissociates to  $H^+$  and  $Br^-$ , thereby decreasing the pH. Irradiation of deca-BDE in THF or toluene in the presence of MNP produced four additional peaks in the EPR spectra with peak intensity ratios of approximately 1:2:2:1 (Figure 3.6-A/B-a' ). This spectral pattern is consistent with the hydrogen (or  $e^-_{aq}$ ,  $H^+$ ) spin adduct of MNP ( $MNP/H^\bullet$ ) (Buettner, 1987; Li *et al.*, 1988). Simulation of experimental spectra yielded hyperfine splitting constants:  $MNP/tert\text{-butyl}^\bullet$  ( $a^N = 15.30$  G and 15.34 G in THF and toluene, respectively) and  $MNP/H^\bullet$  ( $a^N = 14.87$  G and  $a^H = 14.72$  G) in both solvents (Figure 3.7 A/B) (Buettner, 1987; Li *et al.*, 1988). These results suggest that a low yield of photoionization products (solvated electron and aryl radical cation) may be produced from irradiation of deca-BDE.

#### Sources of Hydrogen Involved in the Radical Formation

To gather evidence for our suggestion of  $MNP/H^\bullet$  spin adducts as products of deca-BDE irradiation in THF we used THF-d8 in which all hydrogen atoms are replaced with deuterium atoms. The expected  $MNP/D^\bullet$  spectrum should be quite different than  $MNP/H^\bullet$  because of the different nuclear spins for deuterium ( $I = 1$ ) and hydrogen ( $I = 0.5$ ); in addition the nuclear magneton for deuterium is about 15% of that of hydrogen. Indeed, after irradiation of deca-BDE in THF-d8, the typical EPR peaks of an MNP-hydrogen adduct were basically absent (Figure 3.7 and 3.8-B-1/2), thus supporting our hypothesis that the hydrogen radical was derived from the solvent. However, at our signal-to-noise level the expected weak triplet of triplets signal was not observed, rather a new simple 1:1:1 species appeared along with DTBN. Simulation of experimental spectra yielded hyperfine splitting constants:  $MNP/tert\text{-butyl}^\bullet$  ( $a^N = 15.38$ ) and  $MNP/D^\bullet$  ( $a^N = 13.94$  G and  $a^D = 0.34$  G) (Figure 3.7-C). The addition of solvent protons by inclusion of water (THF-d8:water = 9:1) resulted in no change in the species observed, only in the ratio (Figure 3.7-D). These results suggest that the organic solvent is the main

source for hydrogen radicals. While most nona-BDEs are expected to be further degraded to lower-BDEs (Figure 3.5, path 1) a certain amount of excited nona-BDE could react with MNP (path 2) and produce the MNP/H<sup>•</sup> spin adducts (D) *via* reduction of MNP by electron transfer from the excited state of nona-BDE. If photoionization was a significant process, we would have also expected to see the MNP/H<sup>•</sup> in THF-d8 + water (Mossoba *et al.*, 1982; Moore *et al.*, 1994). This was not observed (Figure 3.7-D). Thus, if photoionization does occur it appears to be a minor process. MNP should capture carbon-centered radicals such as aryl radicals from deca-BDE more effectively than DMPO. The spin adducts of carbon-centered radicals, however, were not definitively observed, probably because the concentration of spin adducts of DTBN was very high and the hyperfine splittings of DTBN are very similar to the splittings of the radicals we were interested in (Janzen, 1971). We were not able to detect the splittings of bromine radicals either, probably, as has been suggested earlier (Symons, 2000a), because the hyperfine splittings of bromine with certain radicals are too small to be detected due to quadrupolar interruption.

#### Photochemistry of the Free Radical Formation of Deca-BDE in the Presence of UV Light

Reductive debromination is probably the main mechanism of photodegradation of PBDEs (Watanabe and Tatsukawa, 1987; Hua *et al.*, 2003; Rayne *et al.*, 2003; Sanchez-Prado *et al.*, 2005; Rayne *et al.*, 2006a). It has been suggested that the homolytic dissociation of aryl-Br bonds leads to the debromination of PBDEs generating aryl and bromine radicals and subsequently lower brominated DEs, PBDFs and other degradation products (Sanchez-Prado *et al.*, 2005; Rayne *et al.*, 2006a). The aryl radicals are then proposed to abstract hydrogen atoms from their matrices thereby completing the reductive debromination process (Rayne *et al.*, 2003; Sanchez-Prado *et al.*, 2005; Rayne *et al.*, 2006a). The analysis of photodegradation products of irradiated BDE 15 (4,4'-



dibromodiphenyl ether) suggested homolytic cleavage of C-Br as a dominant process since no O-aryl bond breakage products were formed, probably because the Br-aryl bond dissociation energy (~335 kJ/mol) is weaker than the O-aryl bond dissociation energy (335 - 390 kJ/mol) (Rayne *et al.*, 2003; Schutt and Bunce, 2004). Other researchers suggest that photodegradation of PBDEs also involve aryl-oxygen bond cleavage with the generation of phenoxy and aryl radicals (Watanabe and Tatsukawa, 1987; Rayne *et al.*, 2006a). We did not detect clear evidence of products of ether bridge cleavage in our GS/MS analysis; however, they may have been below the detection limit after this short term exposure.

Our results with MNP show that irradiation of deca-BDE in THF and toluene produces hydrogen atom spin adducts and that the hydrogen radicals are from the solvents. Simulation data from experiments with DMPO suggest that irradiation of deca-BDE led to the formation of solvent radicals *via* hydrogen abstraction. Thus the primary mechanism of radical formation during PBDE photodegradation in solvents is hydrogen abstraction from matrices, a secondary event following the debromination process of PBDEs *via* homolytic cleavage of C-Br (Figure 3.5).

### Conclusions

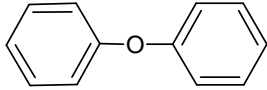
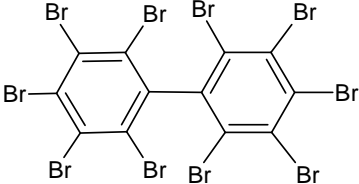
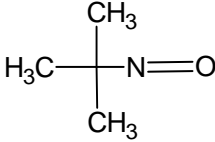
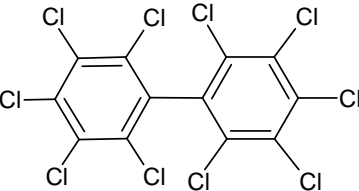
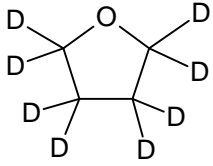
This hydrogen abstraction deserves special attention, since in biological systems, hydrogen abstraction initiates lipid and protein oxidation, thereby producing various radicals and electrophiles which may attack critical cellular macromolecules, including the DNA. For example, irradiation of chlorpromazine produced radicals that homolytically changed sulfhydryl or peptide bonds *via* hydrogen abstraction (Chignell, 1990). The human skin surface is covered with lipids whose unsaturated bonds are subjected to hydrogen abstraction by free radicals. Polyunsaturated fatty acids (PUFA) in surface skin lipids could be more easily involved in hydrogen abstraction than THF because PUFA's bond energy (75-80 kcal/mol at allylic position) is lower than the

dissociation energy of  $\alpha$ -carbon bond of THF (92 kcal/mol) (Wagner *et al.*, 1994; Laarhoven and Mulder, 1997). Indeed, PBDEs in lipid degrade quickly if exposed to sunlight (Peterman and Orazio, 2003). Irradiation of halogenated PAHs in lipids significantly increased lipid peroxides (Herreno-Sánchez *et al.*, 2006). Peroxidation of skin surface lipids deteriorates membrane function (Akitomo *et al.*, 2003). Lipid peroxides from surface skin lipids lead to cell damage in keratinocytes and stimulated cell growth and altered epidermal structure in skin tissues (Picardo *et al.*, 1991). Therefore, our observation of UV-induced radical formation of PBDEs in THF via hydrogen abstraction from its solvent suggests that PBDEs could also be photoreactive and phototoxic on human skin. Radical formation could also occur in skin tissue, since lower brominated BDEs easily penetrate into the skin (Staskal *et al.*, 2005) and may reach the skin after internal uptake (Staskal *et al.*, 2006). UV A and B penetrate the stratum corneum and can lead to cancer in the stratum germinativum. Dermal PCB exposure has been shown to significantly increase the risk of melanoma in linemen, cable splicers and electricians (Loomis *et al.*, 1997). This risk was considered so substantial that NIOSH issued a warning for melanoma risk in these workers (Mazzuckelli and Schulte, 1993) who are co-exposed to UV light, since they are working frequently outdoors (Loomis *et al.*, 1997). PBDEs may be an even greater risk factor, due to the widespread contamination levels and - as shown in this study - significantly stronger activity in radical formation compared to PCBs. Young children may be at particularly high risk, since they have generally higher PBDE contamination levels than adults (Stapleton *et al.*, 2005), more outdoor activity and therefore UV exposure, and higher risk of percutaneous toxicity due to their specific skin structure (Mancini, 2004). This potential risk of skin damage and carcinogenesis by radical formation due to UV-exposure of PBDEs needs urgent clarification.

This is important new information, since it indicates that deca-BDE may have a so far unrecognized, significant mechanism of toxicity. Thus, light exposure of deca-BDE

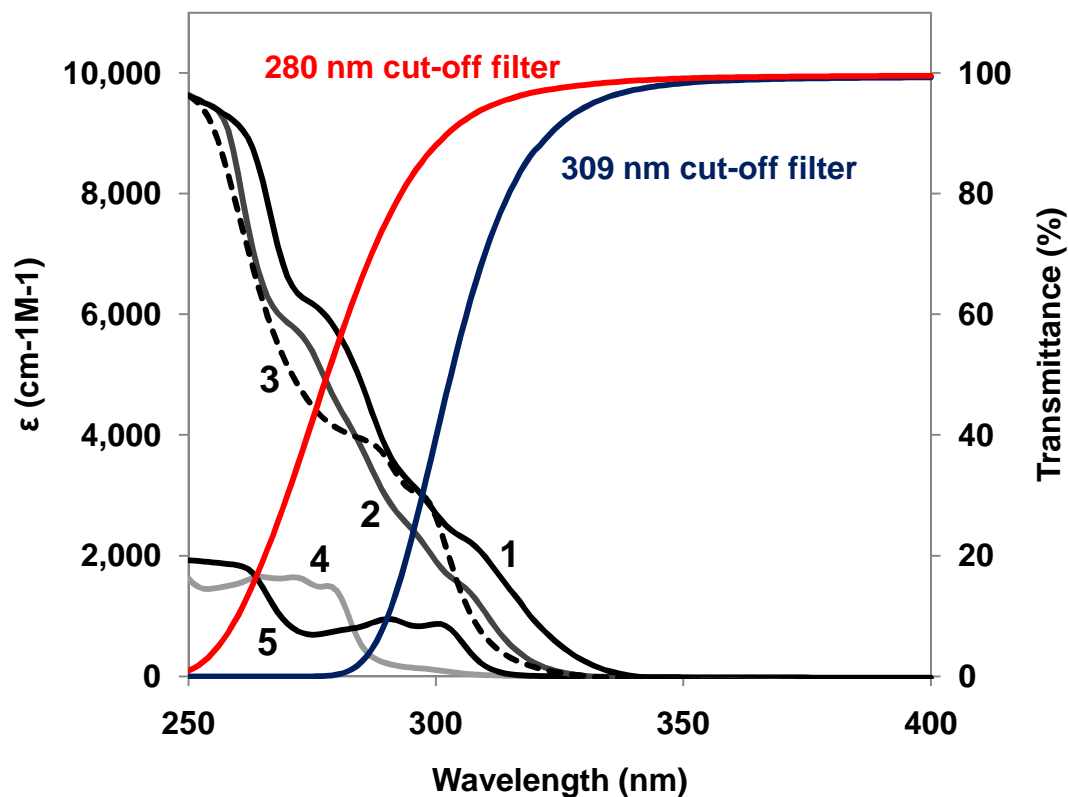
in the skin, may cause serious toxic effects, even carcinogenicity. Therefore additional studies of the consequences of UV irradiation of deca-BDE in biological systems are urgently needed.

**Table 3.1. Molecular structures of the compounds structurally related to deca-BDE, MNP spin trap agent and deuterated THF.**

Name	Molecular structure	Name	Molecular structure
Octa-BDE (DE-79) <sup>1</sup>	N/A	DE	
PBB 209		MNP	
PCB 209		D-THF	

<sup>1</sup> The octa-BDE mixture (DE-79) contains several congeners of PBDEs (see Materials and Methods for composition).

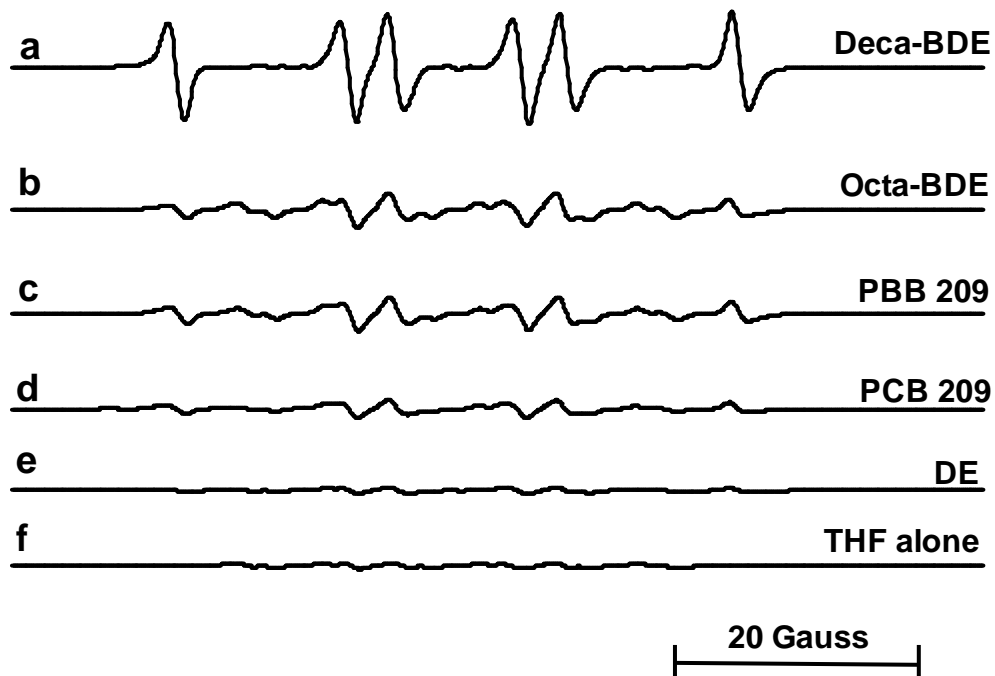
**Figure 3.1.** Absorption spectra of test compounds; transmittance (%) of cut-off filters.



1. deca-BDE (DE-83R); 2. PBB 209; 3. octa-BDE (DE-79) (dotted line); 4. DE; 5. PCB 209. All compounds were dissolved in THF without BHT.

Source: Schott (Duryea, PA, USA; “Optical Glass Filters Datasheets, calculation prog.” ([http://www.us.schott.com/advanced\\_optics/english/download/optical\\_filters\\_download\\_vers.zip?](http://www.us.schott.com/advanced_optics/english/download/optical_filters_download_vers.zip?))) were used to draw the transmission curves for the cut-off filters.

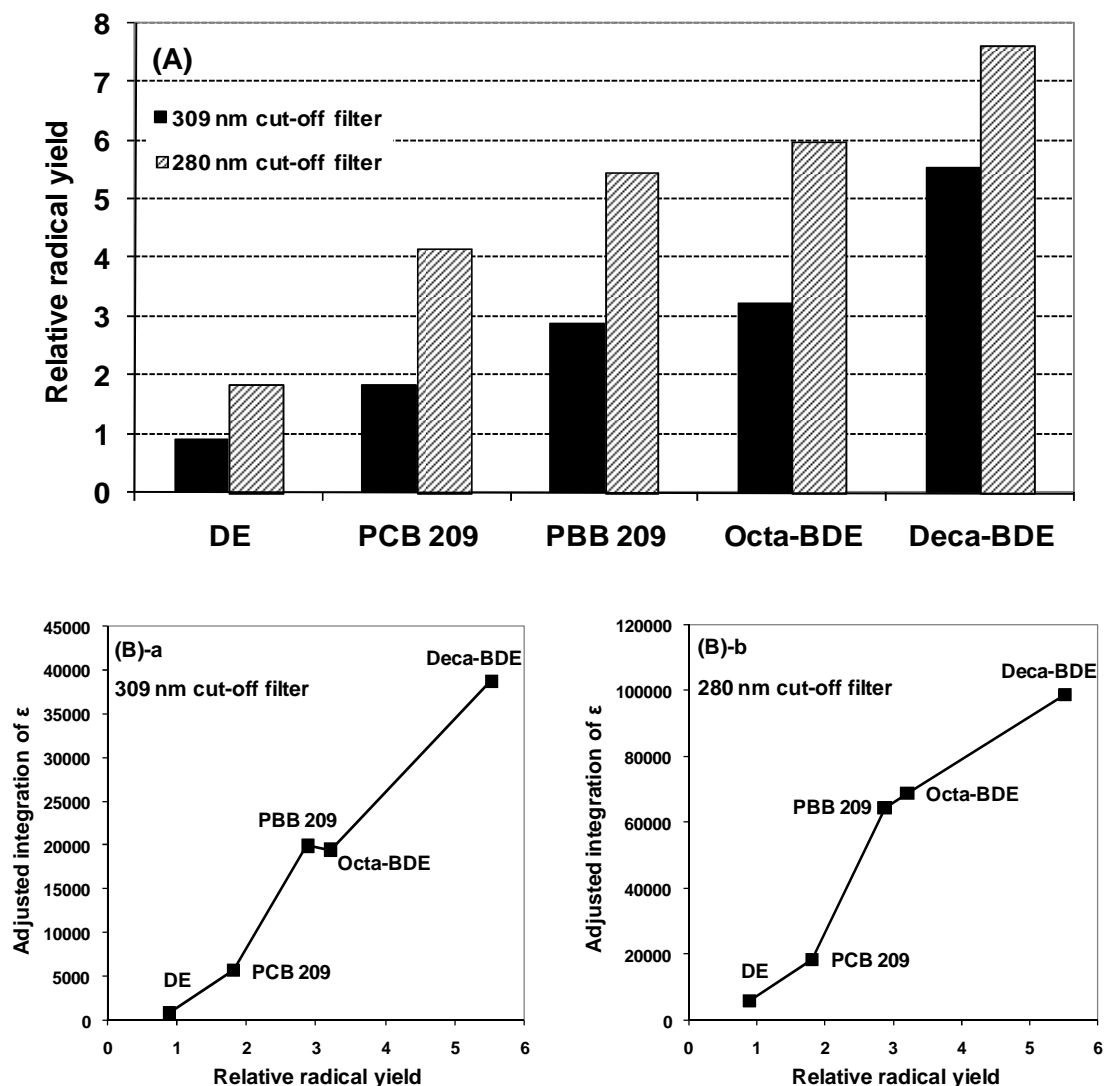
Figure 3.2. EPR spectra of structurally related compounds.



---

Samples were irradiated for 7 minutes. Each compound (1 mM) was dissolved in THF. (a) deca-BDE; (b) octa-BDE; (c) PBB 209; (d) PCB 209; (e) DE; (f) THF alone.

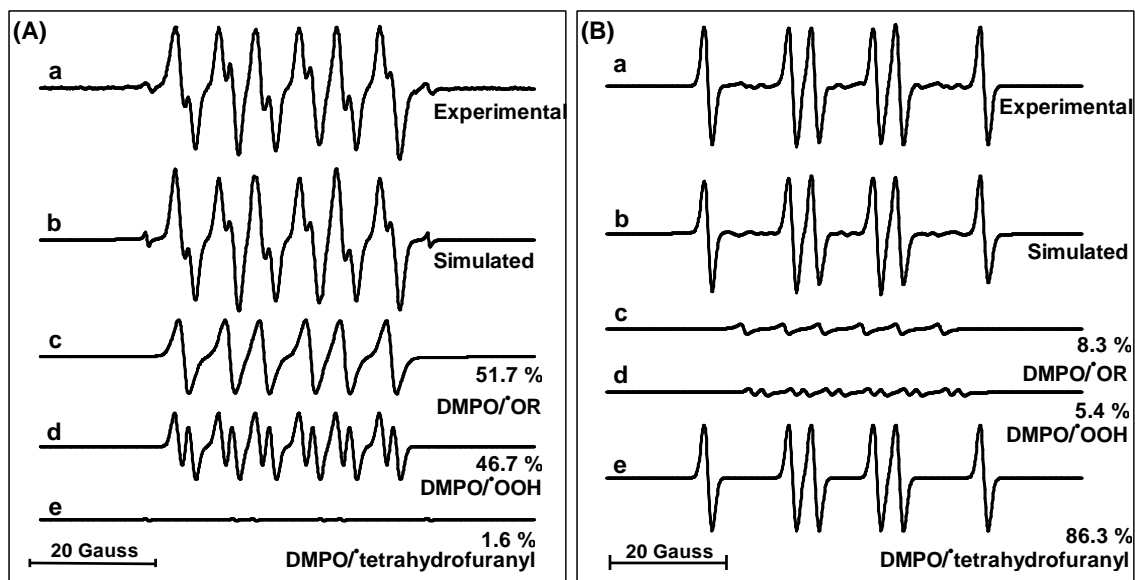
**Figure 3.3. Radical formation by structurally related compounds, relation to UV molar absorption coefficient ( $\epsilon$ ).**



**(A)** radical yield after irradiation with a 309 nm cut-off filter (black bars) or a 280 nm cut-off filter (striped bars). The radical yield was obtained by double-integration of EPR spectra; relative radical yield: ratio of radical yield of each compound to radical yield of THF alone.

**(B)** Radical yield correlated to UV absorption: the area under the absorption curve ( $\epsilon$ ) was determined by a Trapezoid integration; to estimate the actual light absorbed by the sample when employing a cutoff filter, an “adjusted-integration” was determined by the percent transmittance of the cutoff filter at a specific wavelength times the extinction coefficient of the compound at that wavelength in the integration. **(a)** 309 nm cut-off filter; **(b)** 280 nm cut-off filter.

**Figure 3.4. Computer simulations of EPR spectra of DMPO spin adducts in (A) THF with BHT alone, (B) with deca-BDE.**

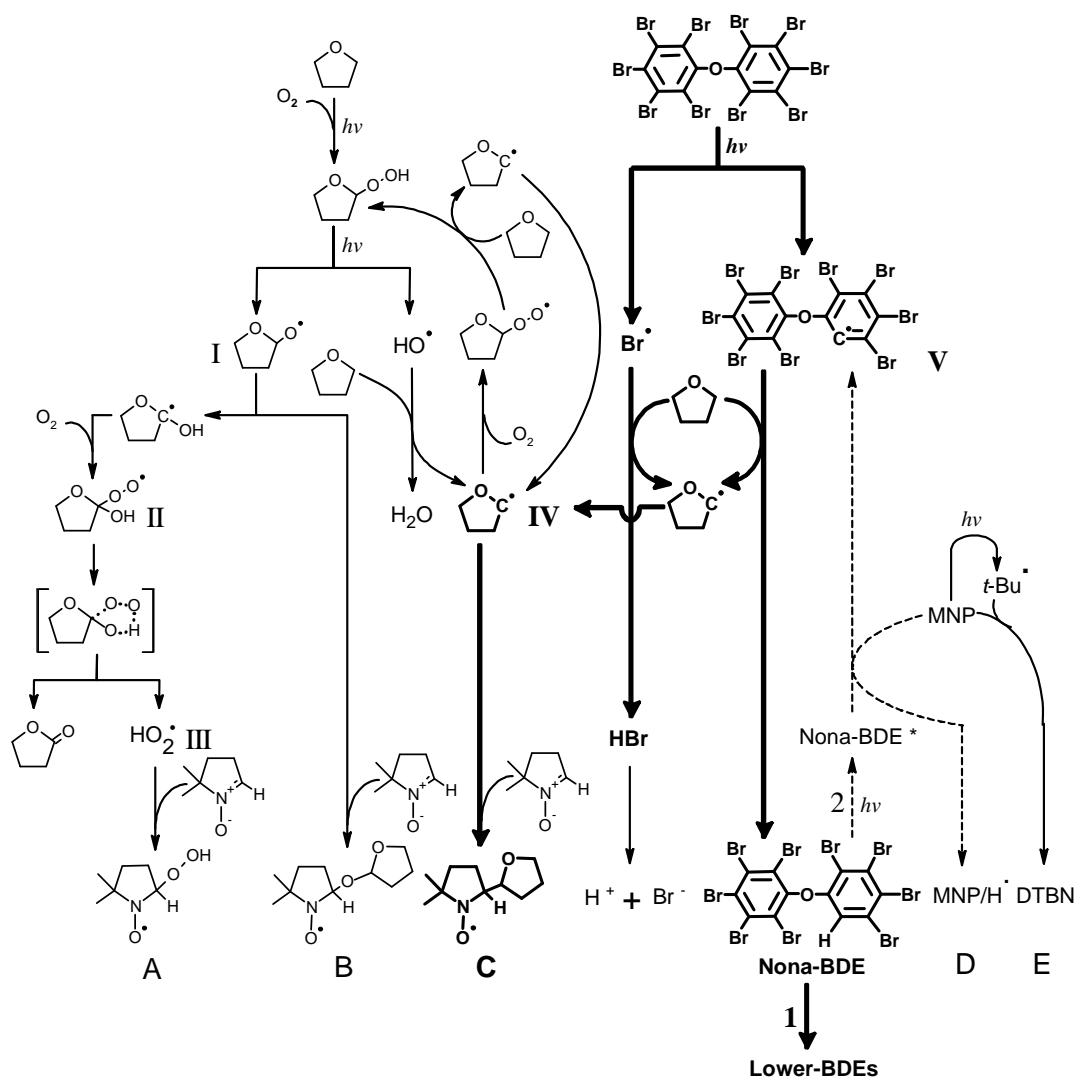


(a.) Experimental spectrum; (b.) Composite computer-simulated spectrum; (c.) component of a. corresponding to DMPO/ $\bullet$ OR adduct (d.) component of a. corresponding to a DMPO/ $\bullet$ OOH adduct (e.) component of a. corresponding to a DMPO/ $\bullet$ tetrahydrofuranyl adduct.

Splitting constants of products are (A) **THF with BHT**: DMPO/ $\bullet$ OR adduct with  $a^N = 13.04$  G and  $a_\beta^H = 7.51$  G; DMPO/ $\bullet$ OOH adduct with  $a^N = 13.03$  G and  $a_\beta^H = 7.07$  G, and  $a_\gamma^H = 2.05$  G; DMPO/ $\bullet$ tetrahydrofuranyl adduct with  $a^N = 14.14$  G and  $a_\beta^H = 17.32$  G (1.6%). (B) **Deca-BDE in THF with BHT**: DMPO/ $\bullet$ OR adduct with  $a^N = 13.04$  G and  $a_\beta^H = 7.05$  G; DMPO/ $\bullet$ OOH adduct with  $a^N = 13.03$  G and  $a_\beta^H = 7.07$  G, and  $a_\gamma^H = 2.05$  G; DMPO/ $\bullet$ tetrahydrofuranyl adduct with  $a^N = 14.22$  G and  $a_\beta^H = 18.00$  G.



**Figure 3.5. Proposed mechanism of radical formation during irradiation of the deca-BDE in THF.**

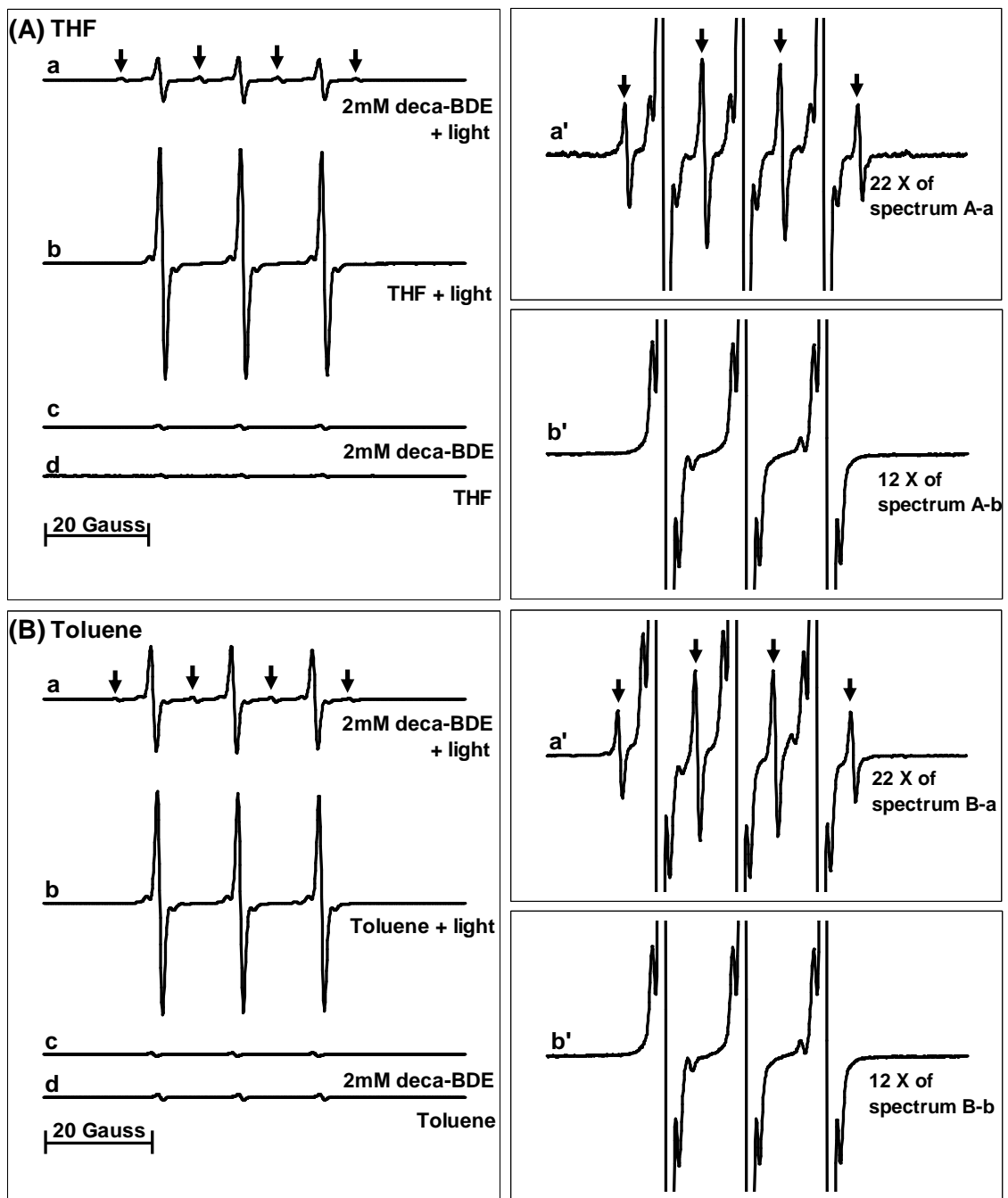


I. Oxygenated tetrahydrofuran radical. II. Tetrahydrofuran hydroperoxyl radical. III. Hydroperoxyl radical. IV. Tetrahydrofuran radical. V. Nona-BDE radical. A. DMPO/•OOH. B. DMPO/•OR. C. DMPO/•tetrahydrofuran. D. MNP/H•. E. MNP/*tert*-butyl• (DTBN).

[ ] indicates the transition state of II. Nona-BDE\* is the excited state of the compound.

For nona-BDE pathway 1 is major and 2 (broken arrow) is minor for further reaction.

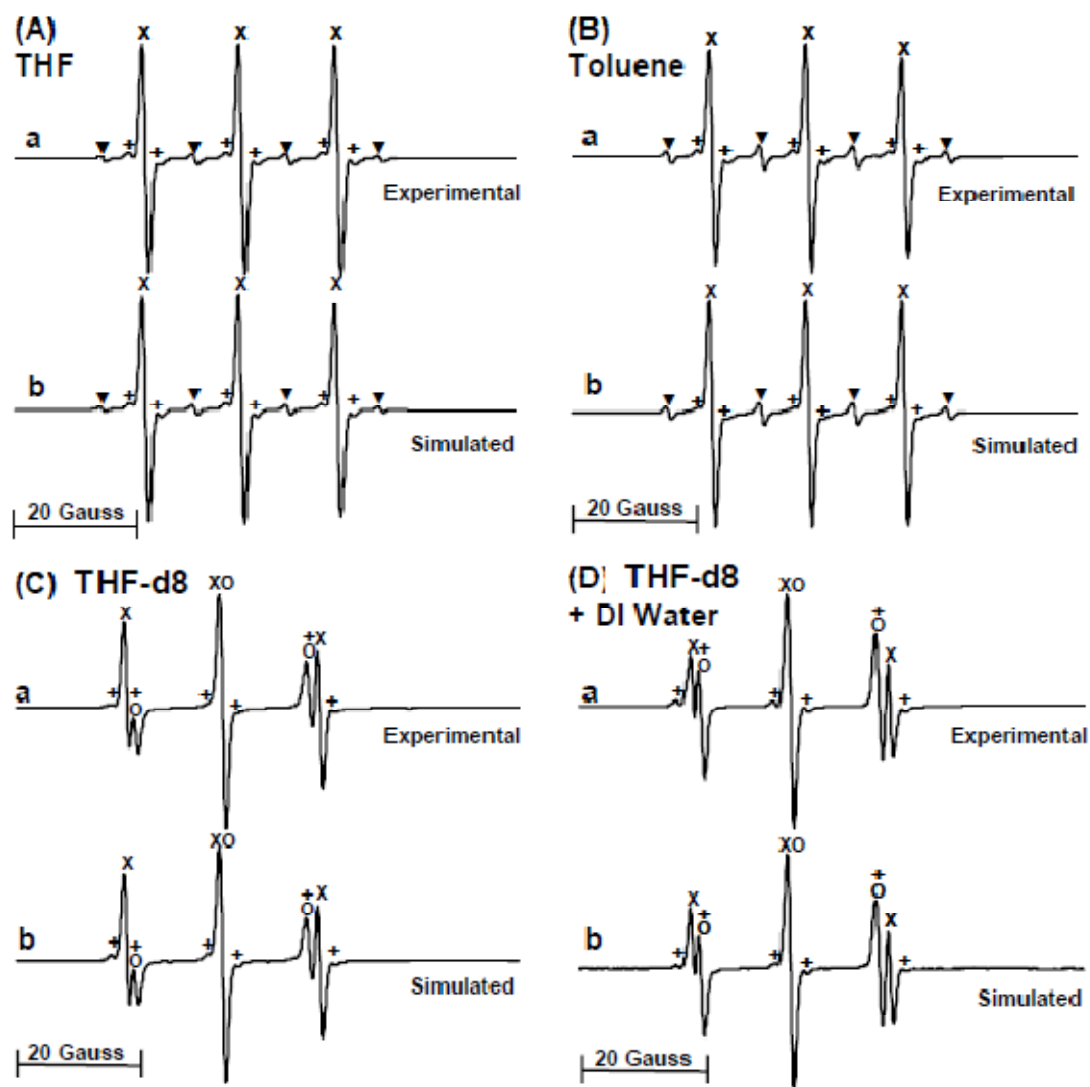
Figure 3.6. EPR spectra produced by MNP adducts in (A) THF, (B) toluene.



(a) deca-BDE + light; (b) solvent alone + light; (a'/b') is spectrum a/b amplified by the factor shown; (c) and (d) controls with no light.

Arrows indicate 1:2:2:1 spectral pattern consistent for the hydrogen (or  $e^-_{aq}$ ,  $H^+$ ) spin adduct of MNP ( $MNP/H^\bullet$ ).

Figure 3.7. Computer simulation of EPR spectra with MNP spin trap.

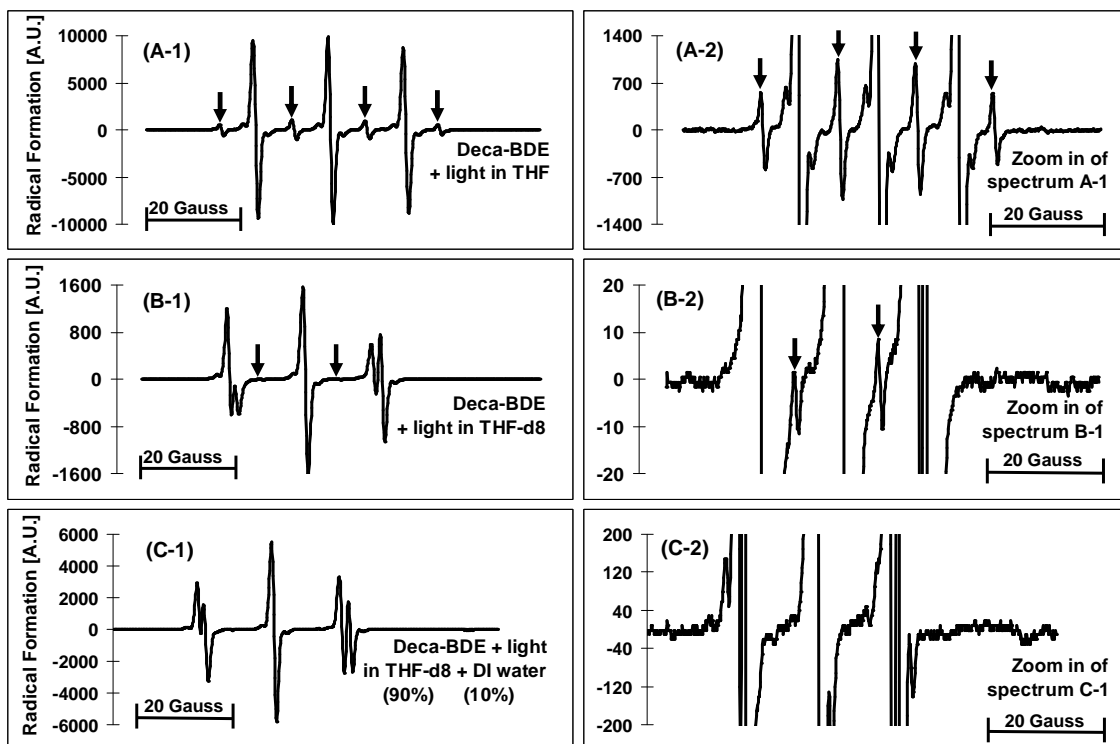


Deca-BDE (2 mM) was dissolved in four different solvents, each containing MNP: **(A)** THF; **(B)** toluene; **(C)** THF-d8; **(D)** THF-d8:DI water (9:1).

For each panel: a. experimental spectrum; b. Composite computer-simulated spectrum. X indicates DTBN; +, DTBN ( $^{13}\text{C}$ ); ▼, MNP/H $^{\bullet}$ ; O, MNP/D $^{\bullet}$ .

Hyperfine splittings are **(A)** X,  $a^{\text{N}} = 15.30$  G; +,  $a^{\text{N}} = 15.30$  and  $a^{\text{C}} = 3.23$  G; ▼,  $a^{\text{N}} = 14.86$  G and  $a_{\beta}^{\text{H}} = 14.66$  G. **(B)** X,  $a^{\text{N}} = 15.34$  G; +,  $a^{\text{N}} = 15.49$  and  $a^{\text{C}} = 3.56$  G; ▼,  $a^{\text{N}} = 14.88$  G and  $a_{\beta}^{\text{H}} = 14.61$  G. **(C)** X,  $a^{\text{N}} = 15.38$  G; +,  $a^{\text{N}} = 15.38$  and  $a^{\text{C}} = 3.49$  G; O,  $a^{\text{N}} = 13.95$  G and  $a^{\text{D}} = 0.36$  G. **(D)** X,  $a^{\text{N}} = 15.69$  G; +,  $a^{\text{N}} = 15.46$  and  $a^{\text{C}} = 4.70$  G; O,  $a^{\text{N}} = 14.15$  G and  $a^{\text{D}} = 0.39$  G.

Figure 3.8. Solvent effects on the radical formation of deca-BDE.



Deca-BDE (2 mM) was dissolved in three different solvent-systems each containing MNP: (A) THF; (B) THF-d8; (c) THF-d8 (90 %) + DI water (10 %).

For each solvent-panel: Spectrum 1 is at the original scale, spectrum 2 is zoomed in (use scales as reference).

Arrows in (A-1) and (A-2) indicate peaks with 1:2:2:1 spectral pattern, indicative of a hydrogen (or  $e^-_{aq}$ ,  $H^+$ ) spin adduct of MNP ( $MNP/H^\bullet$ ).

In THF-d8 (B-1 and B-2), the two peaks with arrows are not identified.

## CHAPTER 4

### BIOLOGICAL EFFECTS OF DECA-BDE/TRICLOSAN, LIGHT, AND THE COMBINATION OF BOTH IN SKIN CELLS

#### Introduction

As described in Chapter 1, dermal contact is one of the main exposure routes of deca-BDE and triclosan and these chemicals could be accumulated in the skin where they could easily be exposed to UV light. It was reported that PBDE concentrations normalized to skin surface area are in the range of 3 - 1970 pg/cm<sup>2</sup> (Stapleton *et al.*, 2008). The backside of a young males hand secretes about 38 µg/cm<sup>2</sup> of surface skin lipids over 3 h (Rajka, 1974). Based on this, we assume that the PBDE levels in skin surface lipid may be in the range of 0.1 – 50 µg/g lipid. In daily life skin is exposed to UV light. It required only 2 min of exposure to sunlight to degrade over 20% of hepta-BDE dissolved in lipids (BDE-183; 25 ng/g lipid) (Peterman and Orazio, 2003). Therefore, the amount and the reactivity of deca-BDE on the skin surface could be high enough to induce a photochemical reaction.

According to a report of the Australian government, 146 µg/kg/day is the estimated exposure level for an adult to triclosan via dermal contact from selected consumer products (NICNAS, 2009). Triclosan is, like deca-BDE, photolytically degraded by UV light, raising the same concerns about possible photoactivation on/in the skin.

Photolysis of deca-BDE and triclosan could produce potential toxicants including the degradation products and free radicals as discussed in Chapter 2, Chapter 3, and other studies (Watanabe and Tatsukawa, 1987; Rayne *et al.*, 2006b; Ustundag and Korkmaz, 2009). Thus, UV-irradiation of PBDEs and triclosan could be expected to cause toxic effects in living systems and the extent and mechanism of these effects need to be understood if we want to design effective protective interventions. This study was

performed to provide critical information about the effects of UV-exposures of PBDEs and triclosan. To validate functionalities of methods used in this study, chlorpromazine which is a classic phototoxicant was employed as a positive control.

## Literature Review

### PBDEs

There are very few studies of phototoxicity of deca-BDE compared to physico-chemical studies of the photodegradation of deca-BDE. One study with photodegradation products of deca-BDE measured changes in AhR agonistic activity with CELCAD (the chick embryo liver-cell assay for dioxins) and the DR-CALUX (the dioxin responsive, chemically activated luciferase expression assay) using rat liver carcinoma cells (Olsman *et al.*, 2006). The photodegradation products of deca-BDE elevated levels of bio-TEQ (bioassay derived TCDD equivalents) compared to that of non-irradiated deca-BDE. The formation of AhR agonists in UV-exposed deca-BDE solution was wavelength-dependent and the maximum level of the formation was recorded in the UVA range (at 330 nm). In the UV-exposed deca-BDE samples, various PBDF congeners including mono to hexabrominated DF were found (Olsman *et al.*, 2006).

The subsequent study of Olsman *et al.* further investigated those PBDF congeners which were produced by irradiation of deca-BDE (Hagberg *et al.*, 2006b). The levels of PBDF and bio-TEQs increased with wider spectral irradiation (UV-ABC > UV-AB, UV-A) while the congener profiles were not wavelength dependent. Based upon the estimated chemically derived TEQs (chem-TEQs) considering the relative potency (REP) factors, it was suggested that non-TCDD like PBDFs mainly contribute to the bio-TEQs.

### Triclosan

In guinea pigs, 1 % triclosan with UV light exposures did not cause skin reactions such as change in skin thickness (NICNAS, 2009). Studies with human subjects reported no phototoxic reaction with exposure to 0.1-2.5 % triclosan for 1h followed by UV light exposure. In photo patch studies of patients with a photo-induced skin disease, 0.3-11.1 % of the patients showed positive response to triclosan with UV light exposure (NICNAS, 2009). In studies lacking detailed information, no phototoxicity was reported in Skh:hairless-1 mice, swine or human subjects whose shoulder blade or back was exposed to triclosan in soap and UV light (NICNAS, 2009).

Overall, while no or only weak phototoxicity of triclosan has been reported, many of the studies did not provide detailed information about their experiments (NICNAS, 2009). In addition, for photo patch studies, usually UVA light is used as a light source (Spielmann *et al.*, 2000). However, the wavelength where maximum absorption of triclosan occurs is around 290 nm, i.e. in the UVB range. Therefore, the experimental design of some of those photo patch studies might not be proper to test the phototoxicity of triclosan.

As described in Chapter 1, the FDA stated that further studies need to be performed to investigate the phototoxicity of triclosan, especially, concerning the conversion of triclosan to dioxin-like compounds and the effects of exposure of solar affected skin to triclosan (FDA, 2008).

### Chlorpromazine

Much more is known about the phototoxicity of chlorpromazine (CPZ). Chlorpromazine (CPZ) is one of the classic phototoxicants. It is a chlorinated heterocyclic polyaromatic hydrocarbon and used as a positive control for a variety of phototoxicity studies (Figure 4.1). In HaCaT, UVA irradiation of CPZ causes apoptosis (Kurita *et al.*, 2007). In human skin fibroblasts, cell growth inhibition and interaction

with DNA were found to be involved in phototoxicity of CPZ (Ljunggren *et al.*, 1980). In mouse lymphoma cells, irradiation of CPZ with UVA and UVB light caused cytotoxicity and genotoxicity (Struwe *et al.*, 2007). Irradiation of CPZ increased oxidative stress by enhancing free radical formation in mouse skin (Buettner *et al.*, 1987).

The photoreaction including photosensitization of CPZ involves cleavage of the chlorine bond producing chlorine radical and aryl radicals such as a promazinyl radical which may generate sulfur-centered radicals from sulfhydryl bonds and secondary radicals from peptide bond oxidation via hydrogen abstraction (Chignell *et al.*, 1985; Chignell, 1990; Struwe *et al.*, 2007). Additionally, peroxy radicals and radicals located on the sulfur atom are also found after the UV exposure. Promazinyl radicals are suggested to be both phototoxic and photoallergic by covalent interaction with proteins and thereby production of antigens (Chignell *et al.*, 1985). Promazinyl radicals are also suggested to react with DNA and cause genotoxicity, while pre-irradiated CPZ did not show genotoxic effects, indicating that the genotoxicity is due to short-lived free radicals (Nałęcz-Jawecki *et al.*, 2008). Photoionization could produce promazinyl cation radicals, however while the cation radicals might not be involved in the observed biological effects since they need UVC light exposure for their formation (Chignell *et al.*, 1985; Chignell, 1990; Struwe *et al.*, 2007). Superoxide anion is also possibly related to the phototoxicity of CPZ while singlet oxygen might not be important for the toxicity (Chignell *et al.*, 1985).

In HaCaT cells, glutathione (GSH) decreased after cells were exposed to CPZ and UV light (Reid *et al.*, 2007). In primary rat hepatocytes, photodegradation products of chlorpromazine at concentration higher than 100  $\mu$ M caused toxic effects including leakage of intracellular enzymes such as GPT (Glutamic-pyruvic transaminase) and GOT (glutamic-oxaloacetic transaminase) and detachment of cells (Castell *et al.*, 1987). In addition, 100 mM of the photodegradation products interrupted the production of albumin in hepatocytes in culture.



## Research Hypothesis

Our research hypothesis is that deca-BDE and triclosan have phototox activity in human skin cells and the toxic effects include cytotoxicity and growth inhibition, oxidative stress and genotoxicity.

## Materials and Methods

### Experimental Design

UV absorbance of chemicals of interest was measured first to determine if they should be tested for their phototoxic potential. If the UV absorbance of those chemicals was above a certain minimum level indicating photoreactivity, the chemicals were regarded as candidates for further tests of phototoxicity. A combination of toxicological end points including cytotoxicity, growth inhibition, oxidative stress, and genotoxicity were measured to investigate the phototoxic potential of the candidate compounds.

### Materials

#### Chemicals

DE-83R (>98% BDE-209) was obtained from Great Lakes Chemical Co. (West Lafayette, IN). Triclosan (Irgasan DP300) and chlorpromazine-hydrochloride (CPZ) was purchased from Sigma (C8138, Saint Louis, MO). Na<sub>2</sub>EDTA was obtained from Sigma (E-5134, St. Louis, MO). NaCl was obtained from rpi (S23025-3000.0, Mt. Prospect, IL). Tris (BP152-1) and Triton X-100 (BP151-500) were purchased from Fisher (Fair Lawn, NJ).

#### Cell Culture

HaCaT keratinocytes were obtained from Dr. C. Svensson and Dr. A. Klingelutz (Univ. of Iowa). Primary human fibroblasts were kindly provided by Dr. A. Klingelutz (Univ. of Iowa). Earl's balanced salt solution (EBSS) and Hank's balanced salt solution

(HBSS) with calcium chloride and magnesium chloride, Dulbecco's Modified Eagle Medium (DMEM), P/S (100 units/ml penicillin and 100 mg/ml streptomycin) and TrypExpress were purchased from Invitrogen (Grand Island, NY). Fetal bovine serum (FBS) was obtained from Atlanta Biologicals (Lawrenceville, GA). Flat-bottom polystyrene 12, 24 and 48-well plates were purchased from BD Falcon (Franklin Lakes, NJ). 0.20  $\mu$ M sterile filters were purchased from Corning (NY) and Comet Assay kit, from Trevigen (Gaithersburg, MD).

#### Irradiation and UV-VIS Spectroscopy

A quartz cuvette was purchased from Starna Cells (Cat. No. 3-Q-10, Atascadero, CA). Pyrex glass culture dishes were purchased from Fisher Scientific (Pittsburgh, PA).

### Methods

#### Irradiation

The light sources were 15 W broadband (270-400 nm, peak at 312 nm, X-15B) and 15 W narrowband (peak at 365 nm, X-15A) lamp (Spectronics, Westbury, NY) (Figure 4.2). A plastic plate lid was placed between UV lamps and samples to reduce the amount of short UVB light (< 290 nm) which could be highly toxic to cells (Figure 4.2) (Schirmer *et al.*). The light intensity was measured using an IL1400 BL radiometer with UV GAL.NIT detector (International Light Inc., Peabody, MA). The intensities of the light from the broadband and narrowband lamps were 140-210  $\mu$ W/cm<sup>2</sup> and 70-80  $\mu$ W/cm<sup>2</sup>, respectively, depending on the distance between the lamps and samples. The range of light intensity and energies which was used for our studies, is in the range of UV irradiation from natural sunlight (Table 4.1), while the range of natural UV irradiation varies depending upon locations where they are measured. Irradiation was performed in a biological safety cabinet.

### Spectral Changes after UV Irradiation

The deca-BDE mixture was dissolved in DMSO and diluted to 25  $\mu\text{M}$  in Hank's balanced salt solution (HBSS). Triclosan and chlorpromazine were dissolved in ethanol and diluted to 25  $\mu\text{M}$  in HBSS. Each solution in a Pyrex glass dish was exposed to UV light whose energy was 100  $\text{mJ}/\text{cm}^2$ . During the irradiation, samples were mixed by a magnetic stirrer. Absorption spectra at 250-400 nm of non-irradiated and irradiated samples were measured with a Perkin-Elmer Lambda 650 UV/Vis spectrophotometer at room temperature using a standard 1 cm quartz cuvette. Molecular extinction coefficients ( $\epsilon$ ,  $\text{L mol}^{-1} \text{cm}^{-1}$ ) of non-irradiated compounds were calculated by dividing the absorbance (= the sample absorbance – the solvent absorbance) by the concentration to determine if the compounds have sufficient absorption of UV light for photochemical reactions (OECD, 2004). If the coefficients are higher than 10, the compounds absorb light significantly (OECD, 2004). Absorption spectral changes after UV irradiation were also examined to study the formation of photodegradation products.

### Cell Culture Experiment

All cells were cultured in DMEM with 10 % FBS, and P/S (10 units/ml penicillin and 10 mg/ml streptomycin) at 37°C in humidified air with 5%  $\text{CO}_2$ . Cells were trypsinized by TrypExpress and sub-cultured every 2-3 days when cells reached about 80 % confluence. All materials for cell culture experiments were sterilized by autoclaving or disinfection with 70 % ethanol. Deca-BDE and triclosan were dissolved in DMSO or DMF and chlorpromazine was dissolved in PBS or ethanol to make their stock solutions. The stock solutions were diluted 1:1000 with EBSS or HBSS for chemical treatment of cells. During the whole procedures of cell culture experiments, special care was taken to minimize unintended exposure of cells or materials to light.

Toxicity studies were performed according to three different protocols, A with confluent cells and mixed narrowband plus broadband lamps (UVA & B), B with

confluent cells and broadband lamps only (UVB-centered) or C with exponentially growing cells and broadband lamps (UVB-centered).

#### Cytotoxicity Test (protocol A) for Studying Dose-response

##### Relationship for Test Compounds and UV Dose

Cytotoxicity was measured with a resazurine assay (a.k.a. alamar blue assay). For this assay, cell viability is determined by measuring the metabolic (redox-) activity of cells using resazurin as indicator dye which is a sensitive method for phototoxicity testing using skin cells (OECD, 2004; Nathalie *et al.*, 2006; Vinardell *et al.*, 2008b). For detection of cell death caused by photoreaction in mouse lymphoma cells (L5178Y), the resazurin assay was more sensitive than Trypan Blue which is used to measure cytotoxicity indicated by breakage of cell membrane integrity (Struwe *et al.*, 2007).

Viable cells reduce resazurin [oxidized form (blue)] to resorufin [fluorescent intermediate (red)] and the viability is determined by measuring the amount of resorufin following exposures compared to the control. In our study, 5 mM resazurin stock in PBS was diluted to 50  $\mu$ M with DMEM. Cell media were replaced with 50  $\mu$ M resazurin and cells were incubated for 1 hr at 37 °C in humidified air with 5 % CO<sub>2</sub>. The fluorescence intensity of resorufin was measured with a Fluor GENios Pro microplate reader (Tecan, Switzerland) (excitation at 535 nm / emission at 590 nm) (O'Brien *et al.*, 2000).

For testing cytotoxicity of menadione as a positive control (Figure 4.7), HaCaT were seeded in a 48-well plate at  $20 \times 10^4$  and grown to their confluence. They were treated with 100  $\mu$ M menadione in EBSS with Ca<sup>2+</sup> and Mg<sup>2+</sup> for 1 h at 37 °C in humidified air with atmospheric CO<sub>2</sub>. The cells were washed with EBSS and incubated with fresh DMEM with FBS for 24 h at 37 °C in humidified air with 5 % CO<sub>2</sub>, and then cytotoxicity was measured with the resazurin test.

For dose-response studies of effects of chemical and UV light (Figure 4.8-4.11), HaCaT and HSF were seeded in 48-well plates at  $20 \times 10^4$  and  $5 \times 10^4$ , respectively, and

grown to their confluence. 1.6-50  $\mu\text{M}$  chlorpromazine hydrochloride (CPZ) working solution was prepared by diluting the stock solution with PBS with  $\text{Ca}^{2+}$  and  $\text{Mg}^{2+}$  (final PBS concentration = 1 %). Triclosan and deca-BDE stock in DMSO were diluted with EBSS with  $\text{Ca}^{2+}$  and  $\text{Mg}^{2+}$  to prepare 0.8-25  $\mu\text{M}$  working solutions (final DMSO concentration = 0.1 %). Before treatment with the compounds, cells were washed with EBSS and then exposed to the compounds for 1 h at 37 °C in humidified air with atmospheric  $\text{CO}_2$ . For each chemical, one plate was exposed to UV light (+UV) and the other plate was not exposed to UV light (-UV). The light source was a set of broadband lamp and narrowband lamps. The doses of UV light were 25, 50, and 100  $\text{mJ}/\text{cm}^2$  which was not very toxic to cells, reducing cell viability by less than 20% based upon preliminary tests (OECD, 2004). Immediately after UV irradiation, working solutions were replaced with fresh media. After 24 h further incubation at 37°C in humidified air with 5%  $\text{CO}_2$ , cytotoxicity was measured with the resazurin test. Only for a dose-response study of deca-BDE and UV light in HaCaT, cells were exposed two times for 48 h and then cytotoxicity was measured.

#### OECD Test (protocol C) Paired with Cytotoxicity Test with UVB (protocol B)

The 3T3 NRU (neutral red uptake) phototoxicity test (NRU-PT) has been used for identifying chemicals which have potential of photo irritation, allergic reaction and genotoxicity (Spielmann *et al.*, 1994; Spielmann *et al.*, 1998a; Spielmann *et al.*, 1998b). This method is suggested in the testing guideline for phototoxic chemicals used by OECD (Organisation for Economic Co-operation and Development) (OECD, 2004; Vinardell *et al.*, 2008a). While the OECD test as originally designed for using Balb/c 3T3 cells and neutral red dye as a cell viability dye, it could also be conducted with other skin cells like spontaneously immortalized human keratinocytes (HaCaT) and dyes such as resazurin using modified protocols (Clothier, 1999; Benavides *et al.*, 2004; Vinardell

*et al.*, 2008a). With different cell lines (3T3 and HaCaT) and dyes (neutral red and resazurin), phototoxicity tests of chemicals like surfactants showed similar results compared to the original OECD test procedure (Benavides *et al.*, 2004). Also with human skin fibroblasts and keratinocytes, the resazurin assay provides comparable results to clinical photo patch tests (Benavides *et al.*, 2004). For our experiments of phototoxicity with the OECD test (Figure 4.12-4.15), the original NRU-PT protocol was modified using resazurin as a cell viability indicator.

The only difference between the previously described cytotoxicity test (protocol A) and the OECD test (protocol C) is that the latter one is performed with subconfluent, exponentially growing cells and the use of two broad-band (UVB-centered) lamps. For each test chemical, 20 and 5 x 10<sup>4</sup>/mL of HaCaT and HSF respectively were seeded in two flat-bottom polystyrene 48-well plates. Cells were grown to sub-confluent (about 50 % confluence). One plate was exposed to UV light (+UV) and the other plate was not exposed to UV light (-UV). After chemical treatment, the UV+ plate was exposed to UV light (100 mJ/cm<sup>2</sup>) from a set of two broadband UV lamps, which is not a toxic dose, reducing cell viability by less than about 20%. The two of broadband lamps were used as a new combination of UV lamps to increase intensity of UVB light which is overlapped with the expected absorption ranges of test chemicals. The light intensity was maintained at 100 mJ/cm<sup>2</sup> to enhance photolytic reaction. The non-irradiated plate (UV-) was kept in the dark during the irradiation. Immediately after UV irradiation, the buffers were replaced with fresh media. After 24 h further incubation at 37 °C in humidified air with 5 % CO<sub>2</sub>, the resazurin assay was performed. Toxicity was determined by comparing sample groups to their solvent controls.

IC<sub>50</sub> values were calculated by regression lines. Two parameters were used to evaluate phototoxicity of chemicals. PIF (Photo-Irritation-Factor) is calculated by the formula  $PIF = IC_{50} (-UV) / IC_{50} (+UV)$  and MPE (mean photo effect) is obtained by comparing dose-response curves of UV+ and UV- (OECD, 2004). The details in the

calculation of the MPE are described in the legend of Table 4.3. There are three categories of phototoxicity based upon the parameters as followings:  $PIF < 2$  or  $MPE < 0.1$  = no phototoxicity,  $2 < PIF < 5$  or  $0.1 < MPE < 0.15$  = probable phototoxicity, and  $PIF > 5$  or  $MPE > 0.15$  = phototoxicity (OECD, 2004). The IC<sub>50</sub>, PIF and MPE values were determined with the public software, Phototox (ver. 1.0) provided by OECD (OECD, 2004). The experiment system was validated by checking PIF and MPE values for CPZ (positive control) which is known as a phototoxicant (OECD, 2004).

To enable a comparison of results with growing cells (OECD test) with those in quiescent cells, the same exposure conditions used in the OECD tests were also used with confluent cultures (protocol B) (Figure 4.12-4.15). This also allowed the comparison of UVA & B (protocol A) and UVB-centered light exposure only.

#### Toxicity of Photodegradation Products

To test toxic effects of photodegradation products (Figure 4.16 and 4.17),  $20 \times 10^4$ /mL of HaCaT cells were seeded in a flat-bottom polystyrene 24-well plate. Sub-confluent cells (about 50% confluence) were incubated with the non-irradiated and irradiated samples from the study of spectral changes of chemicals as described above for 24 h at 37 °C in humidified air with 5% CO<sub>2</sub>. After 24 h incubation, growth inhibition was evaluated by measuring the viability with the resazurin assay.

#### Oxidative Stress

The production of oxidative stress was quantitatively analyzed using a fluorescent probe, 2',7'-dichlorofluorescein-diacetate (DCFH-DA, Molecular Probes, Eugene, OR). UV-induced oxidative stress has been measured with DCFH-DA (Tobi *et al.*, 2000; Chignell and Sik, 2003). DCFH-DA is hydrolyzed in cells to 2',7'-dichlorofluorescein (DCFH), where DCFH is then oxidized to 2',7'-dichloro-fluorescein (DCF) by ROS such as hydrogen peroxide, hydroxyl radical, peroxy radical, and peroxy nitrite anion (Gomes

*et al.*, 2005). The fluorescence dye was dissolved in DMF to make a 5 mM stock solutions and diluted with HBSS to make 5  $\mu$ M working solution. The fluorescence of DCF was measured with the microplate reader (ex. 485 nm/em. 535 nm).

20 x 10<sup>4</sup>/ml of HaCaT were seeded in two flat-bottom polystyrene 24 or 48-well plates and grown to the confluence. 100  $\mu$ M of menadione was used as a positive control for measuring oxidative stress with DCFH-DA dye (Figure 4.7). HaCaT were treated with menadione for 1 h in EBSS at 37 °C in humidified air with atmospheric CO<sub>2</sub>. Cells were washed with EBSS and 5  $\mu$ M of DCFH-DA was added to cells and DCF intensity was measured after 3 h incubation at 37 °C in humidified air with atmospheric CO<sub>2</sub>.

For UV experiments (Figure 4.18 and 4.19), confluent cells were treated with the test chemicals and UV+ plates were exposed to UV light with two of the broadband lamps at 100 mJ/cm<sup>2</sup> while UV- plates were kept in the dark. Immediately after UV exposure, plates were washed with HBSS and 5  $\mu$ M DCFH-DA was added to cells. DCF intensity was measured after 3 h and 24 h incubation at 37 °C in humidified air with atmospheric CO<sub>2</sub>.

### Genotoxicity

The genotoxicity was measured by the COMET assay, also called single cell gel electrophoresis (SCGE), which is a sensitive and cost-effective method to detect a wide range of DNA damage including single strand break. DNA is liberated from cells by lysis, hydrolyzed, unwound, moved by electrophoresis and stained for the observation of DNA damage. The identification and quantification of DNA damage is performed by fluorescent microscopy (Singh *et al.*, 1988).

At the beginning of our study, we considered following a modified version (protocol I) of the traditional protocols used for the Comet assay (Trevigen, 2009; Xie *et*



*al.*, 2010). Cells were seeded at  $40 \times 10^4$ /ml in 12-well cell culture plates and grown to about 90 % confluent status before treatment. Before exposure to test chemicals, 0.7 % agarose (0.7 mg low melting agarose/100 ml PBS) was melted in a water bath at 100 °C for 5 min and cooled down in a water bath to 37 °C for at least 1 h and kept at this temperature. Alkaline solution (> pH 13) was also prepared by adding 200 mM EDTA (Trevigen, Gaithersburg, MD) to 1 M NaOH. Cells in one plate were washed with HBSS and treated with chemicals in HBSS for 1 h in an ambient air and then exposed to 100 mJ/cm<sup>2</sup> of UV light from a set of broadband and narrowband UV lamp while the other plate was treated identically and kept in the dark during the UV exposure. After UV exposure, cells were washed twice with HBSS, trypsinized, mixed with DMEM, transferred to 15 mL tubes, counted, centrifuged at 200 g for 5 min, washed with cold HBSS and then resuspended in cold HBSS to a cell density of  $1 \times 10^5$ /mL. 5 µL of cell suspension were mixed with 50 µL of warm 0.7 % low-melting agarose solution and pipetted onto sample spots of Trevigen Comet Slides (Trevigen, Gaithersburg, MD). The agarose layer mixed with cells was solidified in a refrigerator at 4 °C for 15 min and then the cells were lysed in the refrigerator at 4 °C in lysis buffer (100 mM Na<sub>2</sub>EDTA, 2.5 M NaCl, 10 mM Tris (pH 10.0), 1% Triton X-100) for 40 min. The slides were then immersed into alkaline solution and kept in the solution at RT for 30 min. In a walk-in refrigerator, the slides were parallel placed in an electrophoresis chamber and immersed into pre-chilled alkaline solution. Electrophoresis was conducted for 30 min with 1 V/cm and 300 mA. After electrophoresis, the slides were carefully taken from the chamber, washed three times with deionized water three times and then immersed into 70% ethanol for 5 min. The slides were dried overnight. 50 µL of SYBR green fluorescent dye was placed on each agarose-well spot and kept for 5 min. After the slide had dried completely, Comets were observed with a 10-fold objective of an Axio A1 Imager epifluorescence microscope with an Axio Cam MRm camera (Zeiss, Jena, Germany). To analyze Comets, the Comet Score™ 1.5 software (free at

[http://www.autocomet.com/products\\_cometscore.php](http://www.autocomet.com/products_cometscore.php)) was used. For each sample, 100 cells were randomly selected to measure and calculate parameters including tail length (in pixel), % DNA in tail, tail moment (= tail length X %DNA in tail) and olive moment (= (Tail.mass center - Head.mass center) X %DNA in tail/100). No data are reported here using this protocol I, since all results were negative and inconsistent.

Then we employed a modified Comet protocol (protocol II) to increase the sensitivity of detecting UV induced genotoxicity by reducing the recovery of the DNA damage during the trypsinization (Wischermann *et al.*, 2007; Trevigen, 2009) and short-lived free radical-based lesions could be involved in the mechanism of genotoxicity. For this method, unlike the conventional method, about 750 HaCaT cells in 100  $\mu$ L media were seeded on each sample spot of a Comet slide. The slides were placed in a Petri dish and incubated at 37 °C in humidified air with 5 % CO<sub>2</sub> for 8 h. After cells were firmly attached to the slides, they were washed with HBSS and 100  $\mu$ L of test sample solution was placed on each spot of a slide for 1 h. After treatment, the slides were exposed to 100 mJ/cm<sup>2</sup> of UV light from a set of broadband and narrowband UV lamps. After UV exposure, cells were washed with HBSS and melted warm agarose was placed over the cells immediately. Though cells were well attached on the slides and looked healthy before they were treated, sometimes dead cells were observed under the microscope after washing or chemical treatment and we could not proceed to the next step for the Comet assay following the modified protocol. If cells were healthy and not lost, the next steps after placing agarose on the cells were the same as the protocol I above. In Figure 4.20, the results from the Comet assay following protocol II are shown. Due to the above mentioned technical problems this assay was not repeated. Because DNA could be damaged due to not only genotoxic effects but also cell death activating endonucleases, proper ranges of chemical concentrations need to be determined to avoid false positive genotoxicity (Struwe *et al.*, 2007). It was reported that higher than 50% cell viability measured with resazurin assay does not cause false positive Comet (Struwe *et al.*, 2007).

In our study, concentrations of chemicals which show higher than 60 % viability were used for the Comet assay to avoid false positive results. Based upon preliminary study, 10  $\mu\text{M}$  of chlorpromazine, 6.3, 12.5 and 25  $\mu\text{M}$  of deca-BDE and 100  $\text{mJ}/\text{cm}^2$  of UV light were chosen for the Comet assay.

### Statistical Analyses

Data from every experiment, except the Comet assay with protocol II, are presented as the mean $\pm$ standard deviations. At least triplicates were used for statistical analyses. The student t-test was used to compare means of two groups whose data are normally distributed. The Shapiro-Wilk test was used to see if data are normally distributed. The F-test was used to analyze if the variances of the data are equal. Depending upon the equity of the variances, either the t-test for equal or unequal variance was employed. For the data that are not normally distributed, the Mann-Whitney test was used to compare means of two groups. A p-value less than 0.05 was regarded as significant. SPSS 17 for Windows (SPSS Inc, Chicago, Illinois) and Excel 2007 (Microsoft, Redmond, WA, USA) with statistiXL (version 1.8, statistiXL, Broadway–Nedlands, Australia, [www.statistiXL.com](http://www.statistiXL.com)) were used to perform statistical analyses.

## Results and Discussion

### Absorption Spectra and Their Changes after UV Irradiation

According to the OECD phototoxicity guideline, chemicals do not need to be tested for their phototoxic potential if their molar absorptivities ( $\epsilon$ ,  $\text{L mol}^{-1} \text{cm}^{-1}$ ) are lower than 10 (OECD, 2004). The molecular absorptivities of all three test chemicals were at least 20 fold higher than 10 indicating that their potential of phototoxicity needs to be examined (Table 4.2). For deca-BDE, its molar absorptivity was not determined exactly because its wavelength for the local maximum absorbance could not be chosen while the calculated molar absorptivity at 306 nm was similar to the reference value

(Eriksson *et al.*, 2004). The absorption spectra of CPZ, deca-BDE, and triclosan were changed after UV exposure, suggesting they were photolytically degraded (Figure 4.3-5). For triclosan, its spectral changes were dependent on the irradiation time and the pattern of changes did not seem to be unidimensional, i.e. continuous increase/decrease or left/right shift, probably because some of degradation products were subsequently degraded over time (Figure 4.6). Previous studies also reported spectral changes of triclosan depending upon UV light exposure (Wong-Wah-Chung *et al.*, 2007). The pattern of changes was not similar to our observation possibly because a different light source (UVC at 254 nm) was used for irradiation of triclosan (Wong-Wah-Chung *et al.*, 2007).

#### Cytotoxicity with Confluent Cells and UVA & B:

##### Concentration and UV-dose Response

Menadione was used as a positive control for cytotoxicity measurement with resazurin. Exposure of confluent HaCaT to menadione significantly increased (more than five folds) cytotoxicity compared to its solvent control verifying that resazurin assay works for measuring cytotoxicity (Figure 4.7).

For a dose-response study of CPZ and UV light (Figure 4.8), UV irradiation alone did not alter cytotoxicity of the solvent control. UV irradiation significantly enhanced cytotoxicity of CPZ only at 100 mJ/cm<sup>2</sup> and 50 µM compared to the UV-exposed solvent control while cytotoxicity of non-UV exposed group at the same concentration of CPZ was not significantly different from the corresponding solvent control. Exposures of HaCaT to CPZ at other concentrations did not cause significant increase in cytotoxicity regardless of UV exposure. Therefore, CPZ showed synergistic phototoxicity only at 50 µM.

In the dose-response study of triclosan and UV light (Figure 4.9), UV irradiation alone did not alter cytotoxicity of the solvent control group. Triclosan exposures alone at

12.5 and 25  $\mu\text{M}$  compared to the non-UV exposed solvent controls. In addition, at 12.5  $\mu\text{M}$ , UV irradiation with 25, 50 and 100  $\text{mJ}/\text{cm}^2$  further increased the cytotoxicity of 12.5  $\mu\text{M}$  triclosan suggesting a synergistic cytotoxic effect of triclosan and UV irradiation. At 25  $\mu\text{M}$ , cytotoxicity was dominated by triclosan treatment alone causing  $\geq 90\%$  cell death. Exposures of HaCaT to triclosan at other concentrations did not cause significant increase in their cytotoxicities regardless of UV exposure.

For a dose-response study of deca-BDE and UV light in HaCaT, chemical treatment and UV exposure were done two times for 48 h (Figure 4.10) because preliminary study showed that one time exposure of HaCaT to the highest concentration of deca-BDE and/or UV dose did not affect the cytotoxicity. After the two time exposures, UV irradiation alone did not alter cytotoxicity of the solvent control group except UV light at 100  $\text{mJ}/\text{cm}^2$ , which caused  $\sim 40\%$  cell death. Deca-BDE alone caused only mild cytotoxicity, if any. The cytotoxicity of deca-BDE was significantly enhanced only by 100  $\text{mJ}/\text{cm}^2$  UVA & Band 25  $\mu\text{M}$  of deca-BDE. Exposures of HaCaT to deca-BDE at other concentrations did not cause significant increase in cytotoxicity regardless of UV exposure. In a dose-response study of deca-BDE and UV light in HSF, UV irradiation alone did not increase cytotoxicity of the solvent control group. Overall, as the deca-BDE concentration increased, cytotoxicity increased without UV exposure. While it appears that UV irradiation with deca-BDE treatment did increase cytotoxicity at certain concentrations, it is not possible to conclude that there was a clear difference of cytotoxicity between deca-BDE alone and combined exposures of deca-BDE and UV light due to large standard deviations probably because of loss of HSF after washing and treatment steps.

## Toxicity Test with Growing Cells (OECD test) and Confluent Cells

### OECD Test

The IC<sub>50</sub> values determined in confluent cells exposed to UVA & B and phototoxicity parameters obtained following OECD guidelines (growing cells, UVB-centered) are shown in Table 4.3. As expected, the IC<sub>50</sub> of the UV exposed cells with CPZ treatment was significantly lower than that of the non-UV exposed group (Figure 4.8). The MPE of chlorpromazine in our study (0.38) is in the range of the reference values (0.33-0.63) indicating that our irradiation system and method for measuring phototoxicity were properly working (OECD, 2004). Our PIF value of CPZ was much lower than the reference PIF of CPZ which should be higher than 14.4 (OECD, 2004). It might be because a narrower range of CPZ concentrations was used in our study compared to the reference study which used wider and different ranges of concentrations for the non-UV and UV exposed group. For triclosan, overall, there was no difference of the IC<sub>50</sub> between the non UV-exposed (0.10) and UV exposed group (0.10) except the difference at 8.2  $\mu$ M of triclosan (Table 4.3. and Figure 4.9.). This result suggests that triclosan is not phototoxic, which is reflected in its low PIF and MPE values. For deca-BDE, the IC<sub>50</sub> could not be determined from either the non-UV exposed group or the UV-exposed group because cell viability for the whole range of triclosan concentrations and UV light energies was better than 60 %. Therefore, the PIF could not be calculated and the MPE was very low suggesting that deca-BDE is not phototoxic based upon the OECD test (Figure 4.10).

### Cytotoxicity Test with Confluent Cells, UVB-centered

Irradiation of CPZ significantly enhanced cytotoxicity of CPZ in HaCaT (Figure 4.12). Like the result from the OECD test of CPZ, for UV-exposed group, the viability decreased to about 0 % as CPZ concentration increased while without UV exposure, cell

viability was not reduced to below 70 % even at the highest concentration of CPZ. Compared to the UVA & B exposure (Figure 4.8), UVB-centered light exposure alone was by far more synergistic with CPZ. Irradiation of triclosan did not clearly affect viability of HaCaT and only the highest concentration of triclosan (25  $\mu$ M) lowered viability to below 50 % (Figure 4.13). Compared to the cytotoxicity results with a broadband (max. at 312 nm) and a narrowband (max. at 365 nm) (Figure 4.9), here, no synergistic effect was observed at 12.5  $\mu$ M and UV irradiation of 25, 50 and 100  $\text{mJ}/\text{cm}^2$ . This might be due to the difference in the light sources. It was reported that dioxin compounds such as dichloro-*p*-dioxin (DCDD) were detected in the photolysis of triclosan with UVA light (max. at = 365 nm), which could generate less OH radicals compared to UVC light (max. at 254 nm). No DCDD was found in samples from UVC irradiation of triclosan suggesting that OH radicals could interrupt formation of DCDD by irradiation of UV light (Son *et al.*, 2009). In our study, two UV lamps whose maximum intensity is in the UVB range were used and the light intensity could be high enough to produce more OH radicals compared to UVA light exposure and subsequently reduce the amount of DCDD and the toxicity of the photodegradation products. One additional observation is the higher toxicity of triclosan in growing cells (OECD test) compared to confluent cells. More detailed tests are needed to elucidate whether their higher toxicity is due to cell killing or cell growing inhibition. For deca-BDE, there was no combined effect of UV irradiation on cytotoxicity (Figure 4.14). Irrelevance of deca-BDE concentration, UV irradiation caused almost constant toxicity of about 20-40 % cell death while deca-BDE alone did not cause cytotoxicity.

In HSF, the cytotoxicity was totally dependent on the level of triclosan whereas UV exposure did not have an apparent influence on the cytotoxic effect as it didn't in HaCaT (Figure 4.13 and 4.15). Deca-BDE did not affect the viability of HSF while UV irradiation-induced cytotoxicity (about 20-40 %) as UV did on HaCaT (Figure 4.14. and 4.15.). A previous triclosan study reported that in HSF, 24 h treatment with lower than

17.3  $\mu\text{M}$  of triclosan in cell culture media did not show cytotoxicity and 34.5  $\mu\text{M}$  of triclosan caused about 50 % cell death (Park *et al.*, 2004). HaCaT was more sensitive to triclosan exposure showing that 17.3  $\mu\text{M}$  of triclosan cause about 40 % cytotoxicity and over 90 % of cells exposed to 34.5  $\mu\text{M}$  of triclosan were dead (Park *et al.*, 2004). In contrast, our study showed that HSF is more sensitive to triclosan exposure. The difference between the two studies might be due to the different exposure conditions, i.e. 1 h in buffer vs 24 h in medium.

#### Toxicity of Photodegradation Products

Irradiation of triclosan with 500  $\text{mJ}/\text{cm}^2$  reduced the toxic effect of triclosan on HaCaT cells at a 16  $\mu\text{M}$  concentration, whereas 100  $\text{mJ}/\text{cm}^2$ -pretreatment of triclosan did not significantly influence toxicity. At 8.2  $\mu\text{M}$ , both 100 and 500  $\text{mJ}/\text{cm}^2$  did not affect toxicity (Figure 4.16). There was no significant effect on cell number in deca-BDE and irradiated deca-BDE exposed HaCaT for all concentration of deca-BDE and both of UV energies (100 and 500  $\text{mJ}/\text{cm}^2$ ) (Figure 4.17).

It was hypothesized that irradiation of triclosan enhances the cytotoxicity of triclosan based upon the fact that photodegradation products of triclosan include polychlorinated dibenzo-p-dioxins (PCDDs) and halogenated phenol compounds (Sanchez-Prado *et al.*, 2006). PCDDs cause toxic effects on skin such as chloracne (Birnbaum *et al.*, 2003) and the growth of normal human keratinocytes was inhibited by exposure to TCDD in an *in vitro* study (Loertscher *et al.*, 2001). However, we observed the opposite results. One possible explanation for that is that UV light intensity and dose might not be sufficient for producing enough amounts of certain photodegradation products which could cause toxic effects but enough for degrading triclosan. Another possibility is that some of the toxic photodegradation products could not be taken from the irradiated samples due to their low solubility in aqueous media. Additionally, it is possible that the degradation products are originally not toxic to inhibit growth of HaCaT



cells. Furthermore, as described above, recent research reported that dioxin compounds such as DCDD were detected in the photolysis of triclosan with UVA light (max. at = 365 nm), which could generate less OH radicals compared to UVC light (max. at 254 nm). No DCDD was found in samples from UVC irradiation of triclosan suggesting that OH radicals could interrupt formation of DCDD by irradiation of UV light (Son *et al.*, 2009). In our study, two UV lamps whose maximum intensity is in the UVB range were used and the light intensity could be high enough to produce more OH radicals compared to UVA light exposure and subsequently reduce the amount of DCDD and the toxicity of the photodegradation products.

### Oxidative Stress

Menadione was used as a positive control for oxidative stress measurement using the DCFH-DA fluorescent dye. Fluorescence significantly increased by exposure of HaCaT cells to 100  $\mu$ M of menadione indicating that DCFH-DA assay works for measuring oxidative stress with our experimental conditions (Figure 4.7).

After 3h incubation of cells with DCFH-DA following triclosan and UV exposures, the fluorescence intensities had large variations and there was no clear trend of changes in DCF values over concentrations of triclosan with or without UV irradiation though generally, non-UV exposed groups showed higher DCF values than UV-exposed groups (Figure 4.18). Oxidative stress was measured again at 24 h after loading DCFH-DA to cells. Unlike the measurements at 3 h after the incubation, UV irradiation of triclosan-treated cells caused a gradual and synergistic increases in oxidative stress over triclosan concentrations, whereas fluorescence in non-UV exposed groups did not vary depending on level of triclosan (Figure 4.18). For deca-BDE, both measurements at 3 h and 24 h after DCFH-DA incubation did not show either any effect of deca-BDE alone or combined effect of deca-BDE and UV light. As seen with triclosan, UV light alone reduced the level of oxidative stress (Figure 4.19). The delayed increase in oxidative

stress with triclosan and UV exposures and the decrease in the variations over incubation time could be due to our modified experimental condition. Typically, after DCFH-DA is loaded into cells in balanced salt solution for 1 h, the cells are cultured in cell culture media for some period of time to recover their normal activities and then the media are replaced with fresh balanced salt solution. DCF values are measured immediately after the cells are treated with toxic agents. However, for studies of oxidative stress caused by photoreaction, DCFH-DA could not be loaded before UV exposure because of the possibility of photo-oxidation of DCFH-DA to DCF producing false positive results (Chignell and Sik, 2003). Therefore, the lack of recovery time in our study might delay the oxidation of DCFH by toxicants. Due to this reason, it might not be possible to measure short-lived oxidative stress underestimating the oxidative stress, caused by UV light and chemicals. Because the time period for measuring DCF values was relatively long (24 h), DCF values of DCFH-DA controls without cell were subtracted from all sample values to prevent false positive results from auto-oxidation of DCFH-DA to DCF. The late occurring synergistic effect of triclosan plus UVB-centered light on intracellular oxidative stress needs further evaluation.

### Genotoxicity

Due to technical difficulties, only preliminary results were obtained from an experiment following protocol II and it could not be confirmed that the results are repeatable. The preliminary study showed that as expected irradiation of 10  $\mu\text{M}$  of CPZ significantly increased the genotoxicity compared to the UV or CPZ only exposed HaCaT groups (Figure 4.20). At 6.3, 12.5 and 25  $\mu\text{M}$  of deca-BDE, UV irradiation enhanced genotoxicity compared to their UV only exposed control. Overall, UV irradiation of deca-BDE enhanced genotoxicity compared to UV or deca-BDE exposure only groups.

It was suggested that the promazinyl radicals could be reacted with C-8 of guanosine-5'-monophosphate (GMP) producing DNA adducts to cause genotoxicity via

hydrogen abstraction (Nałęcz-Jawecki *et al.*, 2008). Early in this thesis, we suggested that free radicals such as brominated diphenyl ether radicals are generated via hydrogen abstraction. It is possible that the diphenyl ether radicals interact with genetic materials to cause genotoxic effects.

### Conclusions

Deca-BDE and triclosan were candidates for phototoxicity testing because their UV absorption properties and propensity to cause a photoreaction in the range of UVB and UVA wavelengths relevant for biological systems.

At relatively high concentration of triclosan, mixed irradiation from UVB and UVA-centered lamps synergistically enhanced cytotoxicity in HaCaT while UVB-centered irradiation did not cause a synergistic effect. In addition, UVB-centered irradiation of triclosan did not enhance the cytotoxicity compared to non-UV exposed triclosan. Combined toxicity of triclosan and UV light could be wavelength dependent suggesting that type of light sources affects the composition of the photodegradation products. For deca-BDE, the synergistic cytotoxicity in HaCaT was shown only with repetitive exposures of the highest concentration and highest dose of mixed irradiation from UVB and UVA-centered lamps. Otherwise no synergistic effect was found. The photodegradation products of deca-BDE did not cause inhibition of the growth of HaCaT. Based upon the OECD-related tests with HaCaT, neither triclosan nor deca-BDE is suggested to be a phototoxicant. While the combined effects of chemical and UV light were not affected by the type of cells, HSF were more sensitive to chemical treatment with triclosan and deca-BDE.

With UV irradiation, oxidative stress in HaCaT was generally dependent on the concentration of triclosan while triclosan alone did not change the oxidative stress level suggesting that combined exposures of UV light and triclosan generates unexpected

effects on the oxidative stress. Deca-BDE did not contribute to the level of the oxidative stress which was dominated by UV irradiation.

To our knowledge, this is the first in vitro study of phototoxicity of deca-BDE and triclosan in human skin cells. It would provide general ideas about their phototoxicity and useful information about experimental conditions for future research.

Figure 4.1. Chemical structure of chlorpromazine.

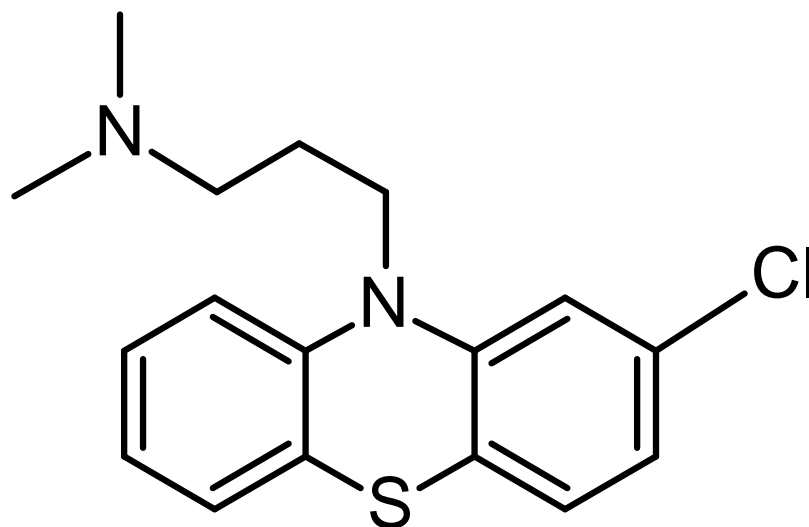
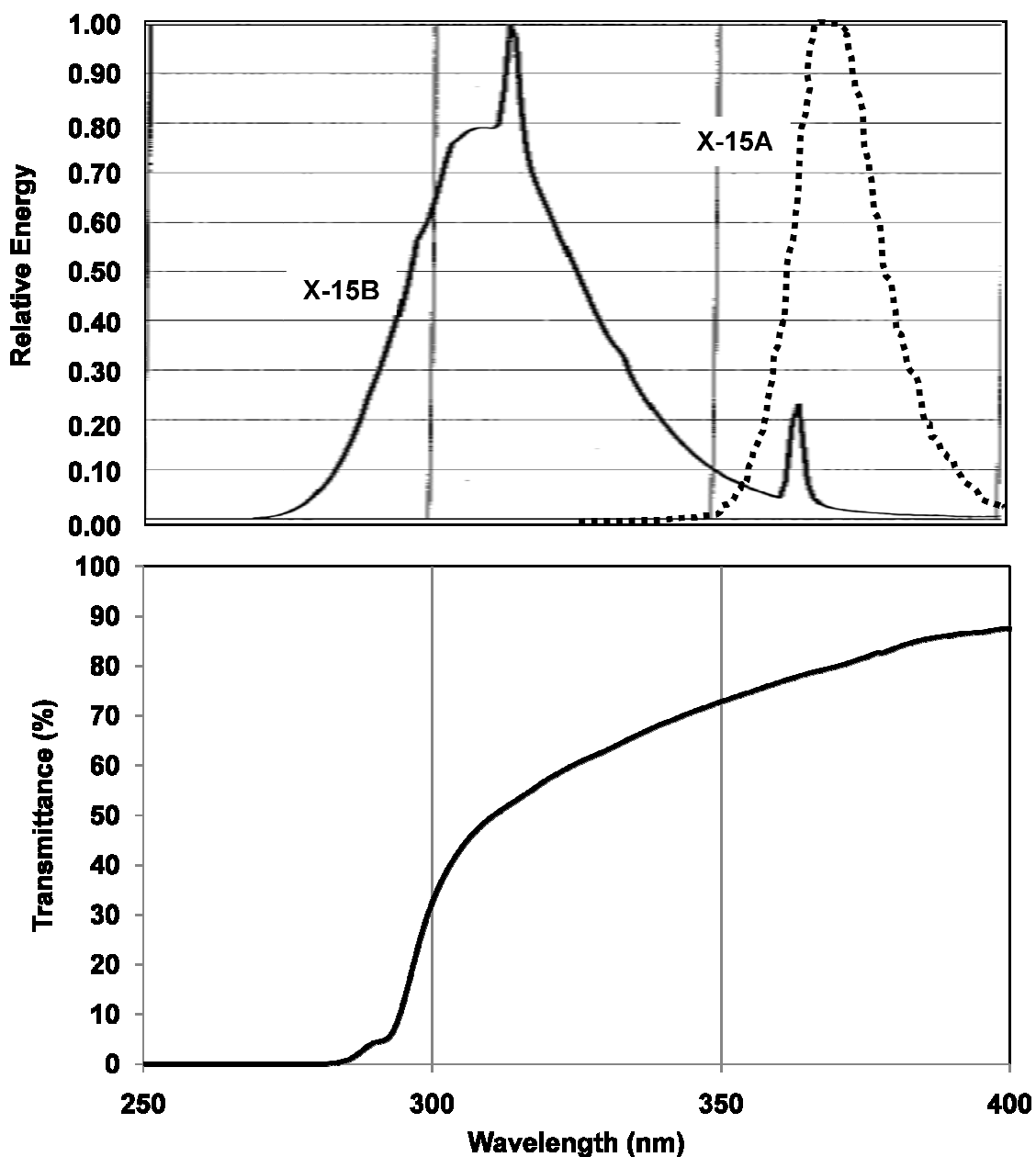


Figure 4.2. Irradiation spectra of UV lamps and absorption spectrum of a plate lid.



Top: Relative spectral energy distributions of X-15B (solid line) and X-15A (dotted line) UV lamps respectively.

Bottom: Transmittance (%) of a plate lid. Data provided from Spectronics (Westbury, NY) were edited to draw the relative spectral energy distribution curve for the UV lamp.

Figure 4.3. Spectral change of chlorpromazine after UV exposure.

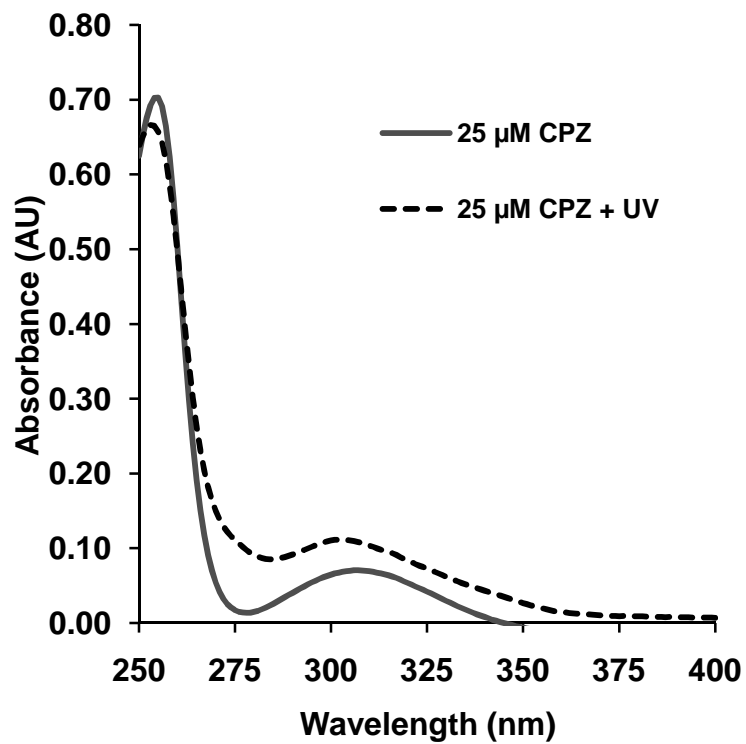


Figure 4.4. Spectral change of triclosan after UV exposure.

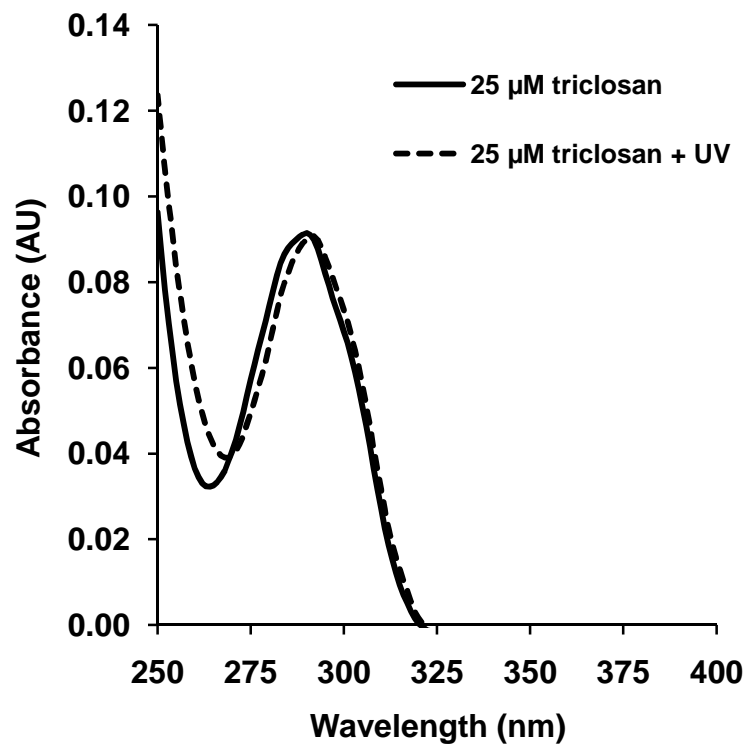




Figure 4.5. Spectral change of deca-BDE after UV exposure.

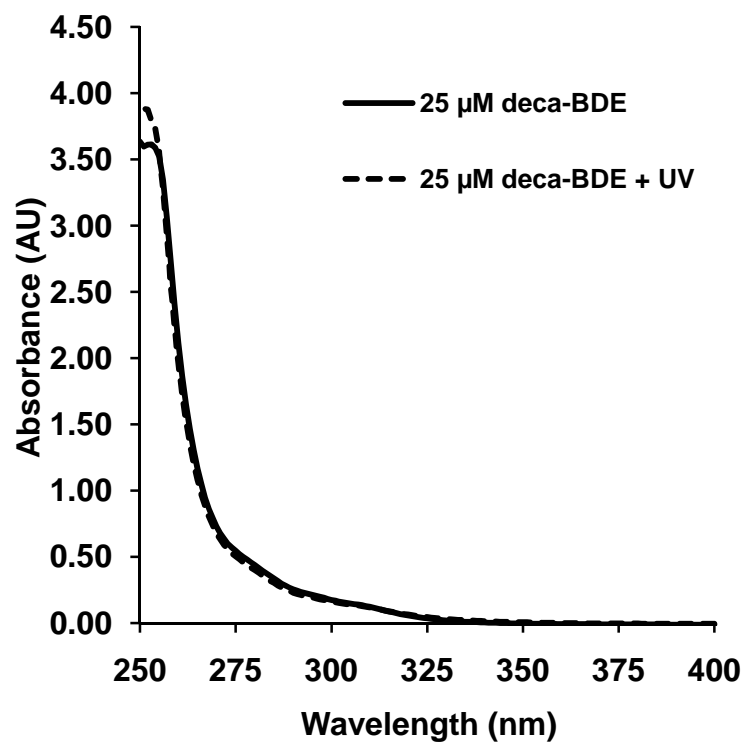


Figure 4.6. UV energy dependent spectral changes of triclosan.

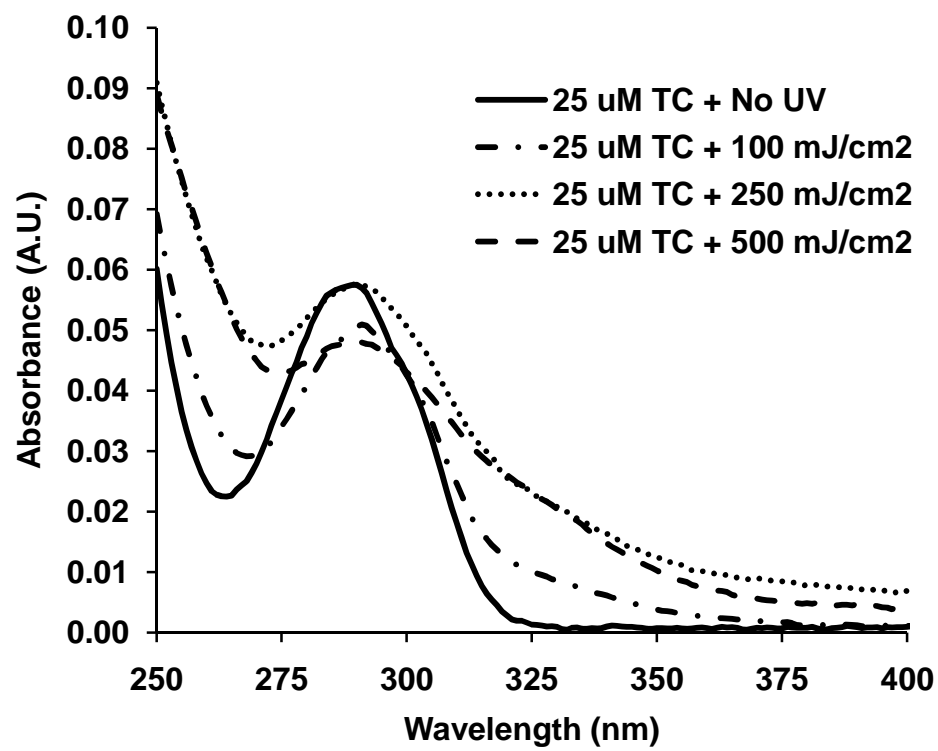
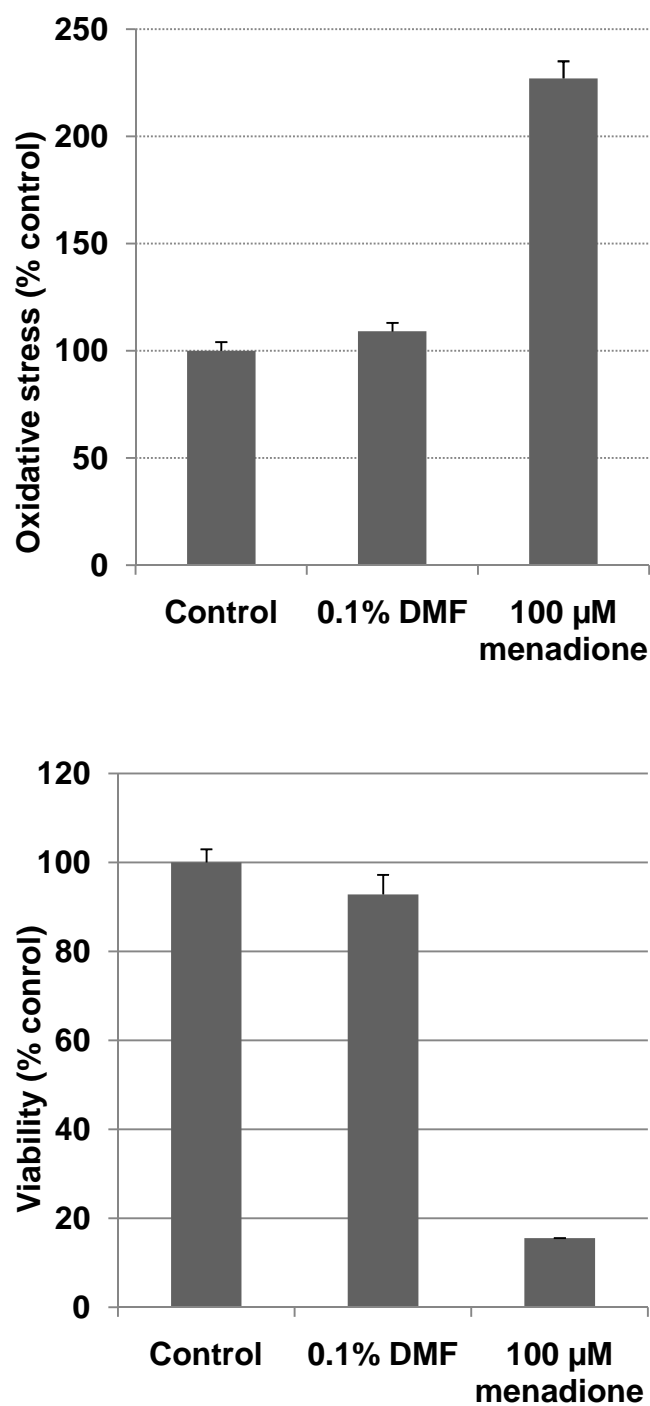
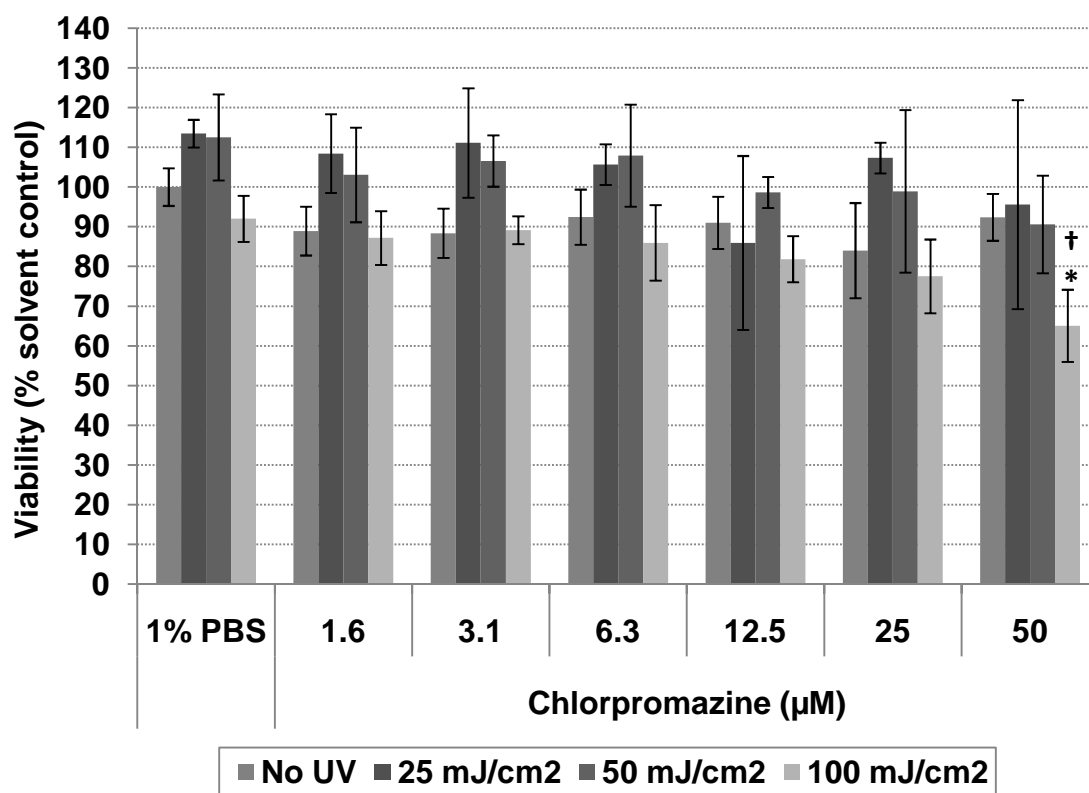


Figure 4.7. Positive control for measurements of oxidative stress and viability.



Oxidative stress was measured with DCFH-DA and cell viability was measured with resazurine. Both assays were working properly with menadione in HaCaT.

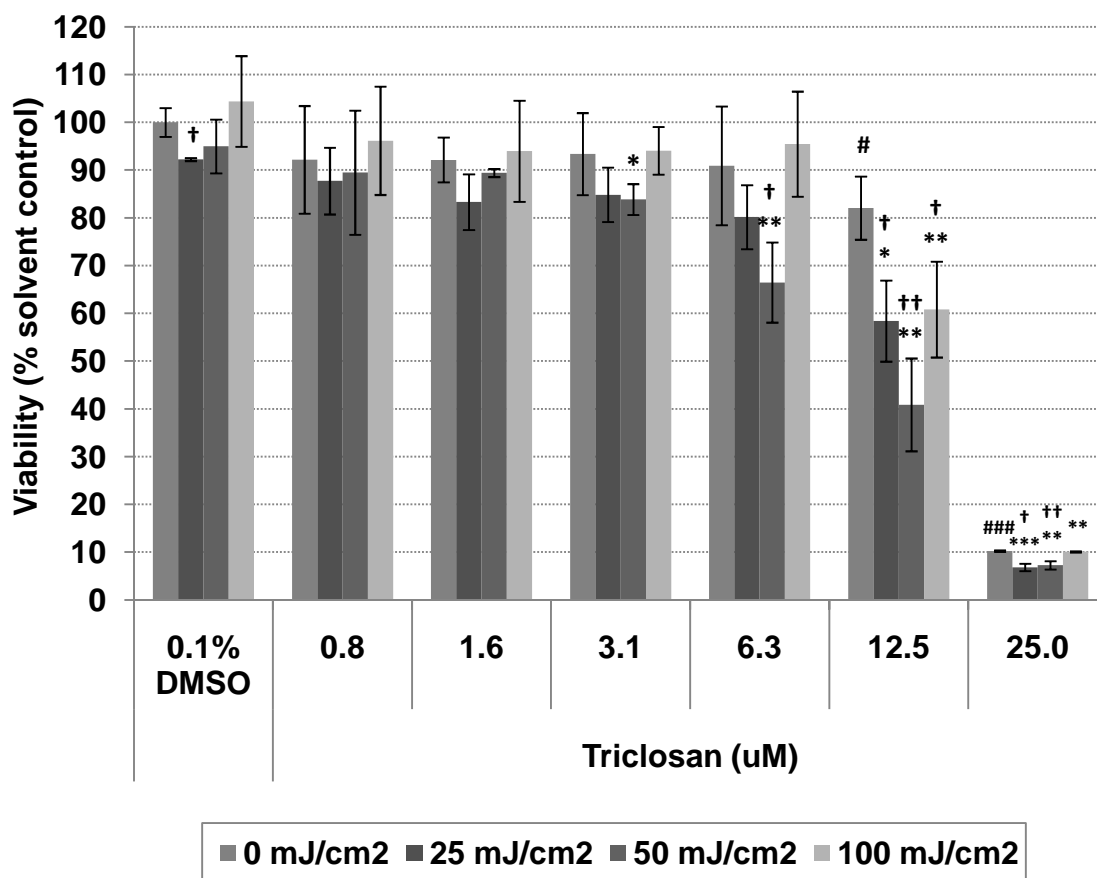
**Figure 4.8. Dose-response study of cytotoxicity of chlorpromazine and UV light on HaCaT.**



† Significantly different from non UV-exposed sample with same chemical treatment;  $p < 0.05$

\* Significantly different from UV-exposed solvent control with same UV energy;  $p < 0.05$

Figure 4.9. Dose-response study of cytotoxicity of triclosan and UV light on HaCaT.

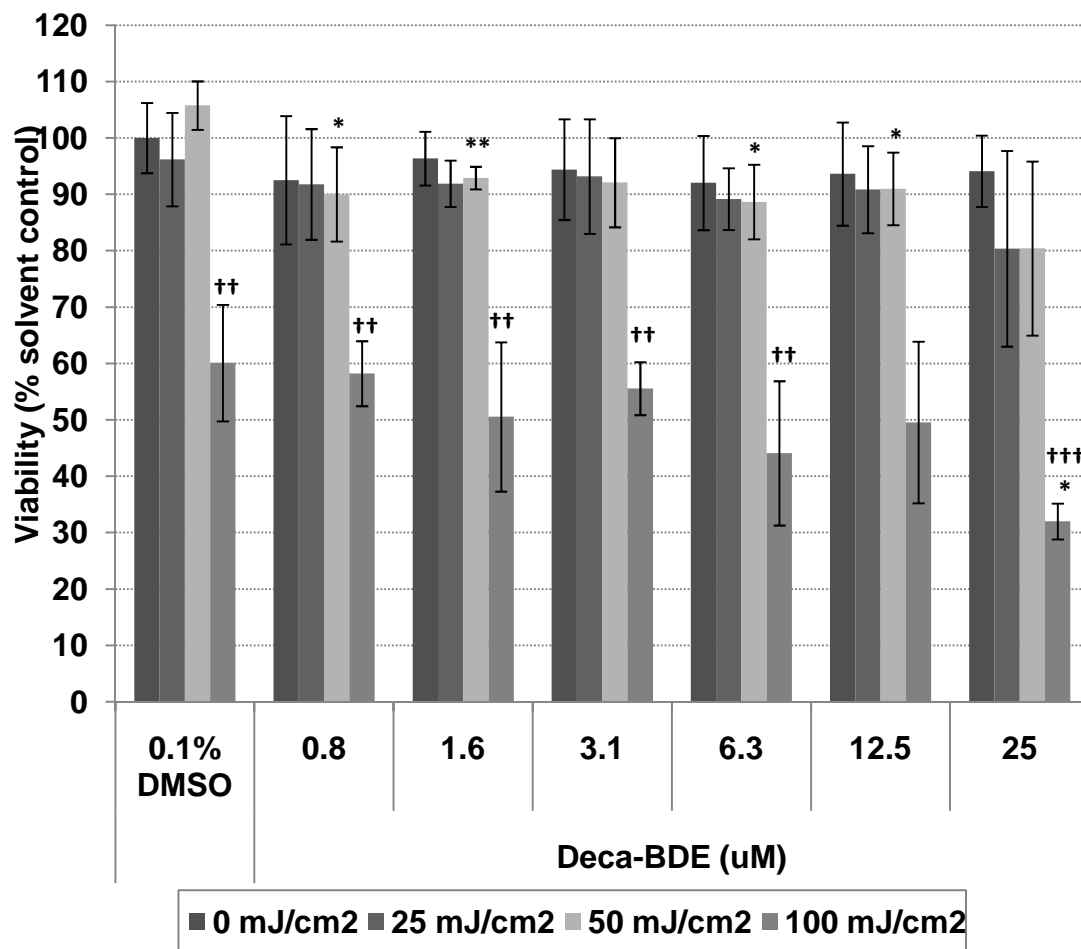


# Significantly different from solvent control;  $p < 0.05$  (#),  $p < 0.001$  (###)

† Significantly different from non UV-exposed sample with same chemical treatment;  $p < 0.05$  (†),  $p < 0.01$  (††)

\* Significantly different from UV-exposed solvent control with same UV energy;  $p < 0.05$  (\*),  $p < 0.01$  (\*\*),  $p < 0.001$  (\*\*\*)

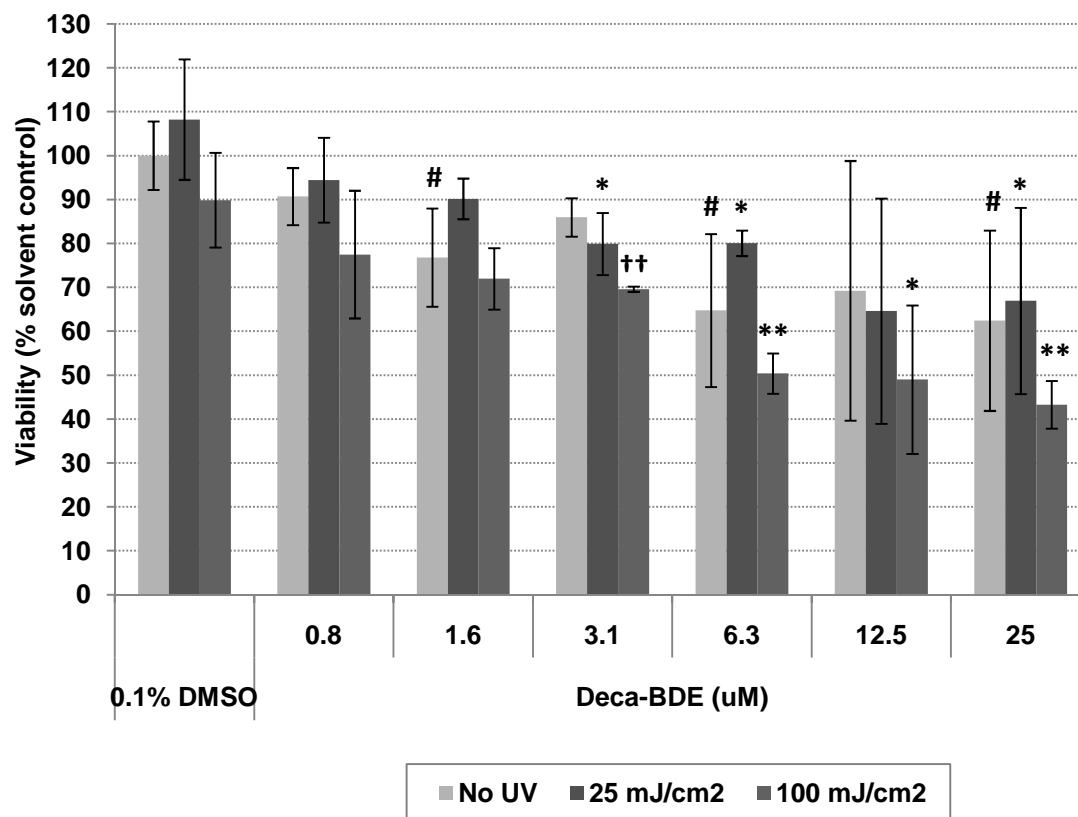
**Figure 4.10. Dose-response study of cytotoxicity of deca-BDE and UV light on HaCaT.**



† Significantly different from non UV-exposed sample with same chemical treatment; p<0.01 (††), p<0.001 (†††)

\* Significantly different from UV-exposed solvent control with same UV energy; p<0.05 (\*), p<0.01 (\*\*)

**Figure 4.11. Dose-response study of cytotoxicity of deca-BDE and UV light on HSF.**

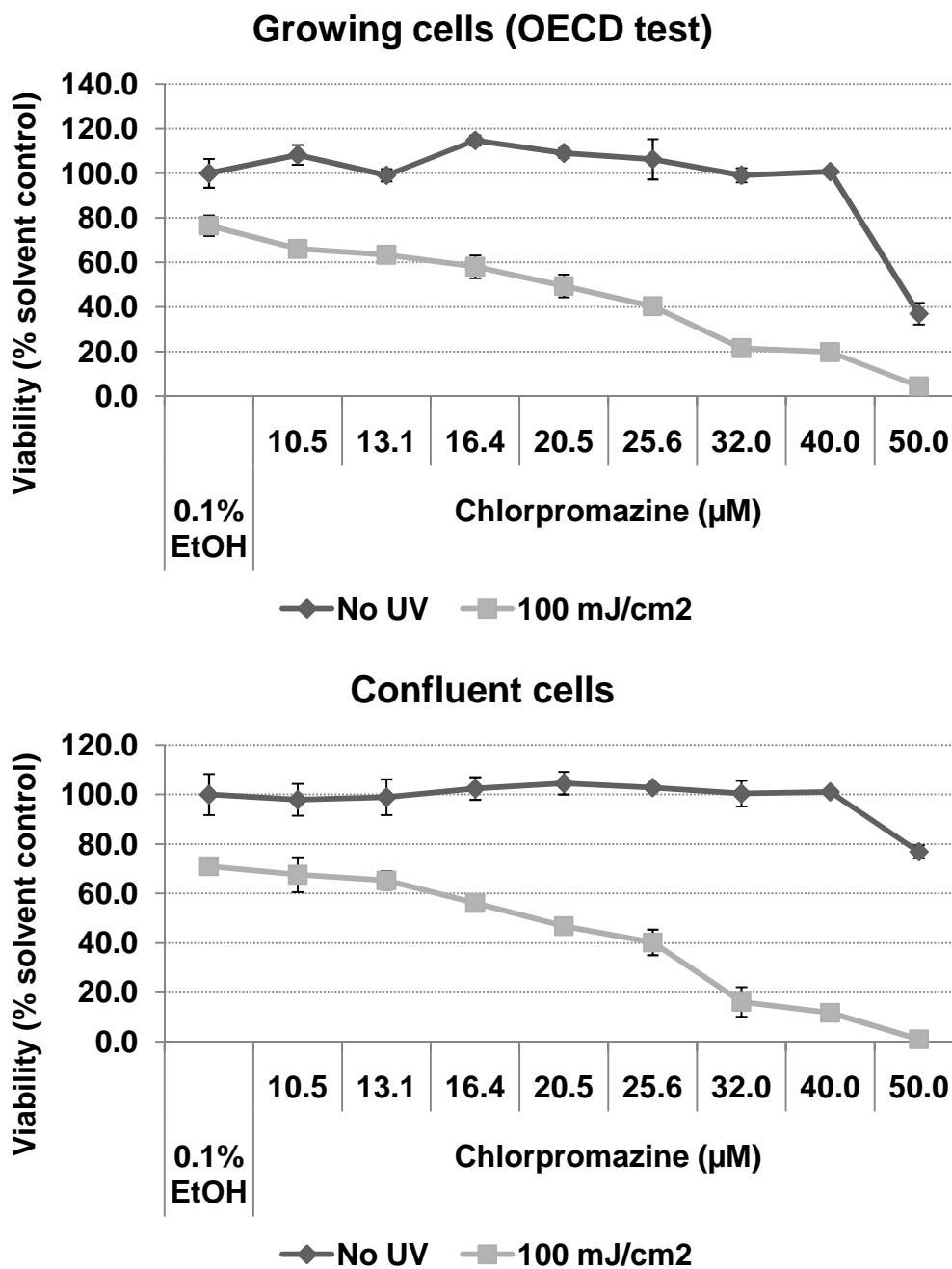


# Significantly different from solvent control;  $p < 0.05$  (#)

† Significantly different from non UV-exposed sample with same chemical treatment;  $p < 0.01$  (††)

\* Significantly different from UV-exposed solvent control with same UV energy;  $p < 0.05$  (\*),  $p < 0.01$  (\*\*)

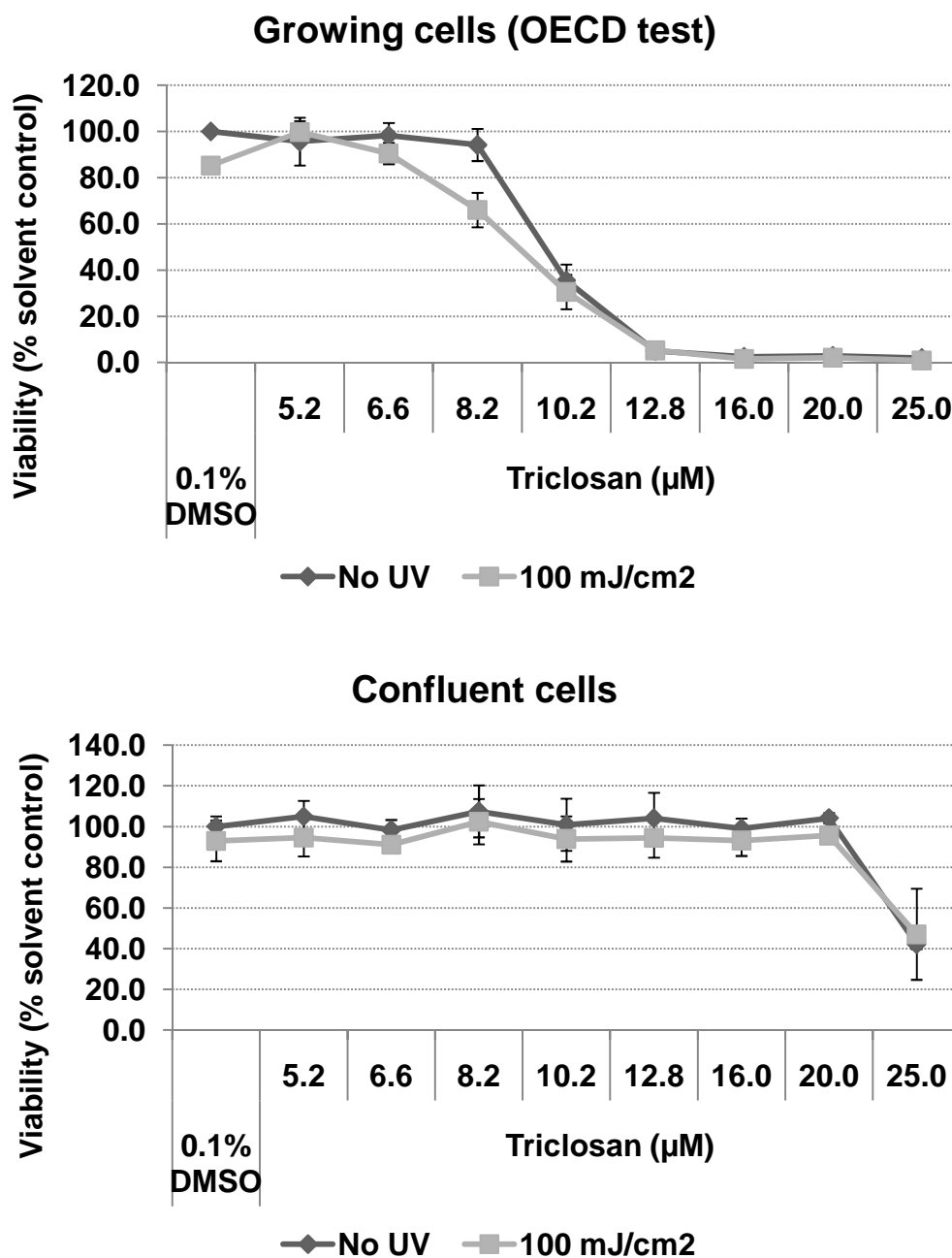
Figure 4.12. Toxicity of combined exposures of exponentially growing (OECD test) and confluent HaCaT cells to UVB-centered light and chlorpromazine.



For exponentially growing cells, the IC<sub>50</sub> for cells exposed to UV and chlorpromazine was much lower than the IC<sub>50</sub> for cells not exposed to UV light. For confluent cells, the IC<sub>50</sub> for the non UV exposed group could not be determined. Both of toxicity data indicate that chlorpromazine has phototoxic effects on HaCaT.

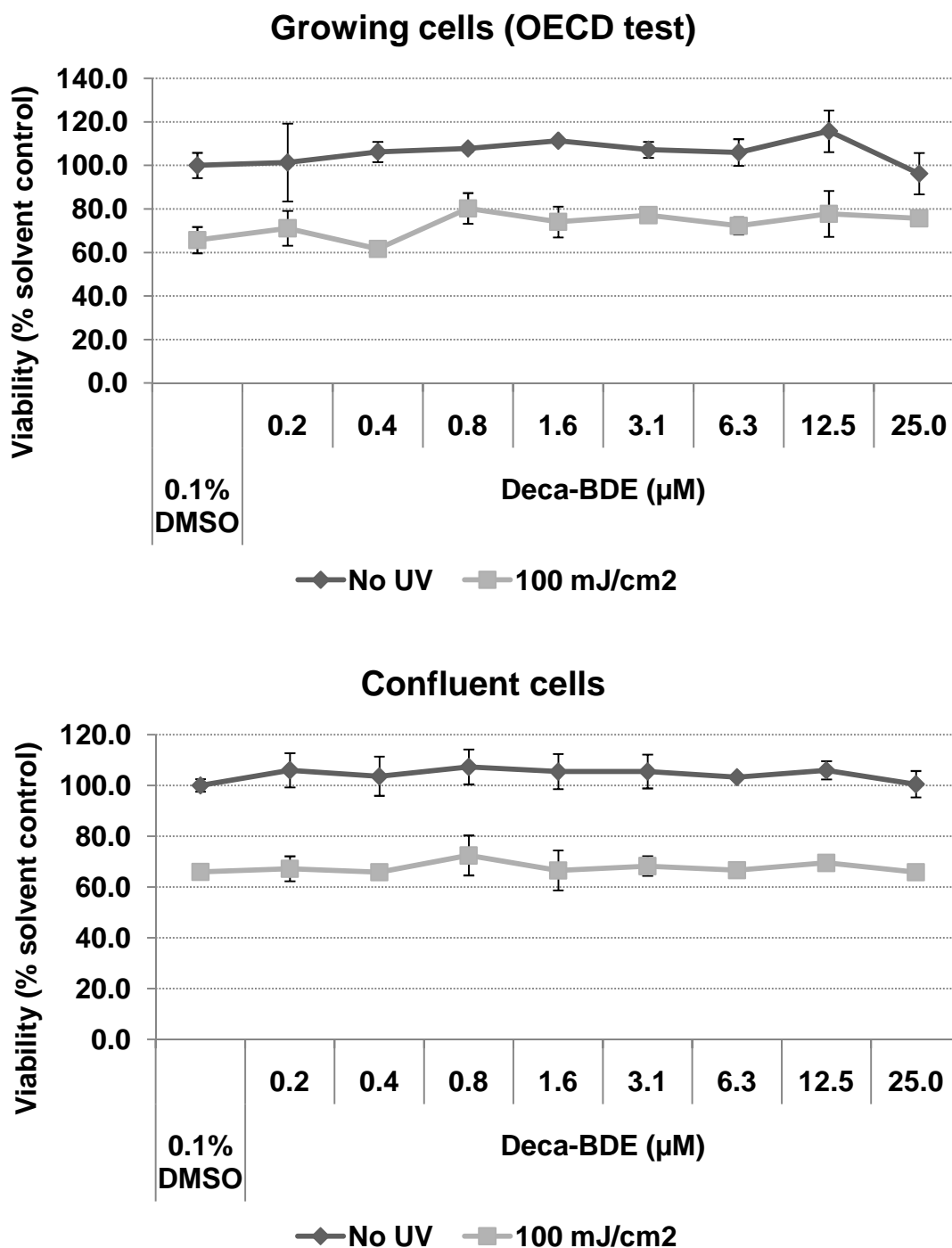


Figure 4.13. Toxicity of combined exposures of exponentially growing (OECD test) and confluent HaCaT cells to UVB-centered light and triclosan.



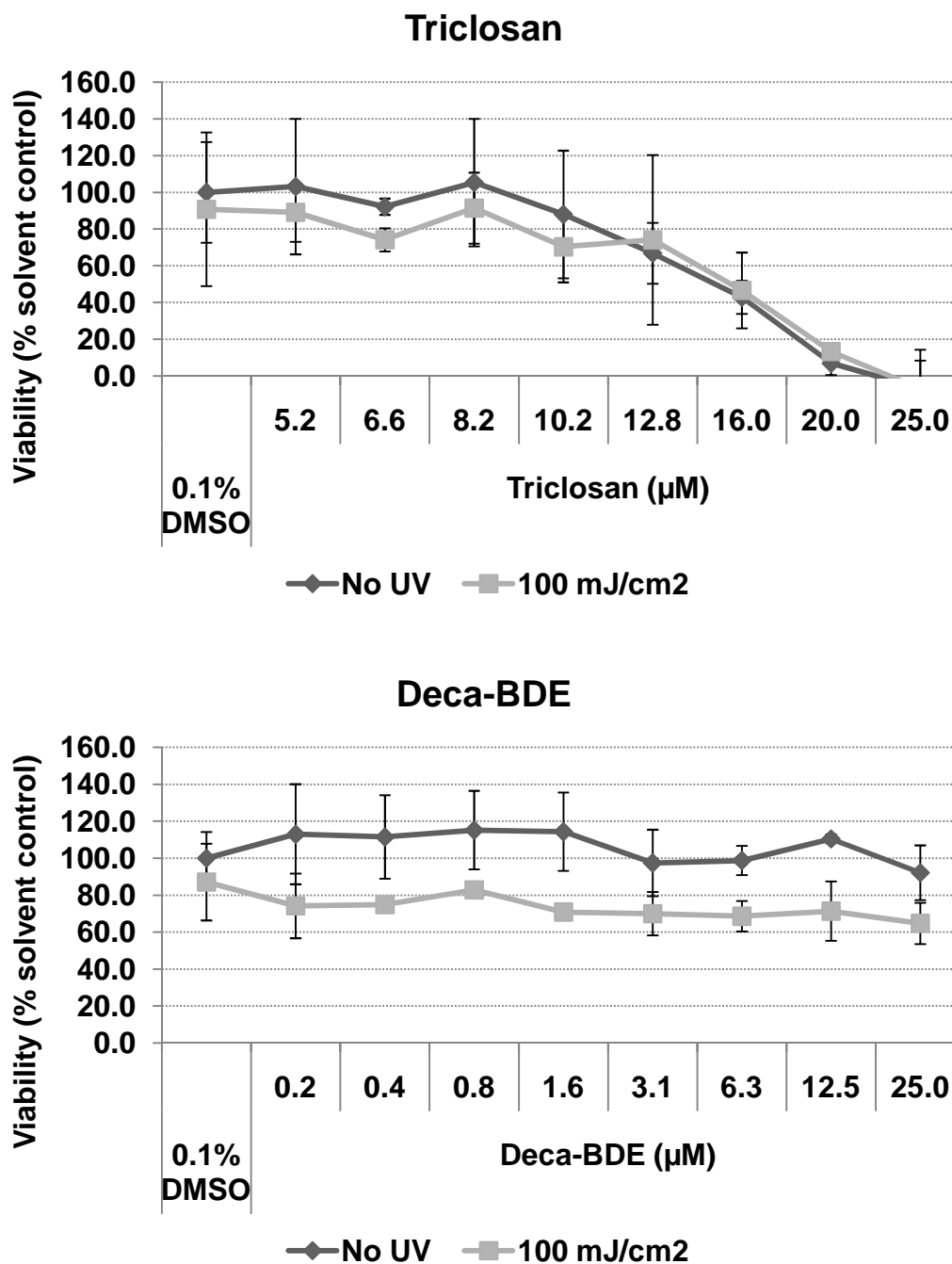
For both growing and confluent cells, the IC<sub>50</sub> for cells exposed to UV and triclosan was not significantly higher than the IC<sub>50</sub> for cells not exposed to UV light. Only with 8.2  $\mu\text{M}$  of triclosan, UV exposure significantly more toxicity of HaCaT cells compared to UV exposed only group.

Figure 4.14. Toxicity of combined exposures of exponentially growing (OECD test) and confluent HaCaT cells to UVB-centered light and deca-BDE.



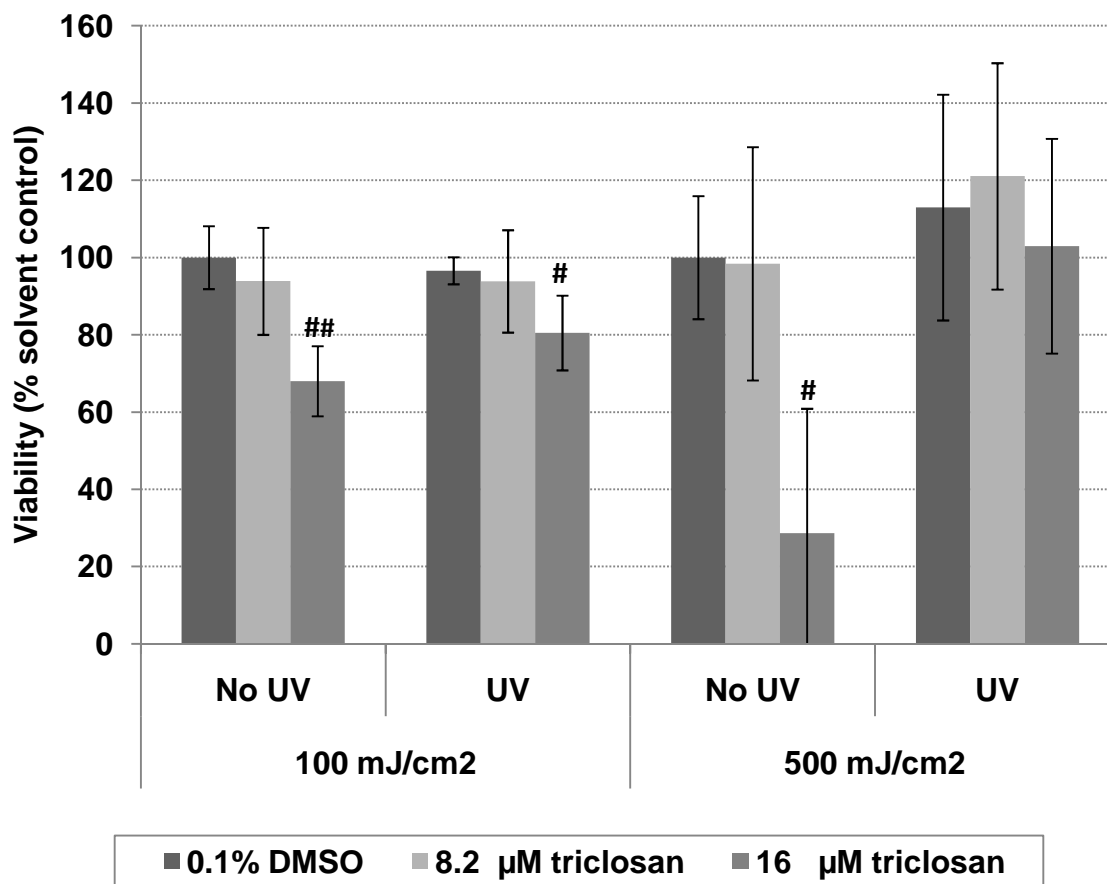
For both growing and confluent cells, there was no combined effect of UV light and deca-BDE exposures on HaCaT.

Figure 4.15. Cytotoxicity of combined exposures of HSF to UV light and triclosan or deca-BDE.



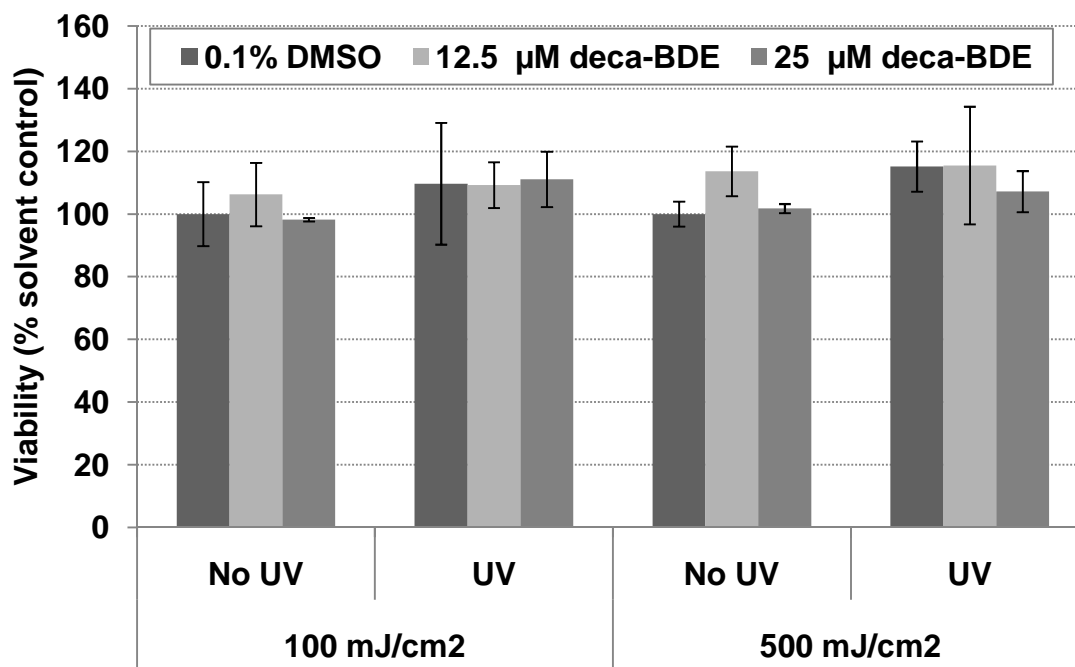
For cytotoxicity, the IC<sub>50</sub> for cells exposed to UVB-centered light and triclosan was not different from the IC<sub>50</sub> for cells treated with triclosan without UV exposure. For triclosan and deca-BDE, the IC<sub>50</sub> values could not be determined.

Figure 4.16. Effects of pre-irradiated triclosan on growing HaCaT cells.



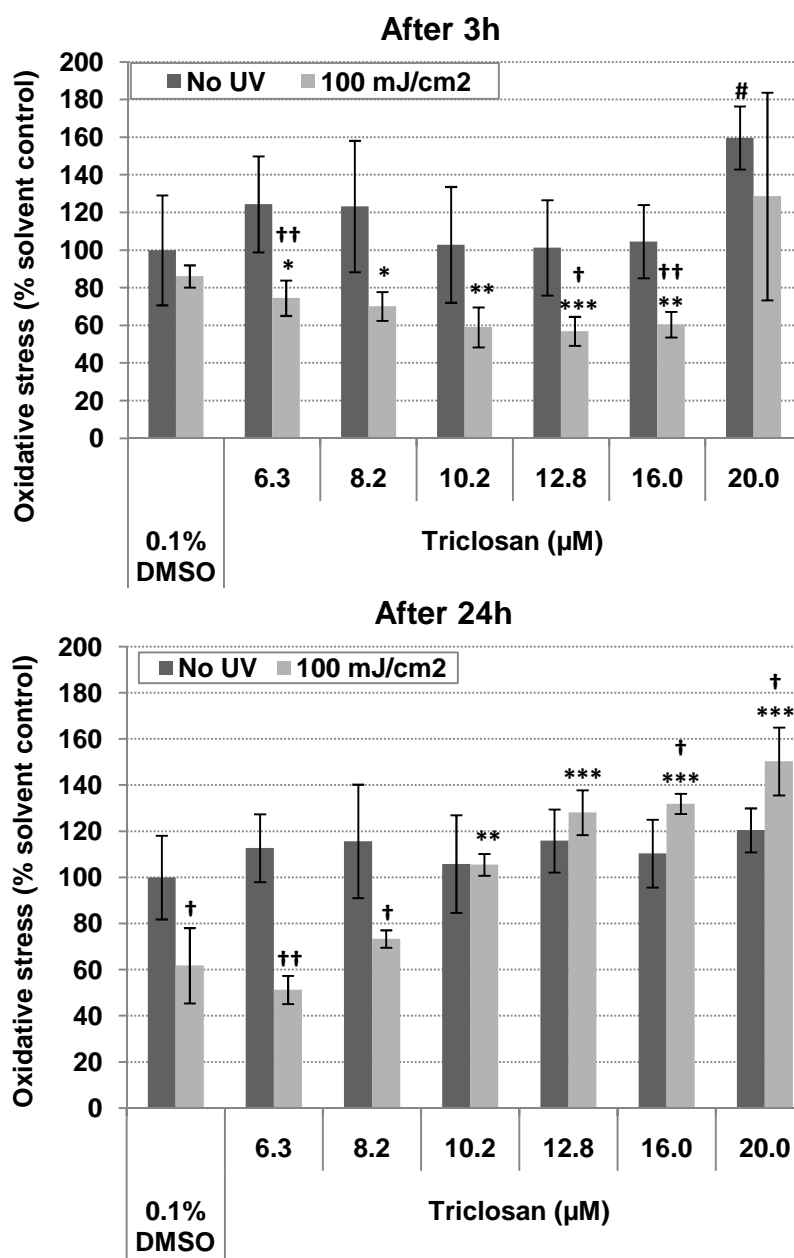
# Significantly different from UV exposed or non-UV exposed solvent control;  $p < 0.05$   
(#),  $p < 0.01$  (##)

Figure 4.17. Effects of pre-irradiated deca-BDE on growing HaCaT cells.



Chemicals were placed in a glass dish covered with a plated lid and exposed to UVB-centered light. HaCaT cells were treated with the pre-irradiated chemicals for 30 min and then further incubated in fresh cell culture media for 24h. After the further incubation, growth inhibition was measured by the Resazurin assay.

**Figure 4.18. Oxidative stress of triclosan and/or UVB-centered light in confluent HaCaT.**



HaCaT were treated with chemicals for 60 min and then exposed to 100 mJ/cm<sup>2</sup> UVB-centered light. DCF values were measured 3h or 24 h after UV exposure.

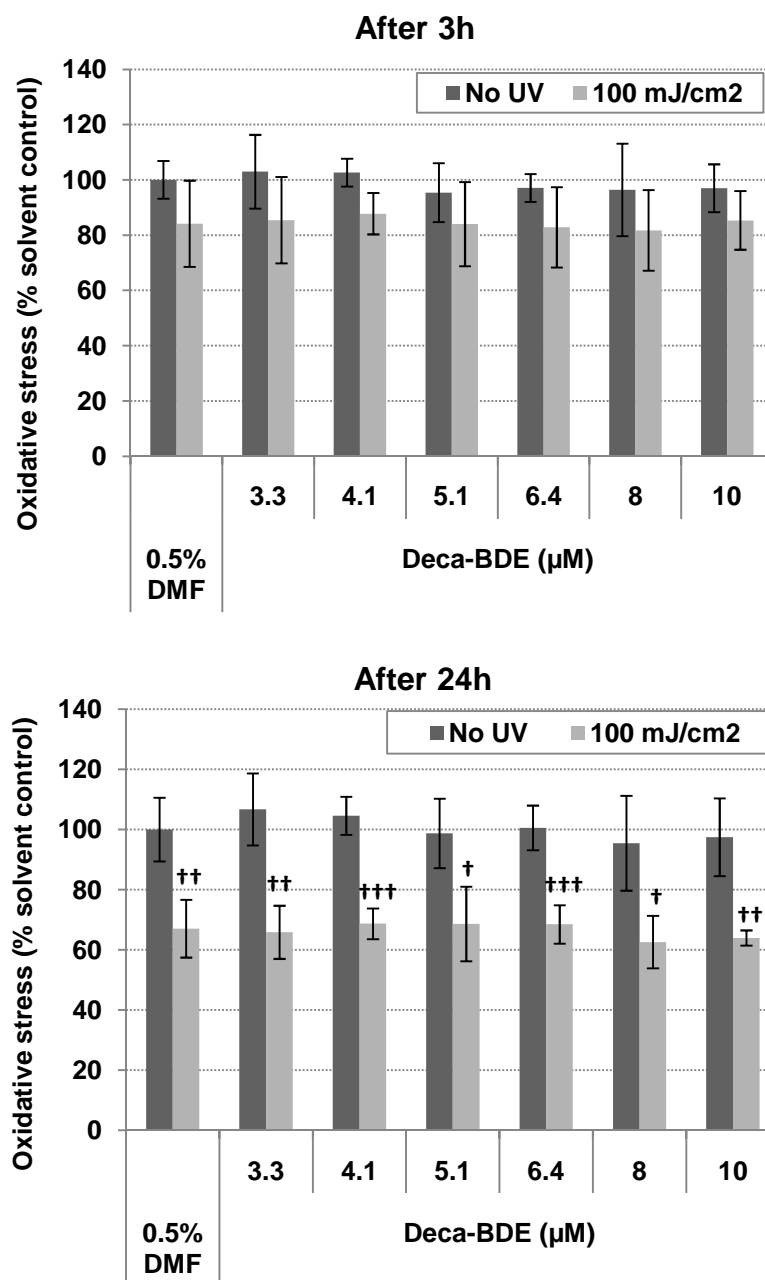
# Significantly different from solvent control; p<0.05 (#)

† Significantly different from non UV-exposed sample with same chemical treatment; p<0.05 (†), p<0.01 (††)

Figure 4.18 continued, above the footnote, p.107.

\* Significantly different from UV-exposed solvent control with same UV energy;  $p < 0.05$   
(\*),  $p < 0.01$  (\*\*),  $p < 0.001$  (\*\*\*)

**Figure 4.19. Oxidative stress of deca-BDE and/or UVB-centered light in confluent HaCaT cells.**



HaCaT cells were treated with chemicals for 60 min and then exposed to 100 mJ/cm<sup>2</sup> UVB-centered light. DCF values were measured 3h or 24 h after UV exposure.

† Significantly different from non UV-exposed sample with same chemical treatment; p<0.05 (†), p<0.01 (††), p<0.001 (†††)



**Figure 4.20. Combined genotoxicity of deca-BDE + UV on HaCaT.**

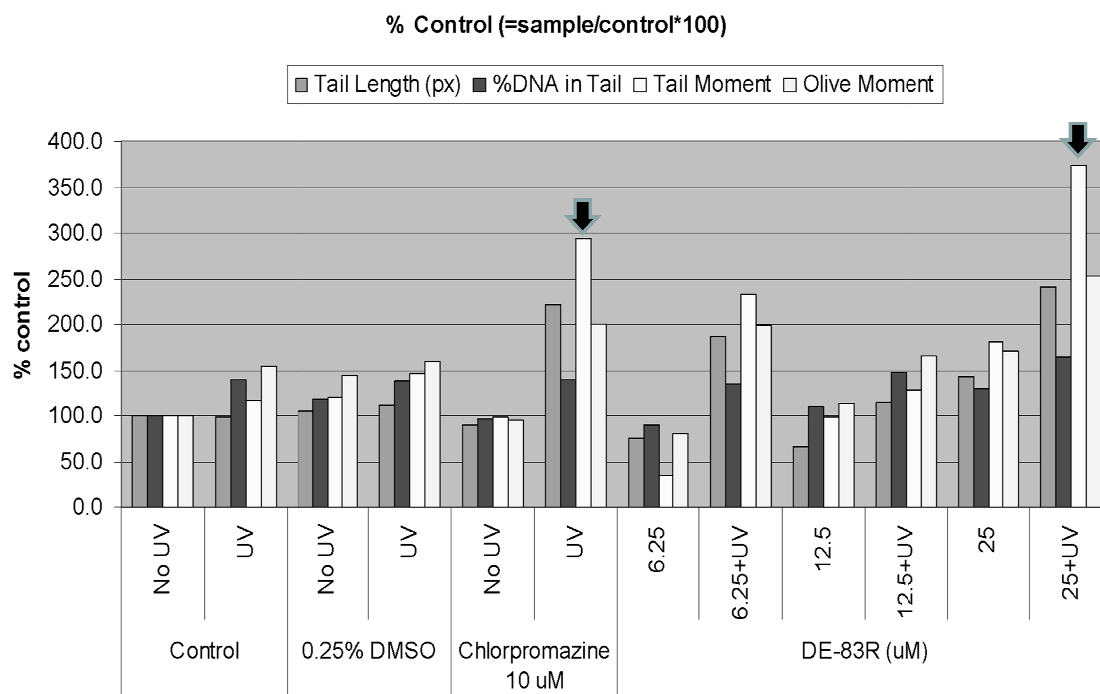


**Table 4.1. Intensity and energy of artificial light sources and natural sunlight.**

<b>Intensity and dose of natural sunlight<sup>1</sup></b>						
<b>Season</b>	<b>Intensity (mw/cm<sup>2</sup>) at noon</b>			<b>Integral daily dose (J/cm<sup>2</sup>)</b>		
	<b>UVB</b>	<b>UVA</b>	<b>Total</b>	<b>UVB</b>	<b>UVA</b>	<b>Total</b>
<b>Spring</b>	0.211	4.20	4.41	4.26	99.4	103.7
<b>Summer</b>	0.243	4.20	4.44	6.19	127.8	134.0
<b>Fall</b>	0.211	3.90	4.11	4.51	97.9	102.4
<b>Winter</b>	0.060	1.78	1.84	1.19	40.3	41.5

<b>Light intensity (mw/cm<sup>2</sup>) of artificial light sources</b>					
<b>Light sources</b>	<b>No lid or filter</b>	<b>Through a plate lid</b>	<b>280 nm filter</b>	<b>307 nm filter</b>	<b>400 nm filter</b>
<b>No room light with a blinder</b>	0				
<b>No room light without a blinder</b>	0.030				
<b>Room White lamp</b>	0.001				
<b>Room Yellow lamp</b>	0.001				
<b>UVB lamp</b>	0.440	0.200			
<b>UVA lamp</b>	0.200	0.080			
<b>UVA + UVB</b>	0.640	0.280			
<b>Xenon lamp</b>			3.50	2.30	

Table 4.1 continued, above the Table material, p.111.

Source: Svobodova, A., Walterova, D., and Vostalova, J. (2006). Ultraviolet light induced alteration to the skin. *Biomedical papers of the Medical Faculty of the University Palacky, Olomouc, Czechoslovakia* **150**, 25-38.

<sup>1</sup>The location for the measurements is not specified in the literature. It should be noted that the range of light intensity and energies of natural UV irradiation varies depending upon locations where they are measured.

**Table 4.2. Molar absorptivities ( $\epsilon$ ) of deca-BDE, chlorpromazine, and triclosan indicate that they need to be tested for phototoxicity.**

<b>Chemical</b>	<b><math>\lambda_{\text{max}}</math> (nm)</b>	<b><math>\epsilon</math> (L mol<sup>-1</sup> cm<sup>-1</sup>)</b>
<b>Chlorpromazine</b>	303	3932
<b>Deca-BDE<sup>1</sup></b>	306	2450
<b>Triclosan</b>	290	3807

Source: Eriksson, J., Green, N., Marsh, G., and Bergman, A. (2004). Photochemical decomposition of 15 polybrominated diphenyl ether congeners in methanol/water. *Environmental science & technology* **38**, 3119-3125.

<sup>1</sup> The molar absorptivity of deca-BDE was cited from the literature.

**Table 4.3. IC50 values and phototoxicity parameters of chlorpromazine, triclosan and deca-BDE.**

	IC50 (µM)		Phototoxicity Parameter	
	No UV	UV	MPE <sup>1</sup>	PIF
<b>Chlorpromazine</b>	45	26	0.38	1.75
<b>Triclosan</b>	10	10	-0.03	0.95
<b>Deca-BDE</b>	NA	NA	-0.02	NA

<sup>1</sup> Detailed information about the calculation of the MPE was quoted from the literature as below:

“It is defined as the weighted average across a representative set of photo effect values. The photo effect (PE<sub>c</sub>) at any concentration (C) is defined as the product of the response effect (RE<sub>c</sub>) and the dose effect (DE<sub>c</sub>) i.e. PE<sub>c</sub> = RE<sub>c</sub> x DE<sub>c</sub>. The response effect (RE<sub>c</sub>) is the difference between the responses observed in the absence and presence of light, i.e. RE<sub>c</sub> = R<sub>c</sub> (-Irr) – R<sub>c</sub> (+Irr). The MPE and dose-effect are given by

$$MPE = \frac{\sum_{i=1}^n w_i PE_{c_i}}{\sum_{i=1}^n w_i} \quad DE_c = \left| \frac{C/C^* - 1}{C/C^* + 1} \right|$$

where C\* represents the equivalence concentration, i.e. the concentration at which the +Irr response equals the –Irr response at concentration C. If C\* cannot be determined because the response values of the +Irr curve are systematically higher or lower than RC(-Irr) the dose effect is set to 1. The weighting factors w<sub>i</sub> are given by the highest response value, i.e. w<sub>i</sub> = MAX [R<sub>i</sub> (+Irr), R<sub>i</sub> (-Irr)]. The concentration grid C<sub>i</sub> is chosen such that the same number of points falls into each of the concentration intervals defined by the concentration values used in the experiment. The calculation of MPE is restricted to the maximum concentration value at which at least one of the two curves still exhibits a response value of at least 10%. If this maximum concentration is higher than the highest concentration used in the +Irr experiment the residual part of the +Irr curve is set to the response value “0”. Depending on whether the MPE value is larger than a properly chosen cut-off value (MPE<sub>c</sub> = 0.15) or not, the chemical is classified as phototoxic.”

Source: OECD (2004). OECD Guideline for testing of chemicals, no. 432: In vitro 3T3 NRU phototoxicity test, Paris, France.

## CHAPTER 5

### SUMMARY AND FUTURE PERSPECTIVES

#### Summary

Deca-BDE is the dominant commercial mixture of PBDEs, accounting for over 80% of global production of PBDEs (US EPA, 2010). It is widely used in a variety of consumer products and easily released into the environment. Deca-BDE accounts for about 30 % of the total estimated BDE-intake for adults (Frederiksen *et al.*, 2009).

Triclosan is a hydroxylated chlorinated diphenyl ether. It is also used in various consumer products, including personal hygiene items, and finds its way into the environment. It was reported that triclosan was a component in all liquid antibacterial soaps and 16% of bar type antibacterial soaps as of 2001 in the U.S. (FDA, 2008). The CDC reported that the levels of triclosan in human urine on average have increased by approximately 40 % from 13.0 µg/L (2003-2004) to 18.5 µg/L (2005-2006) (CDC, 2009).

For deca-BDE and triclosan, dermal contact is a main exposure pathway (FDA, 2008; Frederiksen *et al.*, 2009). PBDE concentrations normalized to skin surface area were found in the range of 3 - 1970 pg/cm<sup>2</sup> (Stapleton *et al.*, 2008). The Australian government reported that 146 µg/kg/day is the estimated exposure level for an adult to triclosan via dermal contact from selected consumer products (NICNAS, 2009). New halogenated hydrocarbons such as PCBs and PBBs, which are structurally related to PBDEs, have been known to undergo photolytic dehalogenation to lower halogenated biphenyls, and may form dibenzofurans, and other by-products from secondary and tertiary reactions (Robertson *et al.*, 1983; Bunce *et al.*, 1989; Miao *et al.*, 1999; Manzano *et al.*, 2004; von der Recke and Vetter, 2007). It has also been reported that deca-BDE and triclosan are photolytically degraded and generate potential toxicants including their photodegradation products and free radicals. In daily life skin is inevitably exposed to

UV light. Therefore, the toxicity of the combined exposures to deca-BDE/triclosan and UV light needs to be investigated to evaluate their potential risk.

I hypothesized that photolysis of deca-BDE and triclosan generates free radicals and degradation products which cause toxic effects including cytotoxicity, growth inhibition, oxidative stress and genotoxicity on skin.

My data from UV spectroscopy confirmed that deca-BDE in our solvent systems absorbs UVB and UVA light which are biologically relevant. A GC-MS study showed that with increasing UV irradiation time, deca-BDE is degraded to lower-BDEs such as three nona-BDE congeners (BDE-206, 207 and 208), one identified octa-BDE (BDE 203), three unidentified octa-BDE congeners and one tentatively identified hexa-BDE. EPR studies with DMPO spin trap revealed that free radicals are produced by deca-BDE in the presence of UVA and UVB light. Irradiation time and deca-BDE concentration were positively related to free radical formation, suggesting that they are main factors dominating the free radical formation.

To explore the mechanism of the radical formation, I conducted an SAR study using EPR and UV spectroscopic techniques with structurally related compounds, such as deca-BDE, octa-BDE, PCB 209, PBB 209, and DE. The highest radical yield was obtained from irradiation of deca-BDE followed by, in order, octa-BDE, PBB 209, PCB 209 and DE. The UV absorption abilities of those compounds were positively related to the radical yields. The compounds which absorb relatively lower wavelengths had greater increase in radical yields with a 280 nm cut-off filter compared to the radical yields with 309 nm cut-off filter, confirming the close relationship of the absorption properties and the free radical formation. The study also suggested that presence of a halogen atom and an ether bond enhances free radical formation. To explore the debromination and hydrogen abstraction steps suggested to be involved in free radical formation, EPR studies were performed with a MNP spin trap and an isotope of THF. The results showed that hydrogen abstraction is involved in the radical formation and the

reaction occurs between the deca-BDE and the solvent, suggesting that the related hydrogen is originated from solvents. Simulation of EPR data confirmed that the dominant free radicals which were formed during the irradiation of deca-BDE were solvent radicals which were produced by hydrogen abstraction during the debromination process. Therefore, I concluded that the debromination of deca-BDE generates free radicals and those free radicals abstract hydrogen atoms from the solvents and subsequently the solvent radicals are generated. In biological systems, hydrogen abstraction is also an important process which is related to produce free radical species like lipid peroxides causing toxicity.

From our biological studies of triclosan, light, and the combination of both in human skin cells such as HaCaT and HSF cells, I found that at relatively high concentrations of triclosan and mixed irradiation from UVB and UVA-centered lamps synergistically enhanced cytotoxicity in HaCaT, while UVB-centered irradiation did not cause the synergistic effect in either confluent or growing cells.- However, the toxic effect caused in proliferating HaCaT cells by pre-irradiated triclosan, presumably by the degradation products, was reduced by UVB-centered irradiation. These results suggest that the combined toxicity of triclosan and UV light could be wavelength-dependent and therefore complicated to predict, not the least because the type of light source would affect the composition of the photodegradation products and thereby the toxicity.

For deca-BDE, a synergistic cytotoxicity in HaCaT was shown only with repetitive exposures of the highest concentration and highest dose of mixed irradiation from UVB and UVA-centered lamps. Otherwise no synergistic effect was found. The photodegradation products of deca-BDE did not cause inhibition of the growth or toxicity of HaCaT cells. Using OECD test guidelines (proliferating cells, UVB-centered light) with HaCaT, neither triclosan nor deca-BDE were found to be a phototoxicant. While this overall outcome of test chemical and UV light exposure were not affected by the type of cells, HSF were more sensitive to chemical treatment with triclosan and deca-BDE.



With UV irradiation, oxidative stress in HaCaT was generally dependent on the concentration of triclosan while triclosan alone did not change the oxidative stress, suggesting that combined exposures of UV light and triclosan generates unexpected effects on the oxidative stress level. Deca-BDE did not contribute to the level of the oxidative stress which was dominated by UV irradiation. Although a Comet experiment showed an unexpected increase in genotoxicity in the presence of deca-BDE and UV light, the result was not repeated due to technical difficulties, and further experiments should be conducted.

In conclusion, the data suggest that deca-BDE is photolytically active in the presence of biologically relevant UVB and UVA light and generates free radicals by UV irradiation via debromination and hydrogen abstraction processes, which could be involved in a toxification mechanism in biological systems. Within my experimental conditions, deca-BDE and triclosan had no or weak phototoxic potential in human skin cells although a potential toxicologic mechanism for triclosan is probably through an increase in oxidative stress. To my knowledge, this is the first research to report the free radical formation of UV irradiation of deca-BDE by a direct detection of free radicals using the EPR technique. In addition, our biologic study is the first report to investigate phototoxicity of deca-BDE and triclosan in human skin cells.

#### Future Perspectives

Recent studies have reported that high levels of PBDEs are found in indoor dust of homes and work places and outdoor dust of places near the source of PBDEs in the air such as electronic waste processing facilities (Lorber, 2007; Stuart *et al.*, 2008; D'Hollander *et al.*, 2010; Muenhor *et al.*, 2010). As discussed above, dermal absorption is a main exposure pathway for humans, and dermal toxicity of PBDEs should be evaluated to estimate the potential risk of PBDE exposure. The FDA suggested further studies of dermal toxicity of triclosan to obtain proper dermal toxicity data for evaluation

of its risk. Specifically, animal studies of skin carcinogenesis and phototoxicity were suggested by the agency. Currently, the FDA is in the process of a scientific and regulatory review of triclosan used in products regulated by FDA (FDA, 2010). The U.S. EPA is also joining their studies to conduct the effects of triclosan on changes in endocrine effects (EPA, 2010). However, there are relatively few studies of phototoxicity of PBDEs and triclosan.

My study presents first data concerning the phototoxicity of deca-BDE and triclosan in skin cells and useful information on experimental conditions. Additionally, further studies should be conducted to obtain more extensive information on dermal phototoxicity of deca-BDE and triclosan.

For future research, reconstructed skin tissues can be used to provide experimental conditions, which have similar components and structure to human skin (Marionnet *et al.*, 2010). Chemicals whose water solubility is relatively low such as deca-BDE and triclosan are more easily transferred to skin cells in a reconstructed skin tissue model where media are located under the skin structure and test chemicals could be placed on the surface of the structure. Cell viability, oxidative stress, and genotoxicity could also be investigated using a reconstructed skin model (Marionnet *et al.*, 2010).

Determination of CYP activities could also be useful as biomarker for the formation of the photodegradation products of PBDEs and triclosan such as lower BDEs and dioxin compounds which cause changes in CYP activities (Stapleton *et al.*, 2009). Changes in CYP activities could be detected by measuring 7-ethoxyresorufin O-deethylase (EROD) activities for CYP 1A/B and 7-methoxyresorufin O-demethylation (MROD) for CYP 1B. CYP mRNA expression could also be measured by quantitative real-time PCR (qPCR). Measuring induction of mRNA expression of CYP1A1, 1A2, 1B1 and 2S1 could be useful because those genes are known to be induced by TCDD exposures in mouse and human skin (Swanson, 2004). A human liver carcinoma cell line such as HepG2 could also be included for CYP activity and gene expression studies

because of their higher levels of CYP expression compared to skin cells, although our HaCaT cells have very good CYP inducibility and could also serve as indicator cells.

Additionally, phototoxicity studies of PBDE metabolites could be valuable.

PBDEs are transformed chemically and metabolically to OH-PBDEs which are ubiquitously found in the environment and humans and may also be naturally produced by certain marine organisms (Raff and Hites, 2006; Hamers *et al.*, 2008; Stapleton *et al.*, 2009; Wan *et al.*, 2009). Recent studies report that like other hydroxylated derivatives of halogenated diphenyl ethers such as triclosan, OH-PBDEs are converted to dioxin compounds such as polybrominated dibenzo-p-dioxins (PBDDs) by solar or artificial UV light irradiation in aqueous environments (Sanchez-Prado *et al.*, 2006; Bastos *et al.*, 2009; Steen *et al.*, 2009). Therefore, studies of the toxicity of UV-irradiation and OH-PBDE exposures need to be conducted for evaluation of potential risks. My work for this thesis would provide useful information for future studies of OH-PBDEs and UV exposure induced toxicity.

## REFERENCES

- Ahn, M. Y., Filley, T. R., Jafvert, C. T., Nies, L., Hua, I., and Bezares-Cruz, J. (2006). Photodegradation of decabromodiphenyl ether adsorbed onto clay minerals, metal oxides, and sediment. *Environ. Sci. Technol.* **40**, 215-220.
- Akitomo, Y., Akamatsu, H., Okano, Y., Masaki, H., and Horio, T. (2003). Effects of UV irradiation on the sebaceous gland and sebum secretion in hamsters. *J. Dermatol. Sci.* **31**, 151-159.
- Alonso, M., Casado, S., Miranda, C., Tarazona, J., Navas, J., and Herradón, B. (2008). Decabromobiphenyl (PBB-209) activates the aryl hydrocarbon receptor while decachlorobiphenyl (PCB-209) is inactive: Experimental evidence and computational rationalization of the different behavior of some halogenated biphenyls. *Chem. Res. Toxicol.* **21**, 643-658.
- ATSDR (2004). Toxicological profiles. Polybrominated biphenyls and polybrominated diphenyl ethers.
- Bastos, P. M., Eriksson, J., and Bergman, A. (2009). Photochemical decomposition of dissolved hydroxylated polybrominated diphenyl ethers under various aqueous conditions. *Chemosphere* **77**, 791-797.
- Benavides, T., Martínez, V., Mitjans, M., Infante, M. R., Moran, C., Clapés, P., Clothier, R., and Vinardell, M. P. (2004). Assessment of the potential irritation and photoirritation of novel amino acid-based surfactants by in vitro methods as alternative to the animal tests. *Toxicology* **201**, 87-93.
- Bezares-Cruz, J., Jafvert, C. T., and Hua, I. (2004). Solar photodecomposition of decabromodiphenyl ether: products and quantum yield. *Environ. Sci. Technol.* **38**, 4149-4156.
- Birnbaum, L. S., Staskal, D. F., and Diliberto, J. J. (2003). Health effects of polybrominated dibenzo-p-dioxins (PBDDs) and dibenzofurans (PBDFs). *Environment international* **29**, 855-860.
- Bokare, V., Murugesan, K., Kim, Y. M., Jeon, J. R., Kim, E. J., and Chang, Y. S. (2010). Degradation of triclosan by an integrated nano-bio redox process. *Bioresour Technol* **101**, 6354-6360.
- Bothe, E., Schuchmann, M. N., Schulte-Frohlinde, D., and von Sonntag, C. (1978a). HO<sub>2</sub> elimination from  $\alpha$ -hydroxylalkylperoxy radicals in aqueous solution. *Photochem. Photobiol.* **28**, 639-643.
- Bothe, E., Schulte-Frohlinde, D., and von Sonntag, C. (1978b). Radiation chemistry of carbohydrates. Part 16. Kinetics of HO<sub>2</sub><sup>•</sup> elimination from peroxy radicals derived from glucose and polyhydric alcohols. *J. Chem. Soc., Perkin Trans. 2* **5** 416-420.
- BSEF (2010). Brominated Flame Retardant Deca-BDE Decabromodiphenyl Ether.

- Buettner, G. R. (1987). Spin trapping: ESR parameters of spin adducts. *Free Radic. Biol. Med.* **3**, 259-303.
- Buettner, G. R. (1990). On the reaction of superoxide with DMPO/.OOH. *Free Radic. Res. Commun.* **10**, 11-15.
- Buettner, G. R., Motten, A. G., Hall, R. D., and Chignell, C. F. (1987). ESR Detection of Endogenous Ascorbate Free Radical in Mouse Skin Enhancement of Radical Production During UV Irradiation Following Topical Application of Chlorpromazine. *Photochemistry and Photobiology* **46**, 161-164.
- Bunce, N. J., Landers, J. P., Langshaw, J. A., and Nakai, J. S. (1989). An assessment of the importance of direct solar degradation of some simple chlorinated benzenes and biphenyls in the vapor phase. *Environ. Sci. Technol.* **23**, 213-218.
- Castell, J. V., José Gómez-Lechón, M. A., Miranda, M. A., and Morera, I. M. (1987). Toxic effects of the photoproducts of chlorpromazine on cultured hepatocytes. *Hepatology* **7**, 349-354.
- CDC (2009). Fourth National Report on Human Exposure to Environmental Chemicals.
- Chao, H.-R., Shy, C.-G., Wang, S.-L., Chih-Cheng Chen, S., Koh, T.-W., Chen, F.-A., Chang-Chien, G.-P., and Tsou, T.-C. (2010). Impact of non-occupational exposure to polybrominated diphenyl ethers on menstruation characteristics of reproductive-age females. *Environment international* **36**, 728-735.
- Chen, D., and Hale, R. C. (2010). A global review of polybrominated diphenyl ether flame retardant contamination in birds. *Environment international* **36**, 800-811.
- Chignell, C. F. (1990). Spin trapping studies of photochemical reactions. *Pure & Appl. Chem.* **62**, 301-305.
- Chignell, C. F., Motten, A. G., and Buettner, G. R. (1985). Photoinduced Free Radicals from Chlorpromazine and Related Phenothiazines: Relationship to Phenothiazine-Induced Photosensitization. *Environmental Health Perspectives* **64**, 103-110.
- Chignell, C. F., and Sik, R. H. (2003). A photochemical study of cells loaded with 2',7'-dichlorofluorescein: implications for the detection of reactive oxygen species generated during UVA irradiation. *Free radical biology & medicine* **34**, 1029-1034.
- Christen, V., Crettaz, P., Oberli-Schrämmli, A., and Fent, K. (2010). Some flame retardants and the antimicrobials triclosan and triclocarban enhance the androgenic activity in vitro. *Chemosphere* **81**, 1245-1252.
- Clark, D. E. (2001). Peroxides and peroxide-forming compounds. *Chem. Health Saf.* **8**, 12-22.
- Clothier, R. (1999). The Use of Human Keratinocytes in the EU/COLIPA International In Vitro Phototoxicity Test Validation Study and the ECVAM/COLIPA Study on UV Filter Chemicals. *ATLA* **27**, 247-259.

- D'Hollander, W., Roosens, L., Covaci, A., Cornelis, C., Reynders, H., Campenhout, K. V., Voogt, P. d., and Bervoets, L. (2010). Brominated flame retardants and perfluorinated compounds in indoor dust from homes and offices in Flanders, Belgium. *Chemosphere* **81**, 478-487.
- D'Silva, K., Fernandes, A., and Rose, M. (2004). Brominated organic micropollutants-igniting the flame retardant issue. *Crit. Rev. Environ. Sci. Technol.* **34**, 141-207.
- Das, S., Mieden, O. J., Pan, X. M., Repas, M., Schuchmann, M. N., Schuchmann, H. P., von Sonntag, C., and Zegota, H. (1988). Aspects of the HO<sub>2</sub> elimination reaction from organic peroxy radicals: Some recent examples. *Basic Life Sci.* **49**, 55-58.
- de Gruijl, F. R., and van der Leun, J. C. (2002). Physical variables in experimental photocarcinogenesis and quantitative relationships between stages of tumor development. *Front Biosci* **7**, d1525-1530.
- Diener, W., Sorni, M., Ruile, S., Rude, P., Kruse, R., Becker, E., Bork, K., and Berg, P. A. (1998). Panniculitis due to potassium bromide. *Brain Dev.* **20**, 83-87.
- Dunn, R. L., Huwe, J. K., and Carey, G. B. (2010). Biomonitoring polybrominated diphenyl ethers in human milk as a function of environment, dietary intake, and demographics in New Hampshire. *Chemosphere* **80**, 1175-1182.
- EPA (2010). Triclosan Facts. U.S. Environmental Protection Agency, Washington, DC.
- Eriksson, J., Green, N., Marsh, G., and Bergman, A. (2004a). Photochemical decomposition of 15 polybrominated diphenyl ether congeners in methanol/water. *Environ. Sci. Technol.* **38**, 3119-3125.
- Eriksson, J., Green, N., Marsh, G., and Bergman, A. (2004b). Photochemical decomposition of 15 polybrominated diphenyl ether congeners in methanol/water. *Environmental science & technology* **38**, 3119-3125.
- FDA (2008). Triclosan [CAS 3380-34-5] Supporting Information for Toxicological Evaluation by the National Toxicology Program.
- FDA (2010). Triclosan: What Consumers Should Know. U.S. Food and Drug Administration, Washington, DC.
- Fossi, M. C., Casini, S., Bucalossi, D., and Marsili, L. (2008). First detection of CYP1A1 and CYP2B induction in Mediterranean cetacean skin biopsies and cultured fibroblasts by Western blot analysis. *Marine Environmental Research* **66**, 3-6.
- Frederiksen, M., Vorkamp, K., Thomsen, M., and Knudsen, L. E. (2009). Human internal and external exposure to PBDEs - A review of levels and sources. *International Journal of Hygiene and Environmental Health* **212**, 109-134.
- Gevao, B., Jaward, F. M., MacLeod, M., and Jones, K. C. (2010). Diurnal Fluctuations in Polybrominated Diphenyl Ether Concentrations During and After a Severe Dust Storm Episode in Kuwait City, Kuwait. *Environmental Science & Technology*, null-null.
- Godar, D. E. (2006). UV Doses Worldwide. *Photochemistry and Photobiology* **81**, 736-749.

- Gomes, A., Fernandes, E., and Lima, J. L. F. C. (2005). Fluorescence probes used for detection of reactive oxygen species. *Journal of Biochemical and Biophysical Methods* **65**, 45-80.
- Guo, J., Wu, F., Shen, R., and Zeng, E. Y. (2010). Dietary intake and potential health risk of DDTs and PBDEs via seafood consumption in South China. *Ecotoxicology and Environmental Safety* **73**, 1812-1819.
- Hagberg, J., Olsman, H., van Bavel, B., Engwall, M., and Lindstrom, G. (2006a). Chemical and toxicological characterisation of PBDFs from photolytic decomposition of decaBDE in toluene. *Environment international* **32**, 851-857.
- Hagberg, J., Olsman, H., van Bavel, B., Engwall, M., and Lindström, G. (2006b). Chemical and toxicological characterisation of PBDFs from photolytic decomposition of decaBDE in toluene. *Environment international* **32**, 851-857.
- Hagberg, J., Olsman, H., van Bavel, B., Engwall, M., and Lindström, G. (2006c). Chemical and toxicological characterisation of PBDFs from photolytic decomposition of decaBDE in toluene. *Environ. Int.* **32**, 851-857.
- Hall, R. D., Buettner, G. R., and Chignell, C. F. (1991). The biphotonic photoionization of chlorpromazine during conventional flash photolysis: Spin trapping results with 5,5-dimethyl-1-pyrroline-N-oxide. *Photochem. Photobiol.* **54**, 167-173.
- Hamers, T., Kamstra, J. H., Sonneveld, E., Murk, A. J., Visser, T. J., Velzen, M. J. M. V., Brouwer, A., and Bergman, Å. (2008). Biotransformation of brominated flame retardants into potentially endocrine-disrupting metabolites, with special attention to 2,2prime,4,4prime-tetrabromodiphenyl ether (BDE-47). *Molecular Nutrition & Food Research* **52**, 284-298.
- Herreno-Sáenz, D. g., Xia, Q., Chiu, L.-T., and Fu, P. (2006). UVA Photoirradiation of Halogenated-Polycyclic Aromatic Hydrocarbons Leading to Induction of Lipid Peroxidation. *International Journal of Environmental Research and Public Health* **3**, 191-195.
- Herrling, T., Jung, K., and Fuchs, J. (2006). Measurements of UV-generated free radicals/reactive oxygen species (ROS) in skin. *Spectrochimica Acta Part A: Molecular and Biomolecular Spectroscopy* **63**, 840-845.
- Hong, S. H., Kannan, N., Jin, Y., Won, J. H., Han, G. M., and Shim, W. J. (2010). Temporal trend, spatial distribution, and terrestrial sources of PBDEs and PCBs in Masan Bay, Korea. *Marine Pollution Bulletin* **60**, 1836-1841.
- Hu, J., Eriksson, L., Bergman, A., Jakobsson, E., Kolehmainen, E., Knuutinen, J., Suontamo, R., and Wei, X. (2005). Molecular orbital studies on brominated diphenyl ethers. Part II--reactivity and quantitative structure-activity (property) relationships. *Chemosphere* **59**, 1043-1057.
- Hua, I., Kang, N., Jafvert, C. T., and Fabrega-Duque, J. R. (2003). Heterogeneous photochemical reactions of decabromodiphenyl ether. *Environ. Toxicol. Chem.* **22**, 798-804.

- Jansson, B., Asplund, L., and Olsson, M. (1987). Brominated flame retardants -- Ubiquitous environmental pollutants? *Chemosphere* **16**, 2343-2349.
- Janzen, E. G. (1971). Spin trapping. *Acc. Chem. Res.* **4**, 31-40.
- Jurkiewicz, B. A., and Buettner, G. R. (1996). EPR detection of free radicals in UV-irradiated skin: mouse versus human. *Photochemistry and photobiology* **64**, 918-922.
- Kurita, M., Shimauchi, T., Kobayashi, M., Atarashi, K., Mori, K., and Tokura, Y. (2007). Induction of keratinocyte apoptosis by photosensitizing chemicals plus UVA. *Journal of Dermatological Science* **45**, 105-112.
- Laarhoven, L. J. J., and Mulder, P. (1997).  $\alpha$ -C-H bond strengths in Tetralin and THF: application of competition experiments in photoacoustic calorimetry. *J. Phys. Chem. B* **101**, 73-77.
- Li, A. S. W., Cummings, K. B., Roethling, H. P., Buettner, G. R., and Chignell, C. F. (1988). A spin trapping data base implemented on the IBM PC/AT. *J. Magn. Reson.* **79**, 140-142.
- Li, J., Lin, T., Pan, S.-H., Xu, Y., Liu, X., Zhang, G., and Li, X.-D. (2010a). Carbonaceous matter and PBDEs on indoor/outdoor glass window surfaces in Guangzhou and Hong Kong, South China. *Atmospheric Environment* **44**, 3254-3260.
- Li, X., Fang, L., Huang, J., and Yu, G. (2008). Photolysis of mono-through deca-chlorinated biphenyls by ultraviolet irradiation in n-hexane and quantitative structure-property relationship analysis. *J. Environ. Sci. (China)* **20**, 753-759.
- Li, X., Ying, G. G., Su, H. C., Yang, X. B., and Wang, L. (2010b). Simultaneous determination and assessment of 4-nonylphenol, bisphenol A and triclosan in tap water, bottled water and baby bottles. *Environment international* **36**, 557-562.
- Linderholm, L., Biague, A., Månsson, F., Norrgren, H., Bergman, Å., and Jakobsson, K. (2010). Human exposure to persistent organic pollutants in West Africa -- A temporal trend study from Guinea-Bissau. *Environment international* **36**, 675-682.
- Ljunggren, B., Cohen, S. R., Carter, D. M., and Wayne, S. I. (1980). Chlorpromazine Phototoxicity: Growth Inhibition and DNA-Interaction in Normal Human Fibroblasts. *J. Invest. Dermatol.* **75**, 253-256.
- Loertscher, J. A., Sadek, C. S., and Allen-Hoffmann, B. L. (2001). Treatment of Normal Human Keratinocytes with 2,3,7,8-Tetrachlorodibenzo-p-dioxin Causes a Reduction in Cell Number, but No Increase in Apoptosis. *Toxicology and Applied Pharmacology* **175**, 114-120.
- Loomis, D., Browning, S. R., Schenck, A. P., Gregory, E., and Savitz, D. A. (1997). Cancer mortality among electric utility workers exposed to polychlorinated biphenyls. *Occup Environ Med* **54**, 720-728.
- Lorber, M. (2007). Exposure of Americans to polybrominated diphenyl ethers. *J. Expo. Sci. Environ. Epidemiol.*



- MacNeil, J. D., Safe, S., and Hutzinger, O. (1976). The ultraviolet absorption spectra of some chlorinated biphenyls. *Bull. Environ. Contam. Toxicol.* **15**, 66-77.
- Makino, K., Suzuki, N., Moriya, F., Rokushika, S., and Hatano, H. (1981). A fundamental study on aqueous solutions of 2-methyl-2-nitrosopropane as a spin trap. *Radiat. Res.* **86**, 294-310.
- Mancini, A. J. (2004). Skin. *Pediatrics* **113**, 1114-1119.
- Manzano, M. A., Perales, J. A., Sales, D., and Quiroga, J. M. (2004). Using solar and ultraviolet light to degrade PCBs in sand and transformer oils. *Chemosphere* **57**, 645-654.
- Marionnet, C., Pierrard, C., Lejeune, F., Sok, J., Thomas, M., and Bernerd, F. (2010). Different Oxidative Stress Response in Keratinocytes and Fibroblasts of Reconstructed Skin Exposed to Non Extreme Daily-Ultraviolet Radiation. *PLoS ONE* **5**, e12059.
- Mazzuckelli, L. F., and Schulte, P. A. (1993). Notification of workers about an excess of malignant melanoma: a case study. *Am J Ind Med* **23**, 85-91.
- Mekenyan, O. G., Ankley, G. T., Veith, G. D., and Call, D. J. (1994). Qsars for photoinduced toxicity: 1. acute lethality of polycyclic aromatic hydrocarbons to daphnia magna. In *Pub. in Chemosphere, Vol. 28, No. 3, 567-582(1994)*. See also *PB--86-122496 and PB--93-155950*, pp. Pages: (18 p), United States.
- Miao, X.-S., Chu, S.-G., and Xu, X.-B. (1999). Degradation pathways of PCBs upon UV irradiation in hexane. *Chemosphere* **39**, 1639-1650.
- Moore, D. E., Sik, R. H., Bilski, P., Chignell, C. F., and Reszka, K. J. (1994). Photochemical sensitization by azathioprine and its metabolites. Part 3. A direct EPR and spin-trapping study of light-induced free radicals from 6-mercaptopurine and its oxidation products. *Photochem. Photobiol.* **60**, 574-581.
- Mossoba, M. M., Makino, K., and Riesz, P. (1982). Photoionization of aromatic amino acids in aqueous solutions. A spin-trapping, and electron spin resonance study. *J. Phys. Chem.* **86**, 3478-3483.
- Muenhor, D., Harrad, S., Ali, N., and Covaci, A. (2010). Brominated flame retardants (BFRs) in air and dust from electronic waste storage facilities in Thailand. *Environment international* **36**, 690-698.
- Munsch, C., Héas-Moisan, K., Tixier, C., Pacepavicius, G., and Alae, M. Dietary exposure of juvenile common sole (*Solea solea* L.) to polybrominated diphenyl ethers (PBDEs): Part 2. Formation, bioaccumulation and elimination of hydroxylated metabolites. *Environmental Pollution In Press, Corrected Proof*.
- Nałęcz-Jawecki, G., Hajnas, A., and Sawicki, J. (2008). Photodegradation and phototoxicity of thioridazine and chlorpromazine evaluated with chemical analysis and aquatic organisms. *Ecotoxicology* **17**, 13-20.
- Nathalie, D., Yannick, G., Caroline, B., Sandrine, D., Claude, F., Corinne, C., and Pierre-Jacques, F. (2006). Assessment of the phototoxic hazard of some essential oils using modified 3T3 neutral red uptake assay. *Toxicology in Vitro* **20**, 480-489.

- NICNAS, A. G. (2009). Triclosan. Priority Existing Chemical Assessment Report (No. 30). Australian Government.
- Niu, J., Shen, Z., Yang, Z., Long, X., and Yu, G. (2006). Quantitative structure-property relationships on photodegradation of polybrominated diphenyl ethers. *Chemosphere* **64**, 658-665.
- NTP (National Toxicology Program) (1986). Toxicology and carcinogenesis studies of decabromodiphenyl oxide (CAS No. 1163-19-5) in F344/N rats and B6C3F1 mice (feed studies). (U. S. D. o. H. a. H. S. Public Health Service, Ed.), Research Triangle Park, NC.
- O'Brien, J., Wilson, I., Orton, T., and Pognan, F. (2000). Investigation of the Alamar Blue (resazurin) fluorescent dye for the assessment of mammalian cell cytotoxicity. *Eur J Biochem* **267**, 5421-5426.
- OECD (2004). OECD Guideline for testing of chemicals, no. 432: In vitro 3T3 NRU phototoxicity test, Paris, France.
- Olsman, H., Hagberg, J., Kalbin, G., Julander, A., Bavel, B. v., Strid, Å., Tysklind, M., and Engwall, M. (2006). Ah Receptor Agonists in UV-exposed Toluene Solutions of Decabromodiphenyl Ether (decaBDE) and in Soils Contaminated with Polybrominated Diphenyl Ethers (PBDEs) (9 pp). *Environmental Science and Pollution Research* **13**, 161-169.
- Park, J., Lee, J., Jung, E., Park, Y., Kim, K., Park, B., Jung, K., Park, E., Kim, J., and Park, D. (2004). In vitro antibacterial and anti-inflammatory effects of honokiol and magnolol against *Propionibacterium* sp. *Eur J Pharmacol* **496**, 189-195.
- Peterman, P. H., and Orazio, C. E. (2003). Sunlight photolysis of 39 mono-hepta PBDE congeners in lipid. *Organohal. Comp.* **63**, 357-360
- Petreas, M., Nelson, D., Brown, F. R., Goldberg, D., Hurley, S., and Reynolds, P. High concentrations of polybrominated diphenylethers (PBDEs) in breast adipose tissue of California women. *Environment international* **In Press, Corrected Proof**.
- Picardo, M., Zompetta, C., Luca, C., Cirone, M., Faggioni, A., Nazzaro-Porro, M., Passi, S., and Prota, G. (1991). Role of skin surface lipids in UV-induced epidermal cell changes. *Arch. Dermatol. Res.* **283**, 191-197.
- Raff, J. D., and Hites, R. A. (2006). Gas-Phase Reactions of Brominated Diphenyl Ethers with OH Radicals. *The Journal of Physical Chemistry A* **110**, 10783-10792.
- Rajka, G. (1974). Surface lipid estimation on the back of the hands in atopic dermatitis. *Arch. Dermatol. Forsch.* **251**, 43-48.
- Rayne, S., Ikonomou, M. G., and Whale, M. D. (2003). Anaerobic microbial and photochemical degradation of 4,4'-dibromodiphenyl ether. *Water. Res.* **37**, 551-560.
- Rayne, S., Wan, P., and Ikonomou, M. (2006a). Photochemistry of a major commercial polybrominated diphenyl ether flame retardant congener: 2,2',4,4',5,5'-hexabromodiphenyl ether (BDE153). *Environment international* **32**, 575-585.

- Rayne, S., Wan, P., and Ikonou, M. (2006b). Photochemistry of a major commercial polybrominated diphenyl ether flame retardant congener: 2,2',4,4',5,5'-hexabromodiphenyl ether (BDE153). *Environ. Int.* **32**, 575-585.
- Reid, L., Khammo, N., and Clothier, R. H. (2007). An evaluation of the effects of photoactivation of bithionol, amiodarone and chlorpromazine on human keratinocytes in vitro. *ATLA* **35**, 471-485.
- Ricart, M., Guasch, H., Alberch, M., Barcelo, D., Bonnineau, C., Geiszinger, A., Farre, M. L., Ferrer, J., Ricciardi, F., Romani, A. M., Morin, S., Proia, L., Sala, L., Sureda, D., and Sabater, S. (2010). Triclosan persistence through wastewater treatment plants and its potential toxic effects on river biofilms. *Aquat Toxicol.*
- Robertson, L. W., Chittim, B., Safe, S. H., Mullin, M. D., and Pochini, C. M. (1983). Photodecomposition of a commercial polybrominated biphenyl (PBB) fire retardant: High-resolution gas chromatographic analysis. *J. Agric. Food Chem.* **31**, 454-457.
- Sanchez-Prado, L., Llompart, M., Lores, M., García-Jares, C., Bayona, J. M., and Cela, R. (2006). Monitoring the photochemical degradation of triclosan in wastewater by UV light and sunlight using solid-phase microextraction. *Chemosphere* **65**, 1338-1347.
- Sanchez-Prado, L., Llompart, M., Lores, M., Garcia-Jares, C., and Cela, R. (2005). Investigation of photodegradation products generated after UV-irradiation of five polybrominated diphenyl ethers using photo solid-phase microextraction. *J Chromatogr A* **1071**, 85-92.
- Schirmer, K., Chan, A. G. J., Greenberg, B. M., Dixon, D. G., and Bols, N. C. Methodology for demonstrating and measuring the photocytotoxicity of fluoranthene to fish cells in culture. *Toxicology in Vitro* **11**, 107-113.
- Schutt, L., and Bunce, N. J. (2004). Photohalogenation of aryl halides. In *CRC Handbook of Organic Photochemistry and Photobiology* (W. M. Horspool, and F. Lenci, Eds.), pp. 38-31-38-12. CRC Press.
- Singh, N. P., McCoy, M. T., Tice, R. R., and Schneider, E. L. (1988). A simple technique for quantitation of low levels of DNA damage in individual cells. *Experimental Cell Research* **175**, 184-191.
- Söderstrom, G., Sellstrom, U., de Wit, C. A., and Tysklind, M. (2004). Photolytic debromination of decabromodiphenyl ether (BDE 209). *Environmental science & technology* **38**, 127-132.
- Söderström, G., Sellström, U., de Wit, C. A., and Tysklind, M. (2004). Photolytic debromination of decabromodiphenyl ether (BDE 209). *Environ. Sci. Technol.* **38**, 127-132.
- Son, H.-S., Ko, G., and Zoh, K.-D. (2009). Kinetics and mechanism of photolysis and TiO<sub>2</sub> photocatalysis of triclosan. *Journal of Hazardous Materials* **166**, 954-960.

- Spielmann, H., Balls, M., Brand, M., Döring, B., Holzhütter, H. G., Kalweit, S., Klecak, G., Eplattenier, H. L., Liebsch, M., Lovell, W. W., Maurer, T., Moldenhauer, F., Moore, L., Pape, W. J. W., Pfanenbecker, U., Potthast, J., De Silva, O., Steiling, W., and Willshaw, A. (1994). EEC/COLIPA project on in vitro phototoxicity testing: First results obtained with a Balb/c 3T3 cell phototoxicity assay. *Toxicology in Vitro* **8**, 793-796.
- Spielmann, H., Balls, M., Dupuis, J., Pape, W. J., Pechovitch, G., de Silva, O., Holzhütter, H. G., Clothier, R., Desolle, P., Gerberick, F., Liebsch, M., Lovell, W. W., Maurer, T., Pfanenbecker, U., Potthast, J. M., Csato, M., Sladowski, D., Steiling, W., and Brantom, P. (1998a). The International EU/COLIPA In Vitro Phototoxicity Validation Study: Results of Phase II (Blind Trial). Part 1: The 3T3 NRU Phototoxicity Test. *Toxicology in Vitro* **12**, 305-327.
- Spielmann, H., Balls, M., Dupuis, J., Pape, W. J. W., de Silva, O., Holzhütter, H.-G., Gerberick, F., Liebsch, M., Lovell, W. W., and Pfanenbecker, U. (1998b). A Study on UV Filter Chemicals from Annex VII of European Union Directive 76/768/EEC, in the In Vitro 3T3 NRU Phototoxicity Test. *ATLA* **26**, 679-708.
- Spielmann, H., Müller, L., Averbek, D., Balls, M., Brendler-Schwaab, S., Castell, J. V., Curren, R., de Silva, O., Gibbs, N. K., Liebsch, M., Lovell, W. W., Merk, H. F., Nash, J. F., Neumann, N. J., Pape, W. J., Ulrich, P., and Vohr, H. W. (2000). The Second ECVAM Workshop on Phototoxicity Testing. The Report and Recommendations of ECVAM Workshop 42. *ATLA* **28**, 777-814.
- Stapleton, H. M., Dodder, N. G., Offenberg, J. H., Schantz, M. M., and Wise, S. A. (2005). Polybrominated Diphenyl Ethers in House Dust and Clothes Dryer Lint. *Environmental Science & Technology* **39**, 925-931.
- Stapleton, H. M., Kelly, S. M., Allen, J. G., McClean, M. D., and Webster, T. F. (2008). Measurement of polybrominated diphenyl ethers on hand wipes: Estimating exposure from hand-to-mouth contact. *Environ. Sci. Technol.* **42**, 3329-3334.
- Stapleton, H. M., Kelly, S. M., Pei, R., Letcher, R. J., and Gunsch, C. (2009). Metabolism of polybrominated diphenyl ethers (PBDEs) by human hepatocytes in vitro. *Environ Health Perspect* **117**, 197-202.
- Staskal, D. F., Diliberto, J. J., DeVito, M. J., and Birnbaum, L. S. (2005). Toxicokinetics of BDE 47 in female mice: effect of dose, route of exposure, and time. *Toxicol. Sci.* **83**, 215-223.
- Staskal, D. F., Hakk, H., Bauer, D., Diliberto, J. J., and Birnbaum, L. S. (2006). Toxicokinetics of polybrominated diphenyl ether congeners 47, 99, 100, and 153 in mice. *Toxicol Sci* **94**, 28-37.
- Steen, P. O., Grandbois, M., McNeill, K., and Arnold, W. A. (2009). Photochemical Formation of Halogenated Dioxins from Hydroxylated Polybrominated Diphenyl Ethers (OH-PBDEs) and Chlorinated Derivatives (OH-PBCDEs). *Environ Sci Technol* **43**, 4405-4411.
- Struwe, M., Greulich, K.-O., Suter, W., and Plappert-Helbig, U. (2007). The photo comet assay--A fast screening assay for the determination of photogenotoxicity in vitro. *Mutation Research/Genetic Toxicology and Environmental Mutagenesis* **632**, 44-57.

- Stuart, H., Ibarra, C., Abdallah, M. A.-E., Boon, R., Neels, H., and Covaci, A. (2008). Concentrations of brominated flame retardants in dust from United Kingdom cars, homes, and offices: Causes of variability and implications for human exposure. *Environ. Int.* **34**, 1170-1175.
- Sun, S., Zhao, J., Leng, J., Wang, P., Wang, Y., Fukatsu, H., Liu, D., Liu, X., and Kayama, F. (2010). Levels of dioxins and polybrominated diphenyl ethers in human milk from three regions of northern China and potential dietary risk factors. *Chemosphere* **80**, 1151-1159.
- Svobodova, A., Walterova, D., and Vostalova, J. (2006). Ultraviolet light induced alteration to the skin. *Biomedical papers of the Medical Faculty of the University Palacky, Olomouc, Czechoslovakia* **150**, 25-38.
- Swanson, H. I. (2004). Cytochrome P450 expression in human keratinocytes: an aryl hydrocarbon receptor perspective. *Chemico-Biological Interactions* **149**, 69-79.
- Symons, M. C. (2000a). Dibromonitroso benzene sulphonate spin-adducts--why no hyperfine coupling to bromine? *Free Radic Res* **32**, 25-29.
- Symons, M. C. R. (2000b). Dibromonitroso benzene sulphonate spin-adducts - Why no hyperfine coupling to bromine? *Free Radic. Res.* **32**, 25 - 29.
- Tanabe, S., Ramu, K., Isobe, T., and Takahashi, S. (2008). Brominated flame retardants in the environment of Asia-Pacific: an overview of spatial and temporal trends. *J. Environ. Monit.* **10**, 188-197.
- Tobi, S. E., Paul, N., and McMillan, T. J. (2000). Glutathione modulates the level of free radicals produced in UVA-irradiated cells. *J Photochem Photobiol B* **57**, 102-112.
- Trevigen (2009). TREVIGEN® Instructions. CometAssay® Reagent Kit for Single Cell Gel Electrophoresis Assay (Catalog # 4250-050-K). (T. INC., Ed.), GAITHERSBURG, MD.
- US EPA (2008). Reregistration Eligibility Decision for Triclosan. (P. A. T. S. Office of Prevention, Ed.).
- US EPA (2010). An exposure assessment of polybrominated diphenyl ethers. (NCEA, Ed.). National Technical Information Service, Springfield, VA, Washington, DC.
- Ustundag, I. O., and Korkmaz, M. (2009). Spectroscopic, kinetic and dosimetric features of the radical species produced after radiodegradation of solid triclosan. *Radiat Environ Biophys* **48**, 159-167.
- Venkataraman, S., Martin, S. M., Schafer, F. Q., and Buettner, G. R. (2000). Detailed methods for the quantification of nitric oxide in aqueous solutions using either an oxygen monitor or EPR. *Free Radic. Biol. Med.* **29**, 580-585.
- Venkataraman, S., Schafer, F. Q., and Buettner, G. R. (2004). Detection of lipid radicals using EPR. *Antioxidants & redox signaling* **6**, 631-638.
- Vinardell, M. P., Benavides, T., Mitjans, M., Infante, M. R., Clapes, P., and Clothier, R. (2008a). Comparative evaluation of cytotoxicity and phototoxicity of mono and diacylglycerol amino acid-based surfactants. *Food Chem Toxicol* **46**, 3837-3841.

- Vinardell, M. P., Benavides, T., Mitjans, M., Infante, M. R., Clapes, P., and Clothier, R. (2008b). Comparative evaluation of cytotoxicity and phototoxicity of mono and diacylglycerol amino acid-based surfactants. *Food Chem Toxicol* **46**, 3837-3841.
- Vizcaino, E., Grimalt, J. O., Lopez-Espinosa, M.-J., Llop, S., Rebagliato, M., and Ballester, F. Polybromodiphenyl ethers in mothers and their newborns from a non-occupationally exposed population (Valencia, Spain). *Environment international* **In Press, Corrected Proof**.
- von der Recke, R., and Vetter, W. (2007). Photolytic transformation of polybrominated biphenyls leading to the structures of unknown hexa- to nonabromo-congeners. *J. Chromatogr. A* **1167**, 184-194.
- von Sonntag, C. (1988). Peroxyl radicals in aqueous media. *Basic Life Sci.* **49**, 47-54.
- Vonderheide, A. P., Mueller, K. E., Meija, J., and Welsh, G. L. (2008). Polybrominated diphenyl ethers: Causes for concern and knowledge gaps regarding environmental distribution, fate and toxicity. *The Science of the total environment* **400**, 425-436.
- Wagner, B. A., Buettner, G. R., and Burns, C. P. (1994). Free radical-mediated lipid peroxidation in cells: Oxidizability is a function of cell lipid bis-allylic hydrogen content. *Biochemistry* **33**, 4449-4453.
- Wahl, M., Guenther, R., Yang, L., Bergman, A., Straehle, U., Strack, S., and Weiss, C. (2010). Polybrominated diphenyl ethers and arylhydrocarbon receptor agonists: Different toxicity and target gene expression. *Toxicology Letters* **198**, 119-126.
- Wan, Y., Wiseman, S., Chang, H., Zhang, X., Jones, P. D., Hecker, M., Kannan, K., Tanabe, S., Hu, J., Lam, M. H. W., and Giesy, J. P. (2009). Origin of Hydroxylated Brominated Diphenyl Ethers: Natural Compounds or Man-Made Flame Retardants? *Environmental science & technology* **43**, 7536-7542.
- Wang, H., Zhang, Y., Liu, Q., Wang, F., Nie, J., and Qian, Y. (2010). Examining the relationship between brominated flame retardants (BFR) exposure and changes of thyroid hormone levels around e-waste dismantling sites. *International Journal of Hygiene and Environmental Health* **213**, 369-380.
- Ward, J., Mohapatra, S. P., and Mitchell, A. (2008). An overview of policies for managing polybrominated diphenyl ethers (PBDEs) in the Great Lakes basin. *Environ. Int.* **34**, 1148-1156.
- Watanabe, I., and Tatsukawa, R. (1987). Formation of brominated dibenzofurans from the photolysis of flame retardant decabromobiphenyl ether in hexane solution by UV and sun light. *Bull. Environ. Contam. Toxicol.* **39**, 953-959.
- Wischermann, K., Boukamp, P., and Schmezer, P. (2007). Improved alkaline comet assay protocol for adherent HaCaT keratinocytes to study UVA-induced DNA damage. *Mutation Research/Genetic Toxicology and Environmental Mutagenesis* **630**, 122-128.
- Wong-Wah-Chung, P., Rafqah, S., Voyard, G., and Sarakha, M. (2007). Photochemical behaviour of triclosan in aqueous solutions: Kinetic and analytical studies. *Journal of Photochemistry and Photobiology A: Chemistry* **191**, 201-208.

- Xie, W., Wang, K., Robertson, L. W., and Ludewig, G. (2010). Investigation of mechanism(s) of DNA damage induced by 4-monochlorobiphenyl (PCB3) metabolites. *Environment international* **36**, 950-961.
- Yan, C., Huang, D., and Zhang, Y. (2010). The involvement of ROS overproduction and mitochondrial dysfunction in PBDE-47-induced apoptosis on Jurkat cells. *Experimental and Toxicologic Pathology* **In Press, Corrected Proof**.
- Yu, Z., Zheng, K., Ren, G., Zheng, Y., Ma, S., Peng, P., Wu, M., Sheng, G., and Fu, J. (2010). Identification of Hydroxylated Octa- and Nona-Bromodiphenyl Ethers in Human Serum from Electronic Waste Dismantling Workers. *Environmental Science & Technology* **44**, 3979-3985.
- Zeng, X., Simonich, S. L. M., Robrock, K. R., Korytár, P., and Alvarez-Cohen, L. (2008). Development and validation of a congener-specific photodegradation model for polybrominated diphenyl ethers. *Environ. Toxicol. Chem.* **27**, 2427–2435.
- Zhang, C., Liu, F., Liu, X., and Chen, D. (2010a). Protective effect of N-acetylcysteine against BDE-209-induced neurotoxicity in primary cultured neonatal rat hippocampal neurons in vitro. *International Journal of Developmental Neuroscience* **28**, 521-528.
- Zhang, C., Liu, X., and Chen, D. (2010b). Role of brominated diphenyl ether-209 in the differentiation of neural stem cells in vitro. *International Journal of Developmental Neuroscience* **28**, 497-502.